European Commission

JRC TECHNICAL REPORTS

Evaluation of the Accident Damage Analysis Module (ADAM) Tool

Verification and Validation of implemented models in ADAM for Accident Consequence Analysis

FABBRI, L. BINDA, M. WOOD, M.

2018

EUR 29363 EN

Contact information
Name: Luciano FABBRI
Address: JRC Ispra
Email: luciano.fabbri@ec.europa.eu
Tel.: +39 0332 785801

JRC Science Hub
https://ec.europa.eu/jrc

JRC113187

EUR 29363 EN

PDF	ISBN 978-92-79-94668-4	ISSN 1831-9424	doi:10.2760/582513
Print	ISBN 978-92-79-94669-1	ISSN 1018-5593	doi:10.2760/858271

Luxembourg: Publications Office of the European Union, 2018

Fabbri, L., Binda, M. and Wood, M., Evaluation of the Accident Damage Analysis Module (ADAM) Tool , EUR 29363 EN, Publications Office of the European Union, Luxembourg, 2018, ISBN 978-92-79-94668-4, doi:10.2760/582513, JRC113187.

Table of Contents

Abstract

This report summarises the evaluation activity conducted on the Accident Damage Analysis Module (ADAM) developed by the EC Joint Research Centre, with specific reference to the physical effects associated with the concentration toxics after airborne dispersion, the thermal radiation of chemical fires, and the explosion of vapour flammable clouds. Consequence assessment models are characterised by high level of complexity and of uncertainty. It is therefore of paramount importance to assess their limits.

This evaluation activity was conducted on a series of relevant scenarios, by benchmarking the outcome of ADAM with the results obtained by similar software tools and with the experimental data obtained on a series of reference field campaigns, as taken from the literature.

ADAM was funded by the Institutional programme of the EC Joint Research Centre and the EC Directorate General on EU Humanitarian Aid and Civil Protection (DG ECHO) via an Administrative Arrangement on Seveso Capacity Building in EU Neighbour Countries[1].

[1] Administrative Arrangements N° ECHO/SER/2014/691549, N° ECHO/SER/2015/709788, and N° ECHO/SER/2016/732857 between DG ECHO and DG JRC

1 Introduction

The Accident Damage Analysis Module (ADAM) is a tool recently developed by the Joint Research Centre (JRC) of the European Commission (EC) to assist the EU Competent Authorities, responsible for the implementation of the Seveso Directive in their countries, in quickly assessing the potential consequences of an industrial accident. In particular, ADAM is designed to implement the calculation of the physical effects of an industrial accident in terms of thermal radiation, overpressure or toxic concentration that may result from the loss of containment of a flammable or toxic substance. For this purpose, consequence assessment models are used to simulate the possible evolution of an accident. This to support operational decisions associated with the necessary preventive measures to be taken to avoid the occurrence of accidents, but also to aid emergency response in the case of failure of the above measures. In both cases, the accuracy of the predictive models is of paramount importance for the decision making process and the evaluation of these models is strictly necessary to understand their limits and to provide confidence about their robustness and applicability.

The present document summarises the evaluation activity conducted on ADAM with specific reference to the overall consequence assessment cycle, from the critical event, which consists of the unintended release of the dangerous substance (ADAM Module 1) to the physical effects associated with such a release, by including the airborne dispersions of toxics, fires, and vapour cloud explosions (ADAM Module 2). This evaluation activity was conducted on a series of relevant scenarios, by benchmarking the outcome of ADAM with the results obtained by similar software tools and with the experimental data obtained on a series of reference field campaigns, as taken from the literature. A point to note is that all simulations with other software tools –used for benchmarking purpose- were performed by the JRC and have not been independently checked by the software developers.

The first module refers to the implementation of models for *source term calculation* i.e. the estimate of the amount of substance released and the associated parameters that fully characterise the release process due to the assumed loss of containment. This estimate requires the knowledge of the type and amount of substance involved in the accident, the physical and storage conditions, the type and mode of rupture, and the release time. The source terms models are well known and are somehow uniform amongst the different tools for consequence assessment. Thus, Module 1 of ADAM was simply verified by benchmarking the results obtained on a series of different accident types with those obtained using similar software tools commercially available (i.e. PHAST of DNV and EFFECTS of TNO). For the more complex evaluation of flashing of pressurised substance and consequent rainout, the evaluation was conducted by comparing the ADAM results with the data of experimental trials available from the literature.

The second module estimates the physical effects resulting from the accidental development following the loss of containment in terms of: (*i*) concentration of a toxic after airborne dispersion, (*ii*) thermal radiation of the chemical fire, and (*iii*) explosion of the vapour flammable cloud. This calculation is normally influenced by the atmospheric conditions (i.e., air temperature, air stability, wind speed) and by other parameters such as for instance the average time for vapour dispersions or the ignition time or ignition location for flash fires and vapour explosions. Since the associated models are strongly dependent from the assumptions made, this module was submitted to a more intense validation exercise by comparing the model output with the data of the experimental trials available from the literature. In general, the validation of consequence assessment models is not very straightforward. The main difficulty is associated with the need to establish whether the measurement data used to evaluate model performance are accurate enough. In some circumstances, it would be even incorrect to assume that a perfectly accurate model will reproduce measured data. For instance, some fluctuations in the environmental conditions occurring during the field tests might influence significantly the test results and cannot accounted for in the simulations. For this reason, a full validation of models, which are typically designed to describe natural systems, is

practically impossible, as the random nature of the involved process leads to some irreducible uncertainty (Oreskes, 1994). Instead of comparing each single prediction with the corresponding observation, a possible way forward to approach the problem is to group the observations and predictions according to a certain criterion, and then to compare the averaged results. In this respect, model can be only confirmed or evaluated by showing the good agreement between some set of observation data and predictions.

The statistical measures used to evaluate the performance of ADAM to experimental data taken form the literature, were those suggested by Chang and Hanna (Chang, 2004), which are normally applied for the validation of airborne dispersion modelling evaluation and described on Table 1. In the present report the use of these indicators were also extended to the validation of other models such as for instance: the release of a two-phase material from pipe, droplet size, rainout, and the physical effects from fires.

Performance measures of Table 1 are expressed in terms of:

- the predicted values by the models, C_{p_i},
- the observations from the experimental trials, C_{o_i},
- the average values (i.e. $\overline{C_p}$, $\overline{C_o}$) and standard deviations (i.e. $\sigma_{C_p}, \sigma_{C_o}$).

When necessary to establish the confidence intervals on the different model indicators (i.e. to assess the significance of model differences), a Boostrap resampling technique (Efron, 1987) was employed. This procedure essentially involves random sampling from the original data set with replacement from the original sample. The purpose is to generate any number of new sample sets of the same size as the original data set. This approach is normally suggested since the above parameters are not easily transformed by standard procedures to a normal distribution. In the present case, the Boostrap method was applied by resampling 1000 estimates to determine the 95% confidence intervals for each performance level.

In addition to the above quantitative measures, it is often informative to provide scatter plots of predicted vs observed concentration values.

Table 1: Performance measures.

Performance measure	Formula	Description
Fractional Bias (FB)	$FB = \frac{\overline{C_o} - \overline{C_p}}{0.5\ (\overline{C_o} + \overline{C_p})}$	The Fractional Bias (FB) is a measure of mean bias and indicates systematic errors, which allows assessing whether the model underestimates or overestimates the measured values. FB is based on a linear scale and the systematic bias refers to the arithmetic difference between *Cp* and *Co*.
Geometrical mean Bias (MG)	$MG = \exp(\overline{\ln(C_o)} - \overline{\ln(C_p)})$	The Geometrical mean Bias (MG) is also a measure of mean bias and indicates systematic errors, but differently from FB that is based on a linear scale is based on a logarithmic scale. Its use is normally preferred in dispersion related applications because of the wide range of magnitudes involved.
Normalised Mean Square Error (MNSE)	$NMSE = \frac{\overline{(C_o - C_p)^2}}{\overline{C_o} \cdot \overline{C_p}}$	The normalized mean square error (NMSE) is a measure of the overall scatter about the true value and accounts of unpredictable fluctuations. It reflects both systematic and unsystematic (random) errors.
Geometric Variance (VG)	$VG = exp\left[\overline{(\ln(C_o) - \ln(C_p))^2}\right]$	The Geometrical Variance (VG) is, analogously to the NMSE, a measure of the overall scatter about the true value. It is based on a logarithmic scale and its use is normally preferred in dispersion related applications because of the wide range of magnitudes involved.
Correlation Coefficient (R)	$R = \frac{\overline{(C_o - \overline{C_o})(C_p - \overline{C_p})}}{\sigma_{C_o}\ \sigma_{C_p}}$	The correlation coefficient (R) reflects the linear relationship between two variables. It is insensitive to either an additive or a multiplicative factor. A perfect correlation coefficient is only a necessary, but not sufficient condition for accuracy.
Fraction of Predictions within a factor-of-two (FAC2)	FAC2 = fraction of data that satisfies $0.5 \leq \frac{C_p}{C_o} \leq 2$	The fraction of predictions within a factor of two of observations (FAC2) is the most robust measure, because it is not overly influenced by high and low outlier.

2 Source Term (Module 1)

The present chapter reports the results of the benchmarking of ADAM with other available software tools used to calculate the physical effects of accidents. The tools that were considered were EFFECTS of TNO and PHAST of DNV. A point to note is that the specific thermodynamic, fluid mechanic and transport properties used by ADAM and that may influence the release behaviour were collected from a different database if compared to the other reference software tools.

As different accident scenarios, which depend on the type and properties of the stored substance, storage geometry and rupture type, require the use of different models, separate benchmarking had to be conducted to address the different situations. In particular, a first distinction was made depending on the storage thermodynamic conditions (i.e. pressure and temperature), which are particularly influential on the release dynamic. In such a way, the stored substance may be classified as follows:

1. Compressed vapour, when they are superheated with respect to the saturated state at the storage pressure (i.e. the storage temperature is higher than the saturation temperature at the storage pressure). In this case, the release is vapour only.
2. Non-boiling liquid (i.e. pure liquid), when they are subcooled with respect to the saturated state at the storage pressure (i.e. the storage temperature is lower than the saturation temperature at the storage pressure). Typically, this is the case of substances stored as liquids at ambient temperature and pressure such as many petrochemical products (e.g., gasoline, kerosene, diesel oil), but also to refrigerated liquefied gases. In this case, the release could be either liquid or two-phase depending on initial superheat.
3. Pressurised liquiefied gases, when the storage temperature and pressure are in a saturation condition, or the storage pressure is above saturation level. In this case, both liquid and vapour are present in the vessel and the release is two-phase either for the substance flash after release or because of the two-phase mixing within the vessel.

Since in ADAM three different types of damage mechanisms are considered (i.e. failure from vessel hole, from pipe connected to a vessel, and catastrophic rupture of a vessel), by combining these with the above substance types, there are nine different scenario categories, which need to be verified (see table below). The main output of these models under comparison was either the flow rate or the overall amount of the substance released. The overall dynamic was also considered.

	Type of LoC
R1	*Release of compressed gases from vessel*
R2	*Release of compressed gases from pipe*
R3	*Release of non-boiling liquids from vessel*
R4	*Release of non-boiling liquids from pipe*
R5	*Release of pressurised liquids from vessel*
R6	*Release of pressurised liquids from pipe*
CR1	*Catastrophic release of compressed gases from vessel*
CR2	*Catastrophic release of non-boiling liquids from vessel*
CR3	*Catastrophic release of superheated liquids from vessel*

With reference to pressurised liquefied gases, since the process involving the flashing and rainout mechanisms can have different modelling alternatives, it was decided to conduct the evaluation of ADAM by comparing the calculus outcome with the experimental data taken form the literature. The results are given in the last section to this chapter.

2.1 Release of compressed gases (R1 & R2)

The first case used for the benchmarking was the outflow from vessel hole as taken from the Yellow Book (van den Bosch, 2005 paragraph 2.62 page 2.127). This consists of the release of a 100m^3 vessel containing hydrogen stored at a temperature of 288.15K at 50 bara. Although hydrogen is supercritical at these operating conditions (highlighted by ADAM with a pop-up menu), the real gas equation of state provides still a suitable estimate of the gas density. The relevant input parameters for the calculus of the source term are as follows:

Input Parameter	*Value*
Substance	Hydrogen
Storage temperature	288.15 K
Storage overpressure	49 barg
Vessel Volume	100 m^3
Hole Diameter	100 mm
Discharge coefficient	0.62

The discharge coefficient is usually calculated by ADAM and PHAST via an automatic procedure (default setting for both software tool), however it was decided to fix a manual value in this case in order to make a direct comparison with the tabulated values of the Yellow Book, which were also calculated by using a fixed value of 0.62

The result of the comparison is given in Figure 1, where the red curve refers to ADAM, the blue dotted curve was obtained using PHAST 7.22, and the green curve, which is much shorter (i.e. ca. 30s), represents the data as taken from the Yellow Book. In general, a very good match is present, with the Yellow book data that practically superimposes with the ADAM values.

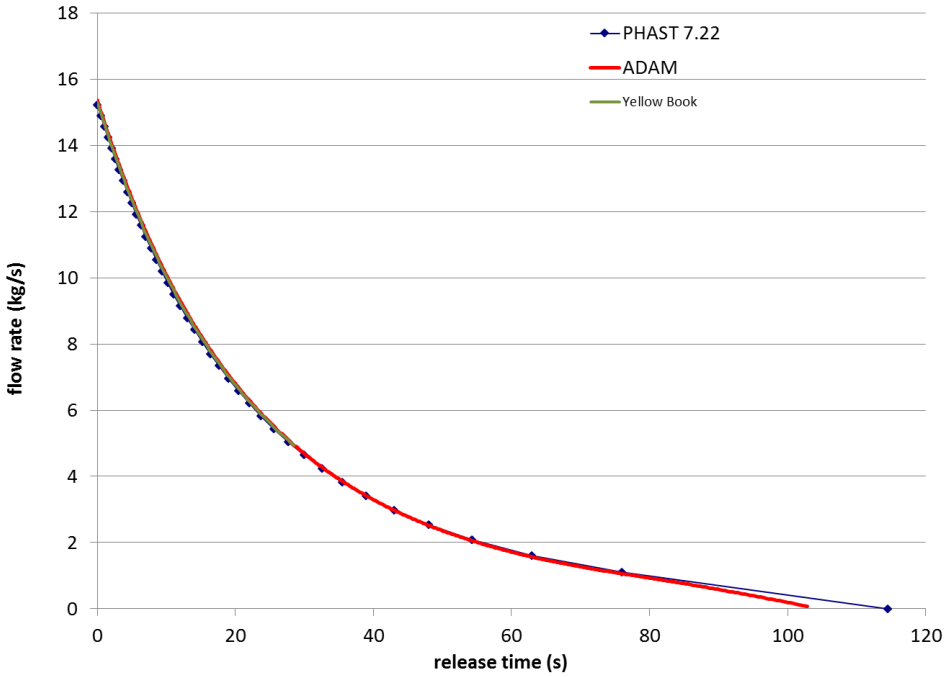

Figure 1: Hydrogen release as from Yellow Book example (Yellow Book, par. 2.62 page 2.127)

Figure 2 represent a more realistic case: the release of ethylene from a 25mm hole in a 0.5 m^3 'bullet' type tank (i.e. cylindrical with hemiheads), where the compressed gas is stored at an absolute pressure of 250 psi at a temperature of -25 °F.

Input Parameter	*Value*
Substance	Ethylene
Storage temperature	-25 °F
Storage overpressure	16.2 barg
Vessel Volume	0.5 m^3
Hole Diameter	25 mm
Discharge coefficient	Automatic (0.865 in EFFECTs)

As it is clear from the figure, there is a very good match between the calculations performed by ADAM and PHAST 6.54, whilst the curve calculated by EFFECTS 5.5 is less conservative. The reason for this is that EFFECTS 5.5, differently from the others, makes use of the ideal gas approximation. This was confirmed by running ADAM with the ideal gas assumption.

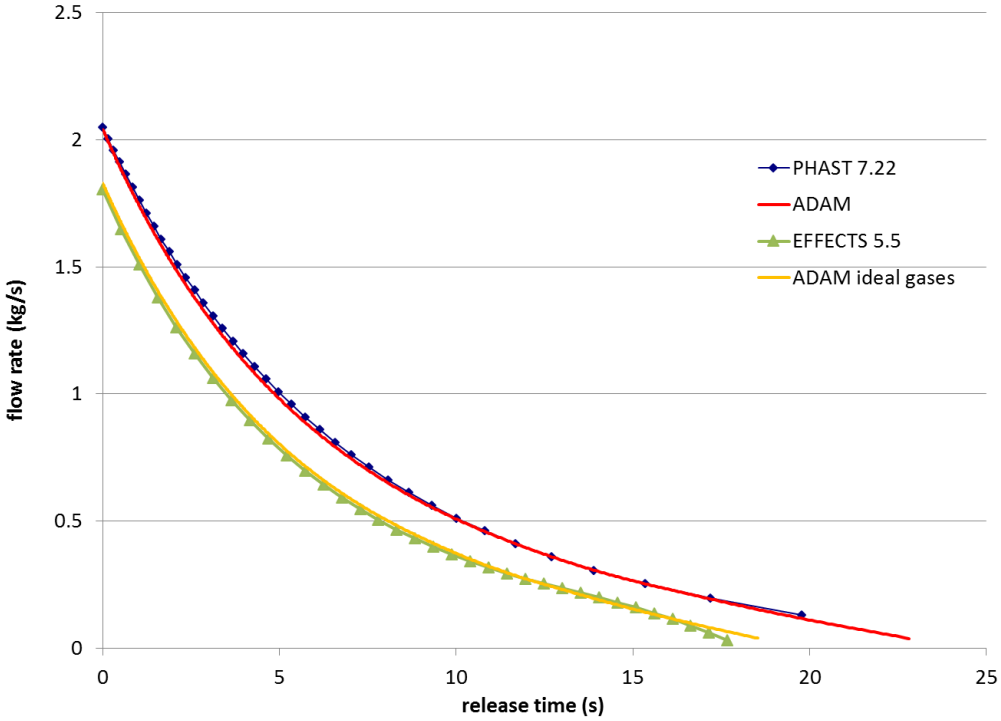

Figure 2: Flow rate vs. time, hole diameter 25mm (Ethylene)

The same release type was also calculated by varying the hole diameter and the storage pressure. For both cases the agreement between the results obtained with ADAM is very good (see Figure 3 and Figure 4).

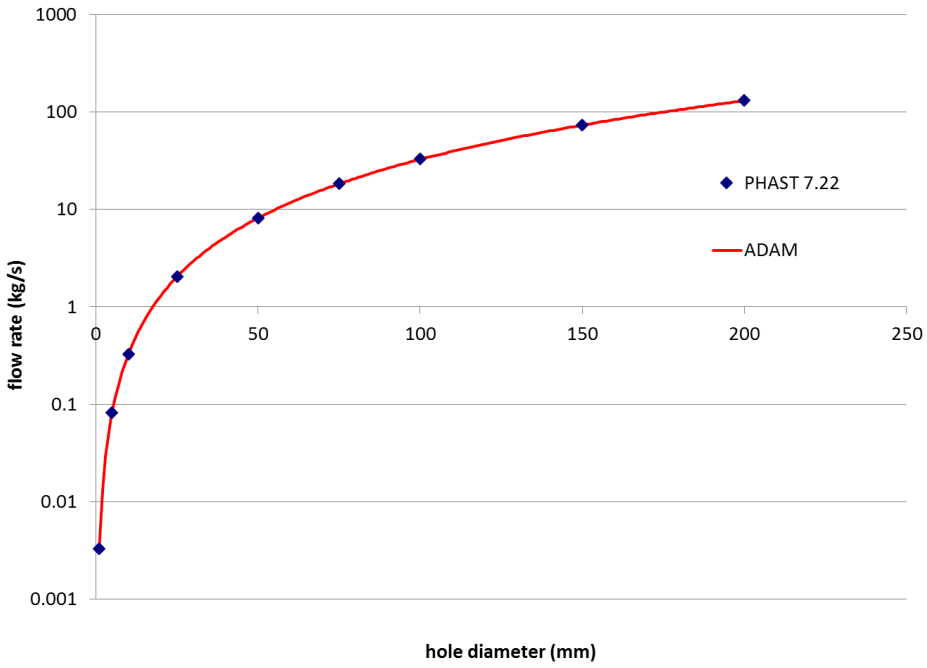

Figure 3: Flow rate vs. hole diameter (Ethylene)

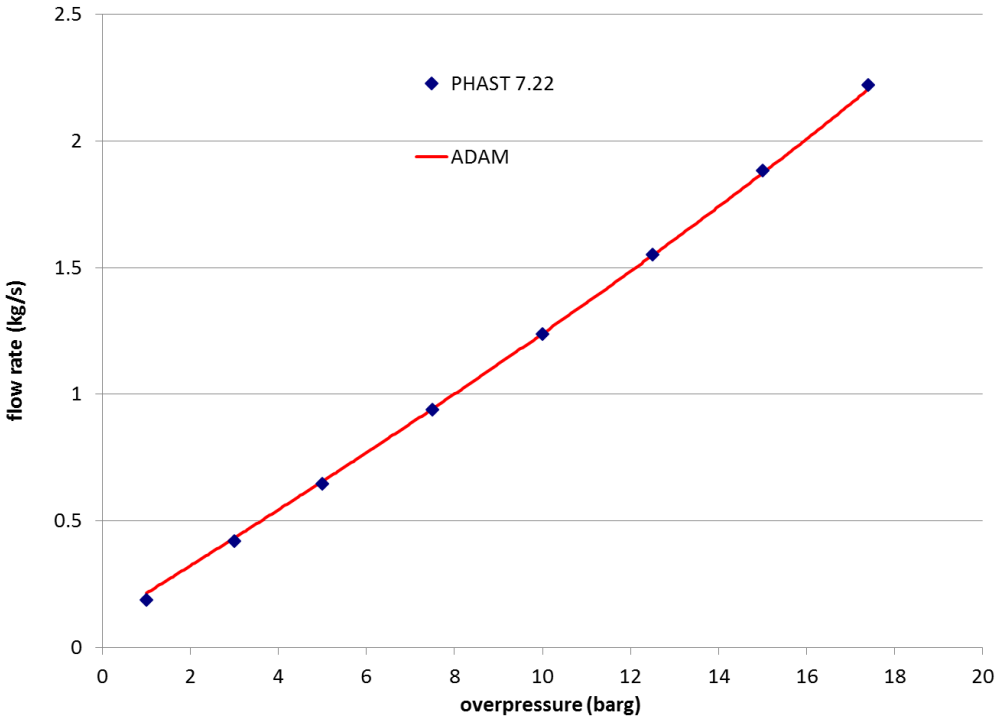

Figure 4: Flow rate vs. storage gauge pressure (Ethylene)

The simulation of the release of a compressed gas from a *pipe* connected to a vessel is reported in Figure 5. This case was obtained by assuming bore pipe rupture of a stainless steel pipe according to the input data given hereunder, and by assuming no other losses within the pipe:

Input Parameter	*Value*
Substance	Methane
Storage temperature	288.15K
Storage overpressure	67.5 barg
Vessel Volume	100 m^3
Pipe inner diameter	154 mm
Piper roughness	0.045 mm
Other losses	none

The two graphs depict the release flow rate as a function of the release time, and refer to the two different distances for the vessel where the pipe rupture takes places, i.e. 10m and 100m, respectively.

Also in this case, a very good agreement is found between ADAM and PHAST.

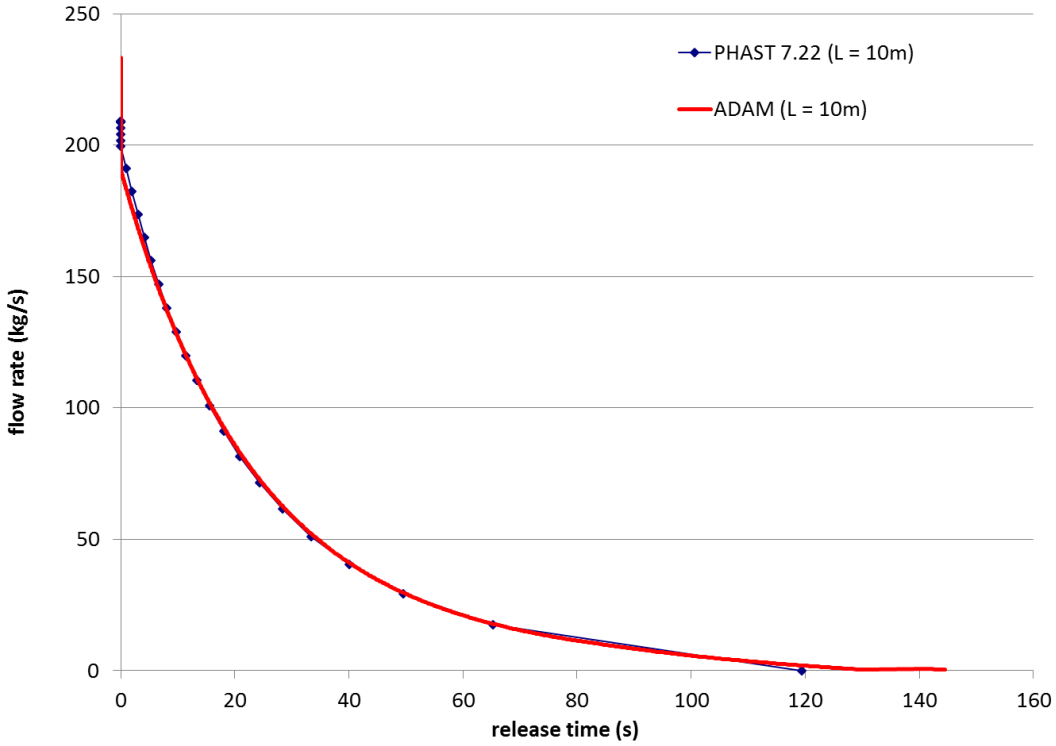

a)

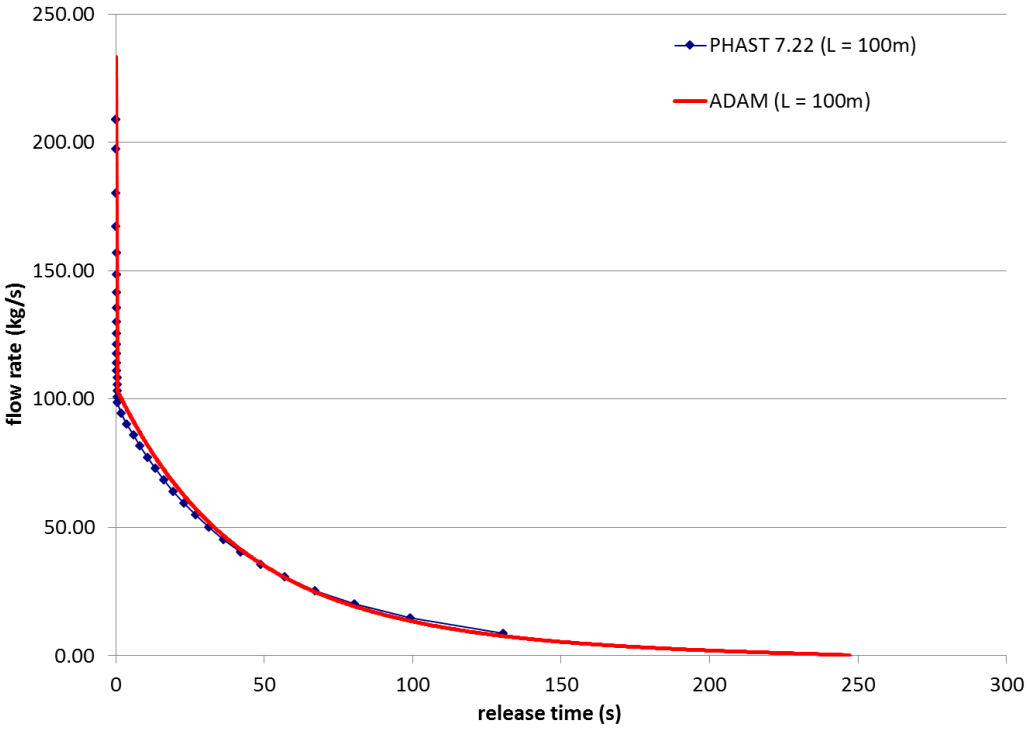

b)

Figure 5: Release of compressed Methane from a pipe. Flow rate vs release time. Pipe length at rupture: a) 10m ; b) 100m

2.2 Release of non-boiling liquids (R3 & R4)

The release of non-boiling liquid can be simulated by assuming that the tank is sealed or atmospheric. In the first case, a depressurization phenomenon will take place during the outflow. This phenomenon will last until the internal pressure added to the hydrostatic weight equals the external pressure. This leads to an oscillating behavior of the flow rate resulting in a gurgling outflow. Both PHAST 7.22 and ADAM model the depressurization of a non-boiling liquid using both assumptions. On the contrary, EFFECTS uses the atmospheric assumption. In order to make the comparison, ADAM was therefore run twice, by using both assumptions.

The result for a release from vessel (i.e. R3) is given in Figure 6, which represents the outflow of a non-boiling substance stored at room temperature with the following input parameters:

Input Parameter	*Value*
Substance	Benzene
Storage temperature	290 K
Storage overpressure	0 (atmospheric)
Tank	Horizontal 10m height, 5m diameter, 70% filling (substance volume 137.45 m^3)
Hole Diameter	100 mm
Release height from bottom	1 m
Discharge coefficient	0.61

In both cases, ADAM reproduces quite well the results of the other tools, even if in the "sealed" talk case, the outflow provided by PHAST, which was obtained by setting the "vacuum relief valve" with the "not operating" option, is somehow more erratic.

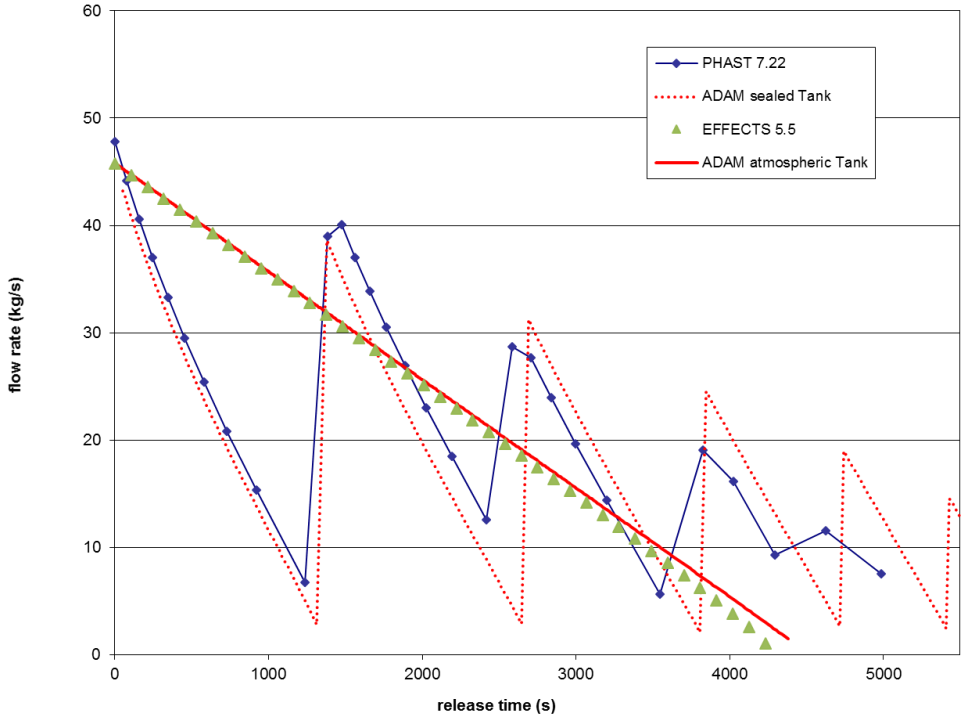

Figure 6: Release of Benzene from vessel (hole: 100mm diameter)

For the release from pipe connected to a vessel (i.e. R4), the result is given in Figure 7. This is the case of benzene outflow from a 101.6 mm diameter pipe, 100m long. Also in this case the agreement for the two cases is rather good.

Input Parameter	*Value*
Substance	Benzene
Storage temperature	290 K
Storage overpressure	0 (atmospheric)
Tank	Vertical 10m height, 5m diameter, 70% filling (substance volume 137.45 m^3)
Pipe	Stainless steel (roughness 0.045mm, inner diameter 101.6mm mm)
Pipe length at rupture	100m
Release height from bottom	1 m
Losses in Pipe	None

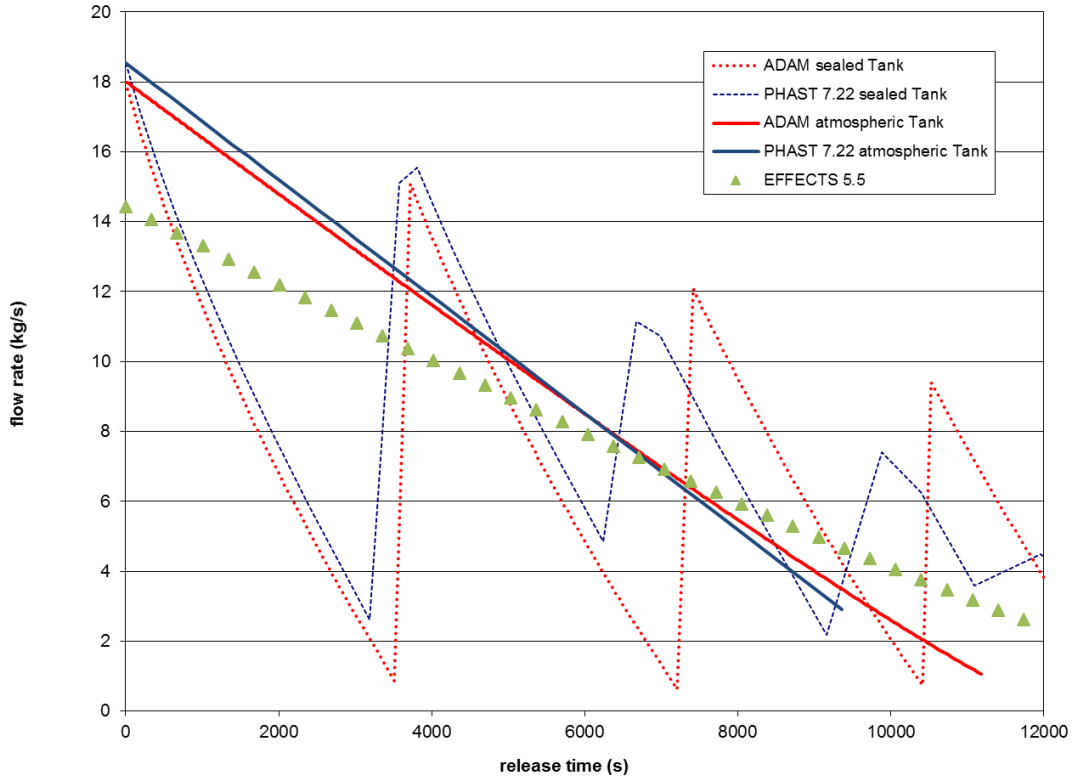

Figure 7: Release of Benzene from pipe connected to a vessel (101.6mm diameter, 100m long)

2.3 Release of liquefied pressurized gases from vessel (R5)

The outflow of a pressurised liquefied gas is definitely more complex if compared to the case of compressed gases and non-boiling liquids. In this case, the outflow generally undergoes to flash after release due to sudden depressurisation. This leads to two-phase releases that are characterised by droplets formation and subsequent rainout of part thereof, which may be cause of reduced concentration of the dispersive cloud. On the other hand, rainout is also cause of extended cloud duration, due to the evaporation of the pool formed by the rainout liquid, which form a secondary source of vapour. For this reason, it is of paramount importance to assess correctly the rainout portion of the outflow.

Two sample cases involving the release from leak in a vessel (i.e. R5) were conducted by using chlorine and propane stored at saturation conditions as reference substances. The input data used for the calculations are given in the table below:

Input Parameter	*Case 1*	*Case 2*
Substance	chlorine	Propane
Storage temperature	290 K	283.15 K
Storage overpressure	5.179 bar (i.e. saturation)	5.353 bar (i.e. saturation)
Tank	Horizontal 10m length, 2.676m diameter, 80% filling (substance volume 45 m^3)	Spherical 19m radius, 80% filling 55.7% (substance volume 2000 m^3)
Hole Diameter	50.8 mm	101.6
Rupture from vessel bottom	0.5 m	1
Discharge coefficient	Automatic calculation	Automatic calculation

Figure 8 and Figure 9 show the flow rate vs the release time for the two cases under investigation. As it can be observed, there is a good match of ADAM with the other tools. The main difference can be noticed at the transition phase, which correspond to the time when the liquid level reaches the exit hole. ADAM is designed to model both the phases of the outflow, i.e. before (hole down) and after this transition (hole up), whilst the others focus on the first phase only, which corresponds to the situation with the liquid level above the exit hole (which is definitely the more significant in terms of the associated consequence effects).

Since the outflow consists of a two-phase substance, it was decided to compare also the calculated vapour quality i.e. the vapour mass fraction in the two-phase mixture. Figure 10 and Figure 11 show calculations performed with ADAM and PHAST (the old version of EFFECT does not allow visualising these data), where a good agreement is found. The behaviour of PHAST at the transition phase for the chlorine case is quite ambiguous since the release tends to became all-liquid, which was not expected.

As previously mentioned, due to the complexity of other aspects associated with a release of a liquefied pressurised substance, i.e. the process of droplet formation and following rainout, the evaluation of ADAM was conducted by comparing the calculated data with the experimental data available in the literature. The following sub-sections provide the result of such a comparisons with reference to: droplet size formation, and rainout effects.

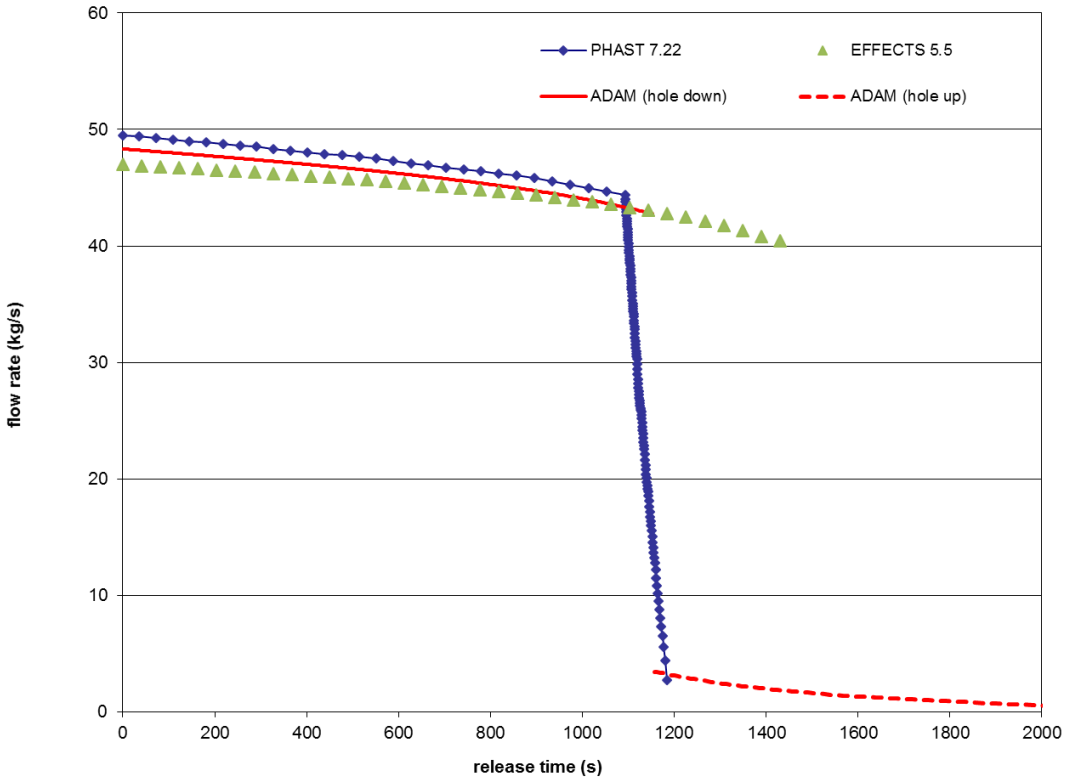

Figure 8: Release of Chlorine from Vessel (Horiz. Cylinder): flow rate vs. release time

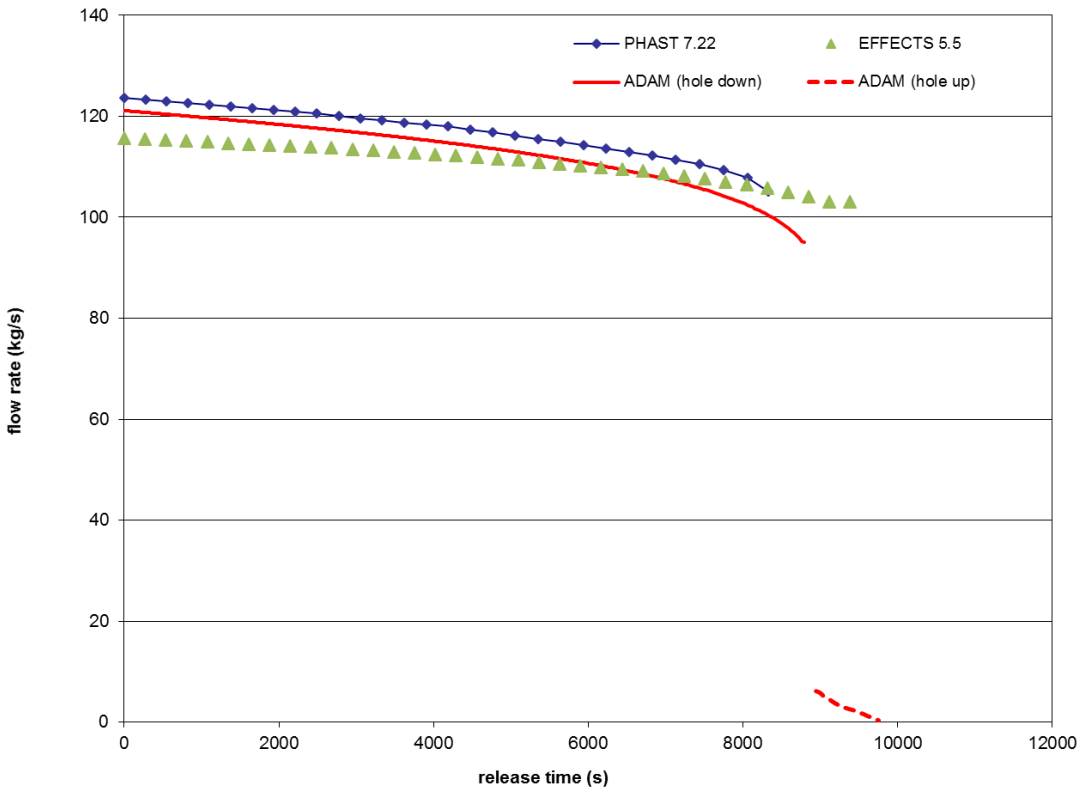

Figure 9: Release of Propane from Vessel (Sphere): flow rate vs. release time

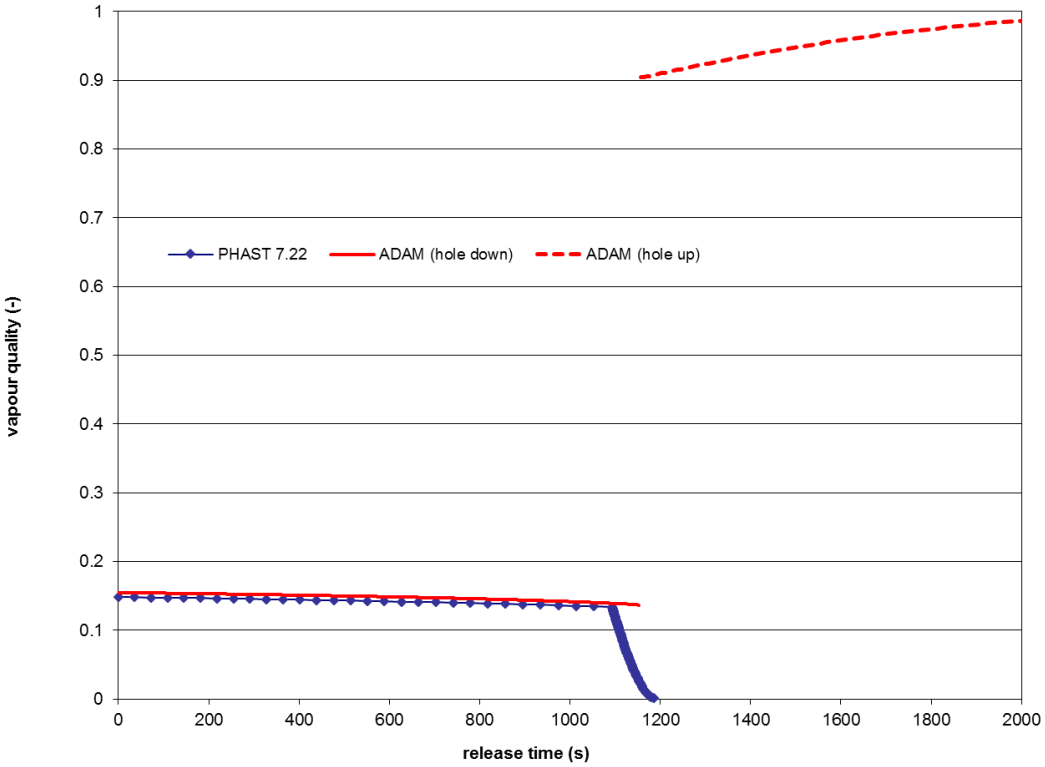

Figure 10: Release of Chlorine from Vessel: vapour quality vs. time

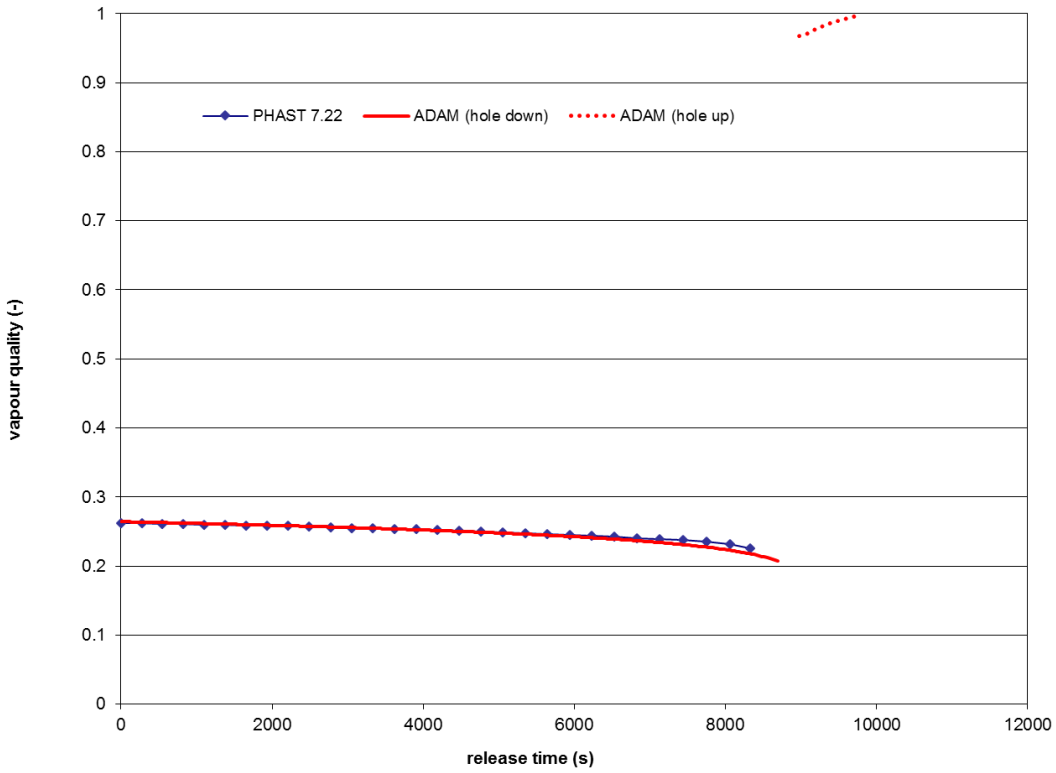

Figure 11: Release of Propane from Vessel: vapour quality vs. time

2.3.1 Droplet size formation

The understanding of the formation of aerosol droplets and their entrainment in a vapour cloud is particularly important since aerosol increase the cloud density and influence the cloud dispersion behaviour. In addition, droplet size is directly associated with the liquid mass fraction falling onto the ground after release (rainout), which is cause of airborne concentration reduction and extended time duration of the dispersion phenomenon.

Despite of the fact that ADAM allows different droplet size correlations, the test was conducted by using the default correlation. This is the modified CCPS correlation (Witlox, 2013), in which the SMD (Sauter Mean Diameter) mechanical break-up value is taken for sub-cooled jets whilst flashing break-up is taken for super-heated jets.

The validation test on droplet size formation was conducted on a series of scaled experiments for substances with a range of volatilities (water, gasoline, cyclohexane, n-butane, propane), which were conducted at Cardiff University (Cleary, 2007; Witlox, 2010). The results of the ADAM calculations were obtained by using the Phase III JIP SMD correlation (Witlox, 2010) and are shown in Figure 12, where the calculated value of the droplet size (i.e., Sauter Mean Diameter), indicated in the graph as 'predicted SMD', was compared to the values obtained experimentally. These values are also compared with those calculated in Witlox, 2010, by using a similar correlation (DNV PHAST). The results are quite similar, with the under predicting data that behave slightly better and those over predicting with a slightly worst tendency. This is also confirmed by the performance measures as shown in the table below:

Table 2: Performance measures for droplet size.

FB	MG	NMSE	VG	P	FAC2
ADAM					
-0.024	0.984	0.129	1.157	0.846	0.889
Witlox 2010					
0.203	1.247	0.183	1.310	0.808	0.861

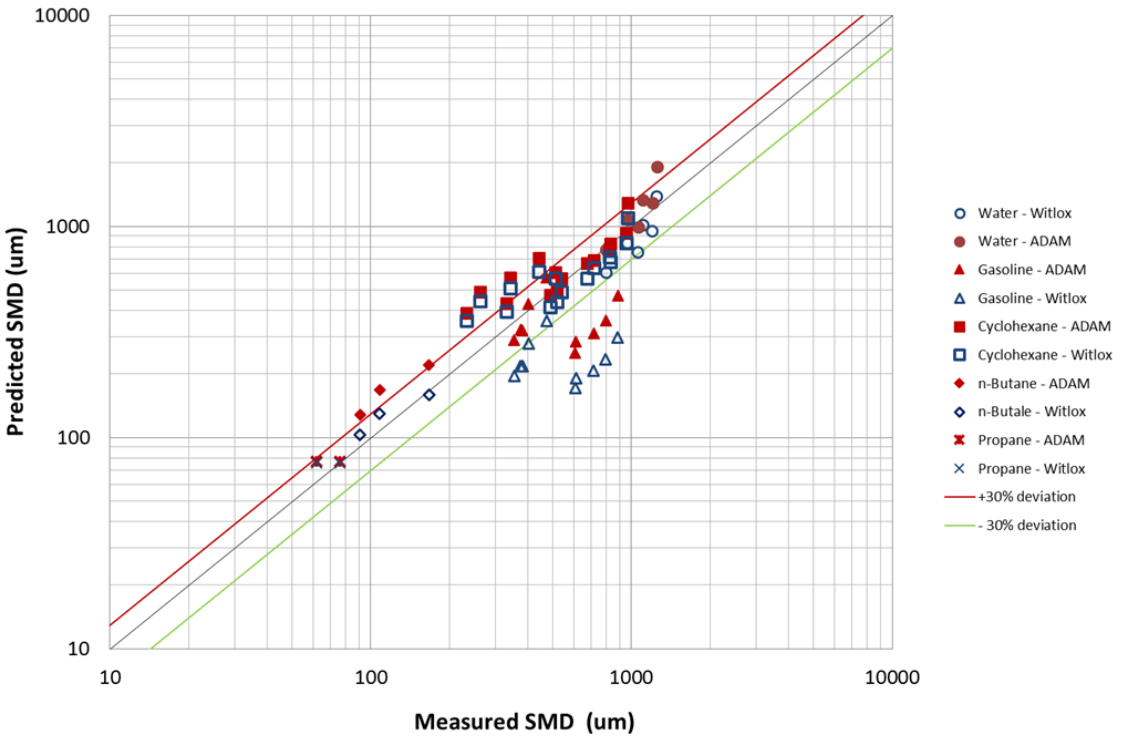

Figure 12: Variation of predicted SMD against measured SMD

2.3.2 Rainout effects

Rainout is the mass of liquid release that is lost from the airborne mass due to droplet impact on the ground. The droplets' size is very influential on the overall rainout. In general, small droplets, typically with SMD <20 μm, will never rainout for most realistic scenarios, by evaporating before landing or carried along the jet.

ADAM models the rainout in two separate steps:

1. The mass fraction of a single droplet reaching the ground after release is estimated by taking into account the motion equation of the droplet, combined with the evaporation process and the related mass flux from the droplet surface to ambient air (i.e. single droplet rainout).
2. Since the droplets formed after the release have not all the same initial size but they follow a distribution with an initial mean value equal to the Sauter Mean Diameter (SMD), the overall rainout is calculated by assuming a certain distribution for the droplets around the SMD value. Two alternative distributions are implemented in ADAM and can be selected in the option menu:

Log-normal distribution*	$p(d) = \frac{1}{\sqrt{2\,\pi}\; d\; ln(\sigma_G)} exp\left\{-.5\left[\frac{ln\left(\frac{d}{SMD}\right)}{ln(\sigma_G)}\right]^2\right\}$
Rosin-Rammler distribution	$\frac{p(d) = a_{RR} b_{RR} \left(\frac{d}{\mathrm{SMD}}\right)^{b_{RR}-1} \exp\left[-a_{RR}\left(\frac{d}{\mathrm{SMD}}\right)^{b_{RR}}\right]}{\mathrm{SMD}}$

**Recommended distribution*

The benchmarking was conducted by comparing the ADAM rainout predictions with the experimental results obtained by the Center for Chemical Process Safety (CCPS) (a Directorate of American Institute of Chemical Engineers), which consisted of a pilot study executed from 1989 to 1991 into two phases and on several substances, i.e., water, trichlorofluoromethane (CFC-11), methylamine, chlorine, cyclohexane (Johnson, 1999).

The ADAM rainout calculations were conducted by using the modified CCPS correlation for the droplet size estimate combined with the different droplets distributions, which can be selected in ADAM in the option menu. The selected droplet correlations was because it seems providing better results on the rainout estimate (Witlox, 2013).

The results of the comparison of these calculations with the CCPS experimental data are depicted in Figure 12-Figure 17, which refer to the different involved substances. The different curves within each figure represent the results obtained by using the different droplet distributions: the purple solid line was obtained by using the log normal distribution with geometric spread equal to 1.4 *(Woodward, 2014),* the green solid line refers to the Rosin-Rammler distribution with parameters calculated (Kay, 2010), whilst the red solid line represents the Rosin-Rammler distribution with fixed parameters as suggested by Elktob (Elkotb, 1982). For comparison, the rainout prediction with the simpler correlation that do not require the full calculation of droplets size is also reported (Lautkaski, 2008), and it is represented by the solid blue line.

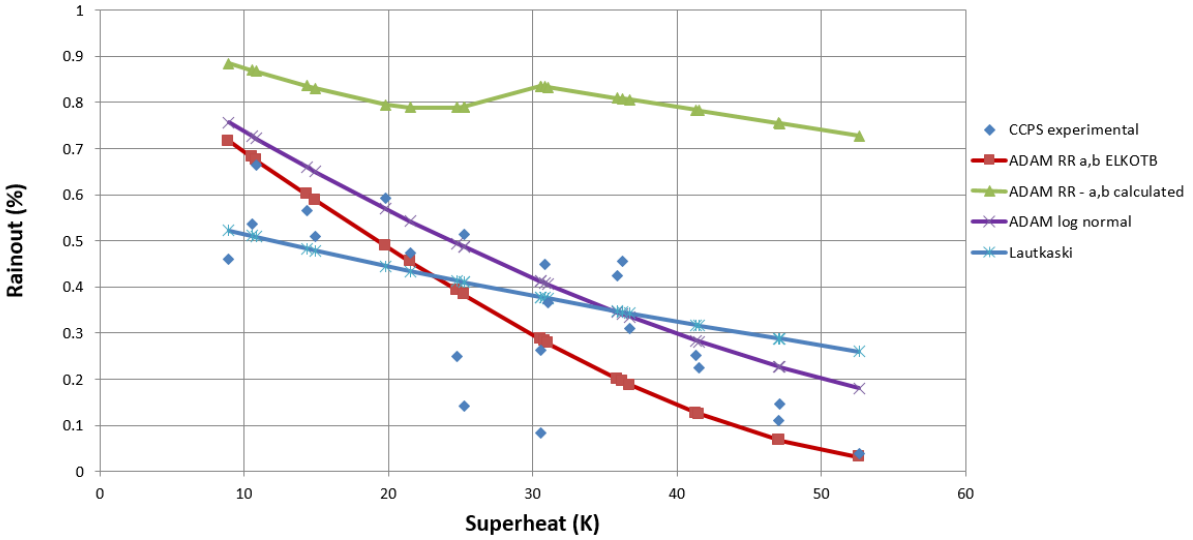

Figure 13: Comparison of the different rainout models implemented in ADAM with rainout CCPS data for Chlorine

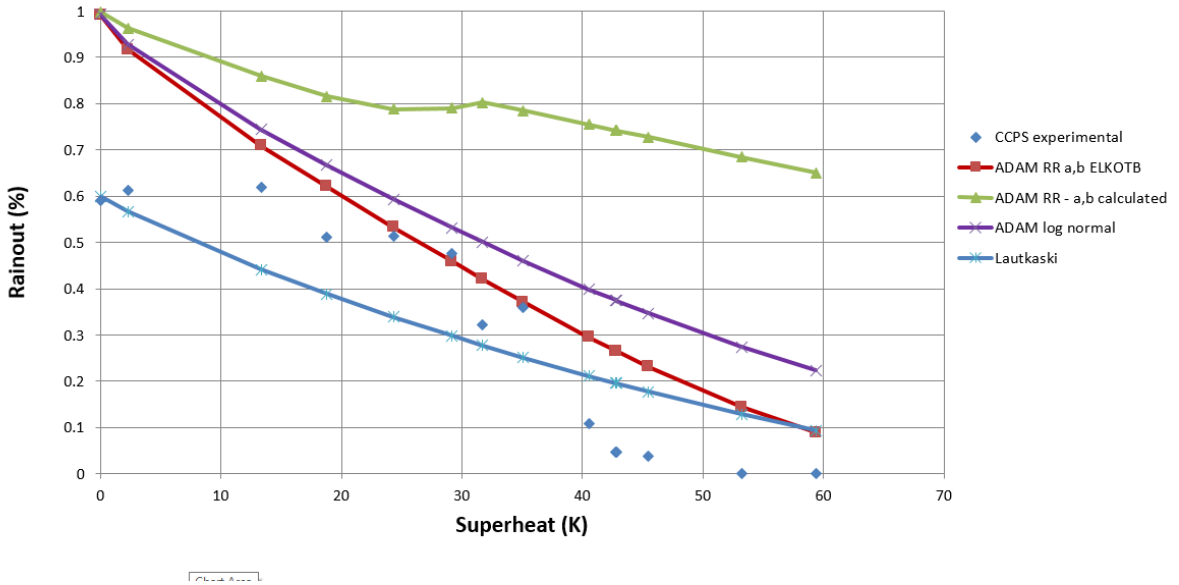

Figure 14: Comparison of the different rainout models implemented in ADAM with rainout CCPS data for CFC11

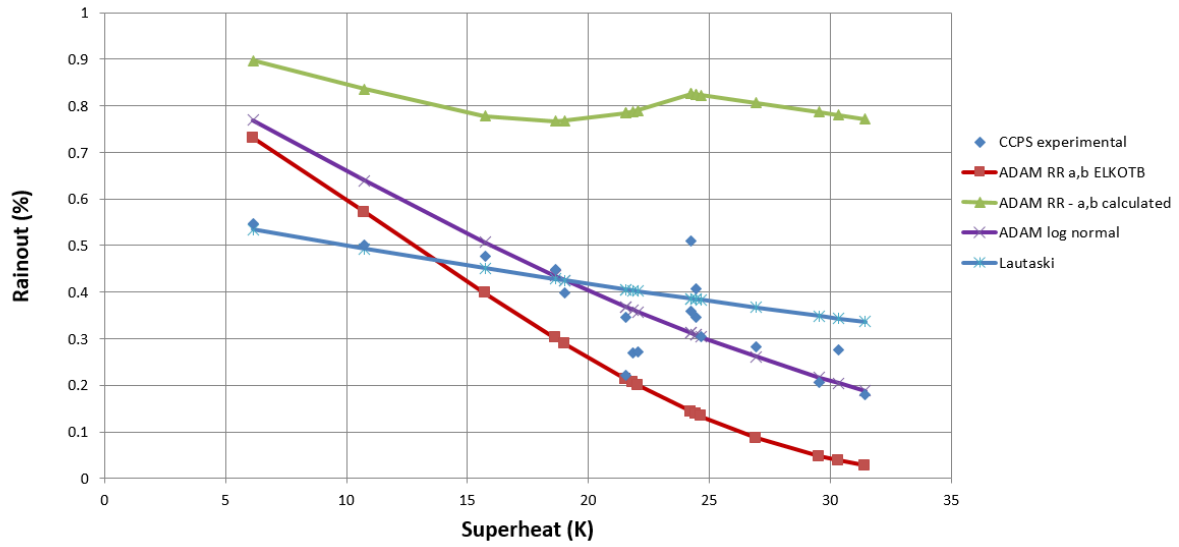

Figure 15: Comparison of the different rainout models implemented in ADAM with rainout CCPS data for Methylamine

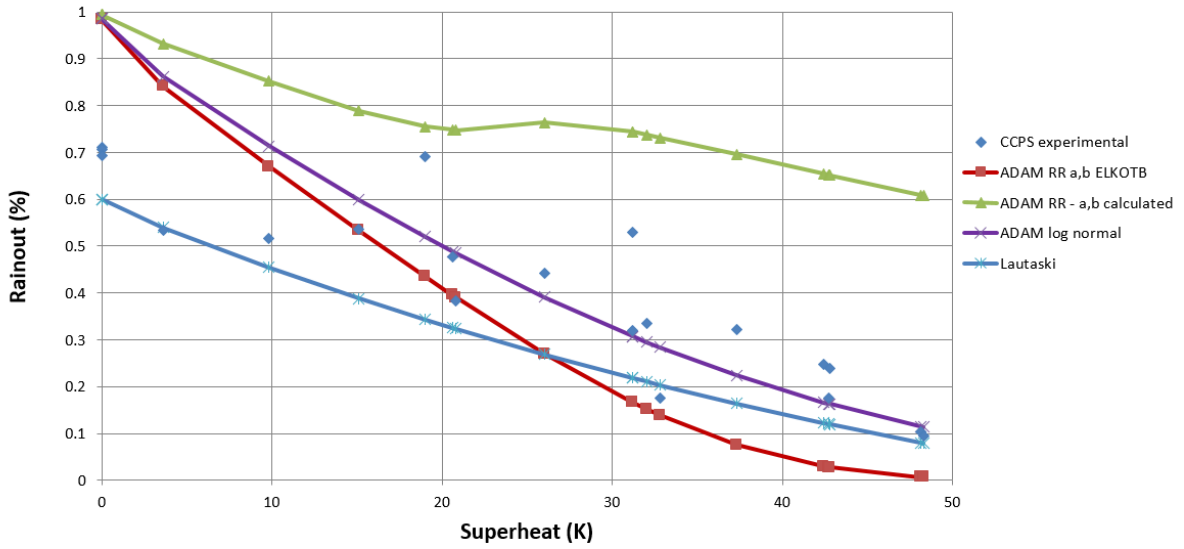

Figure 16: Comparison of the different rainout models implemented in ADAM with rainout CCPS data for Cyclohexane

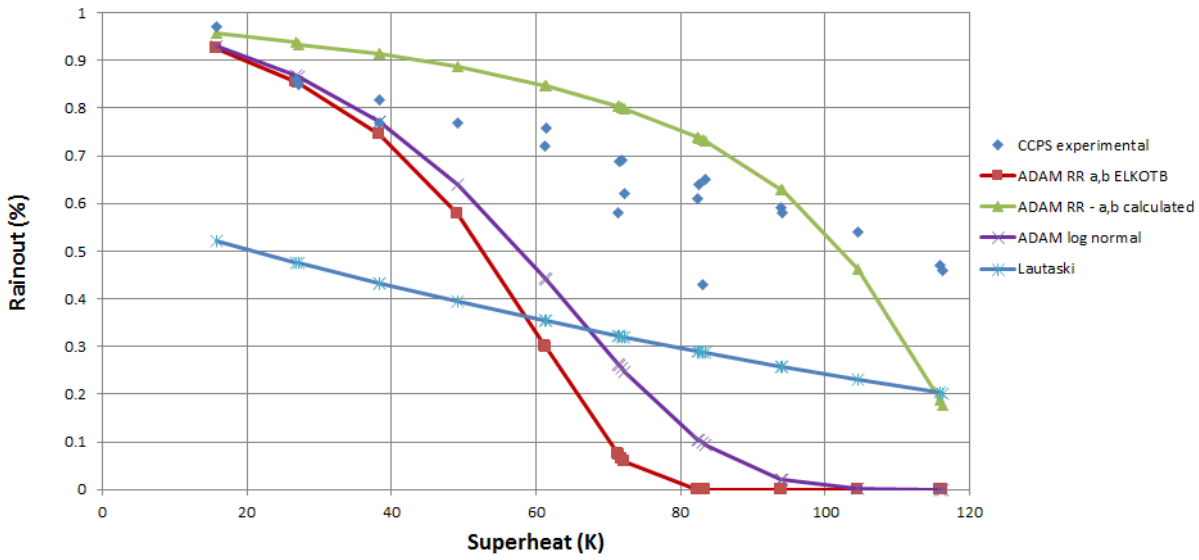

Figure 17: Comparison of the different rainout models implemented in ADAM with rainout CCPS data for water

In order to compare how the different distributions behave, the performance measures to the overall set of measurement/simulation combinations were calculated. The result is given in the table hereunder, which shows that the log normal distribution is definitely the better performing (higher FAC2 lower FB and MMSE, overall). For this reason, this distribution is used in ADAM as the recommended droplet distribution for rainout estimate, and is taken as the default distribution. To visualise the different performance behaviours, the Geometric Variance VG is reported in Figure 18 as a function of the geometrical mean bias MG. A model that "perfectly" reproduces the experimental trials would be placed at the (1,1) point. A model that is characterised by mean bias different from zero and zero random scatter would be placed somewhere along the parabolic line. Thus, this parabola represents the minimum possible value of the geometric variance (VG) for a certain value of the geometrical mean bias (MG). 95% confidence intervals on MG as calculated using the Bootstrap technique are indicated by the horizontal lines, these allow establishing whether the differences amongst the different points are significant, as it is in the present case.

Finally, the data used to calculate the performance measures for the log normal distribution are shown in Figure 19, where the predicted and measured values of rainout of the different trials are graphically compared.

Table 3: Performance measures for rainout modelling. Comparison amongst the different distributions.

FB	MG	NMSE	VG	P	FAC2
Log-Normal distribution*					
0.05	*1.12*	*0.214*	*1.767*	*0.564*	*0.846*
Rosin-Rammler distribution					
-0.50	0.54	0.375	2.075	0.311	0.638
Rosin-Rammler distribution (Elktob)					
0.269	1.774	0.343	2.788	0.663	0.612

* *default distribution in ADAM*

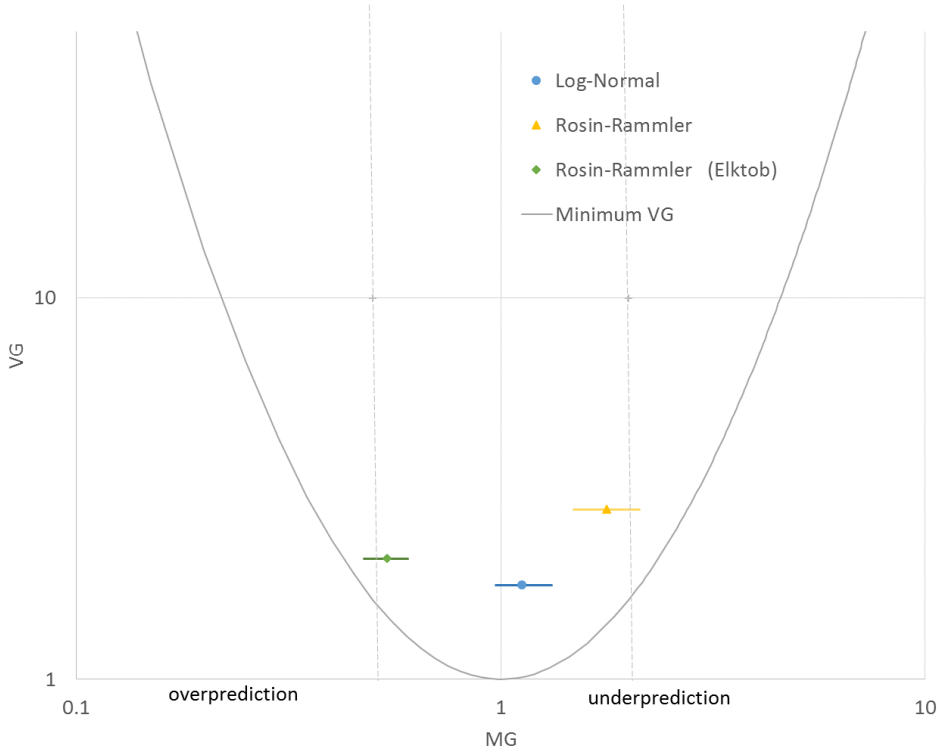

Figure 18: Performance measures (i.e. MG vs VG) for the rainout estimate of the CCPS trials. 95% confidence intervals on MG are indicated by the horizontal lines. The solid parabola represent the 'Minimum VG' curve. The vertical dotted lines represents the 'factor-of-two' between mean predictions and observations

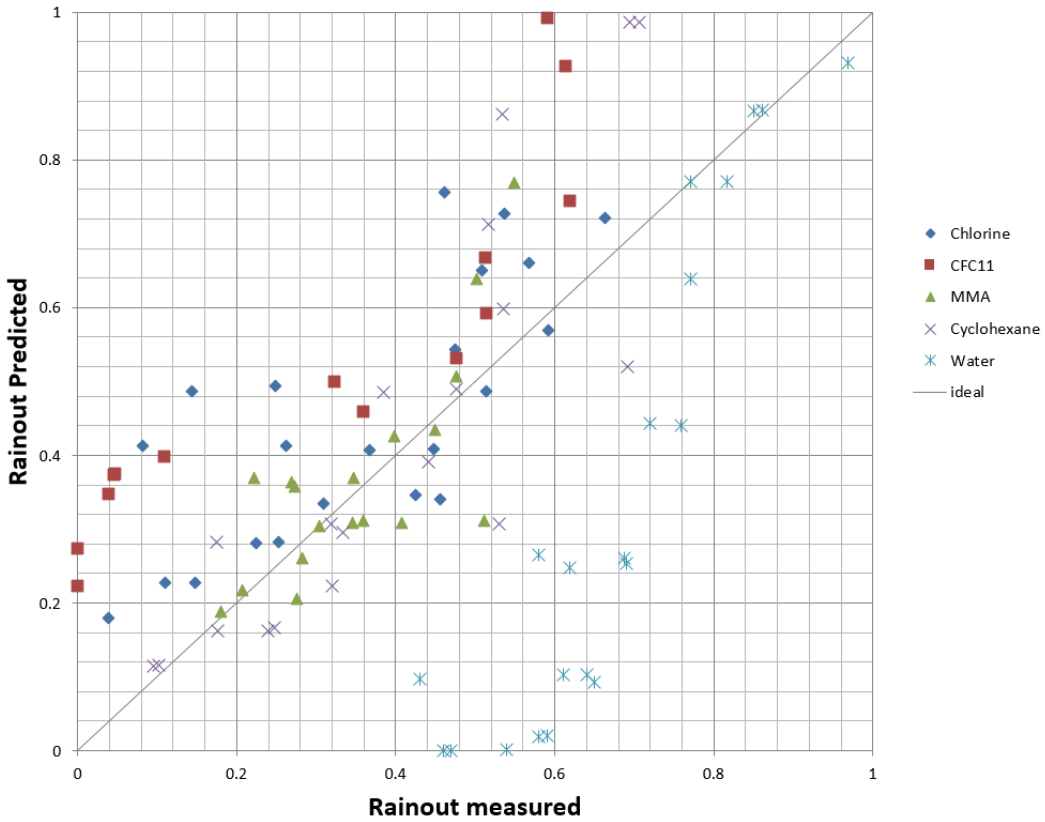

Figure 19: Log normal distribution, scatter plots of predicted vs mesured rainout (%) for the different CCPS trials.

2.4 Release of liquefied pressurized gases from pipe connected to vessel (R6)

The case of release of a superheated fluid from pipe is probably the most complex amongst the different source term scenarios due to the flash occurring within the pipe immediately after the pipe failure. The model implemented by ADAM is the TPDIS model described in Kukkonen, 1990, which is also the recommended method in the Yellow Book.

The validation was conducted by comparing the ADAM results with those obtained in the TRAUMA programme (Wheatley, 1987), and by benchmarking with the results obtained by PHAST on a set of accident scenarios.

2.4.1 TRAUMA programme

The TRAUMA programme was also used by Kukkonen to validate the TPDIS model. The same set of data were also used to verify, the TPDIS implementation in ADAM. The reference scenarios consisted of the discharge of three toxic (i.e., Ammonia, Chlorine and Sulphur Dioxide) and one flammable (i.e. Propane) substances. All the scenarios referred to the full-bore rupture of a pipe connected to a vessel at a length L from the pipe inlet. The calculations were conducted by assuming absence of losses and friction (i.e. ε=0) within the pipe, with the main parameters summarised in the table below:

case	***Substance***	***Vessel***		***Pipe structure***	
		Storage T (C)	Storage P (bar)	L(m)	D(mm)
1	Ammonia	15	7.27	3.32	70
2	Ammonia	15	7.27	3.32	100
3	Chlorine	15	5.79	2.25	40
4	Sulphur Dioxide	15	2.76	2.50	100
5	Propane	15	7.26	1.72	70

The results of ADAM are given in Figure 20, where the discharge flow rate vs the flow rate calculated by TRAUMA is reported. For comparison, the results obtained by using EFFECTS 9.0 and PHAST 6.54 are also given. By considered the TRAUMA data as the reference values, the corresponding quantitative performance measures were calculated as reported in Table 4, which shows the good match of ADAM with the reference simulation (i.e. TRAUMA). Overall ADAM, together the TPDIS model of Kukkonen, PHAST and EFFECTS, tend slightly to over-predict the flow rate if compared to TRAUMA (i.e. FB < 0) but with a very low normalized mean square error (NMSE), which shows the very limited scatter about the reference value. The different performance behaviour is also shown in Figure 21, which depicts the normalised mean square error NMSE vs the fractional bias FB, which is given with its 95% confidence intervals as calculated by using the Bootstrap technique. A model perfectly reproducing the results of TRAUMA would be placed at the (0,0) point.

Table 4: Performance measures to evaluate the R6 case. Comparison between different tools.

	FB	**MG**	**NMSE**	**VG**	**P**	**FAC2**
ADAM	***-0.120***	*0.900*	*0.021*	*1.013*	*0.999*	*1.000*
KUKKONEN	**-0.128**	0.881	0.021	1.016	0.999	1.000
PHAST 6.54	**-0.139**	0.847	0.044	1.045	0.920	1.000
EFFECTS 9.0	**-0.383**	0.688	0.192	1.153	0.997	1.000

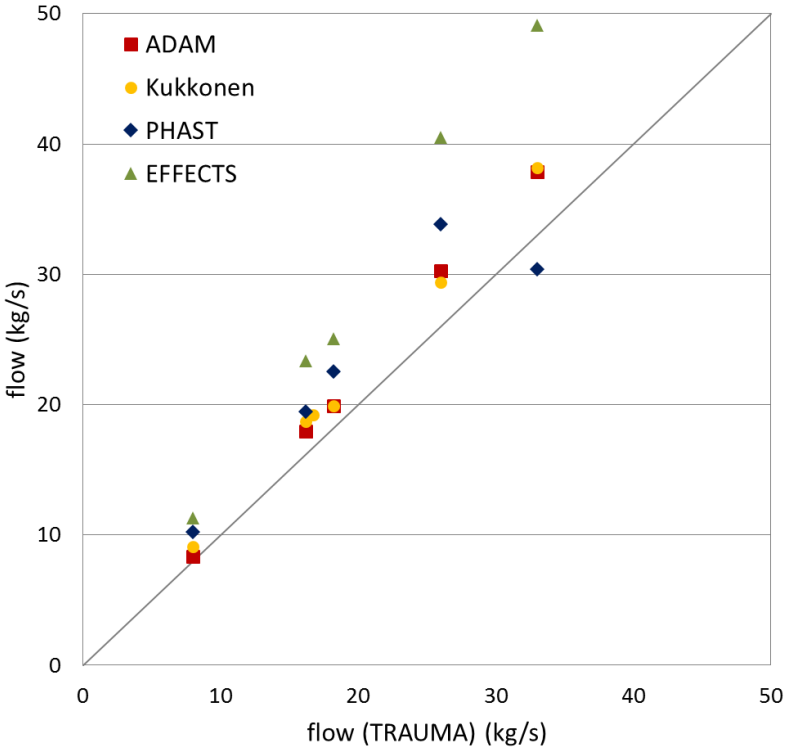

Figure 20: Flow rates for the cases of the TRAUMA programme. Calculated vs reference TRAUMA values.

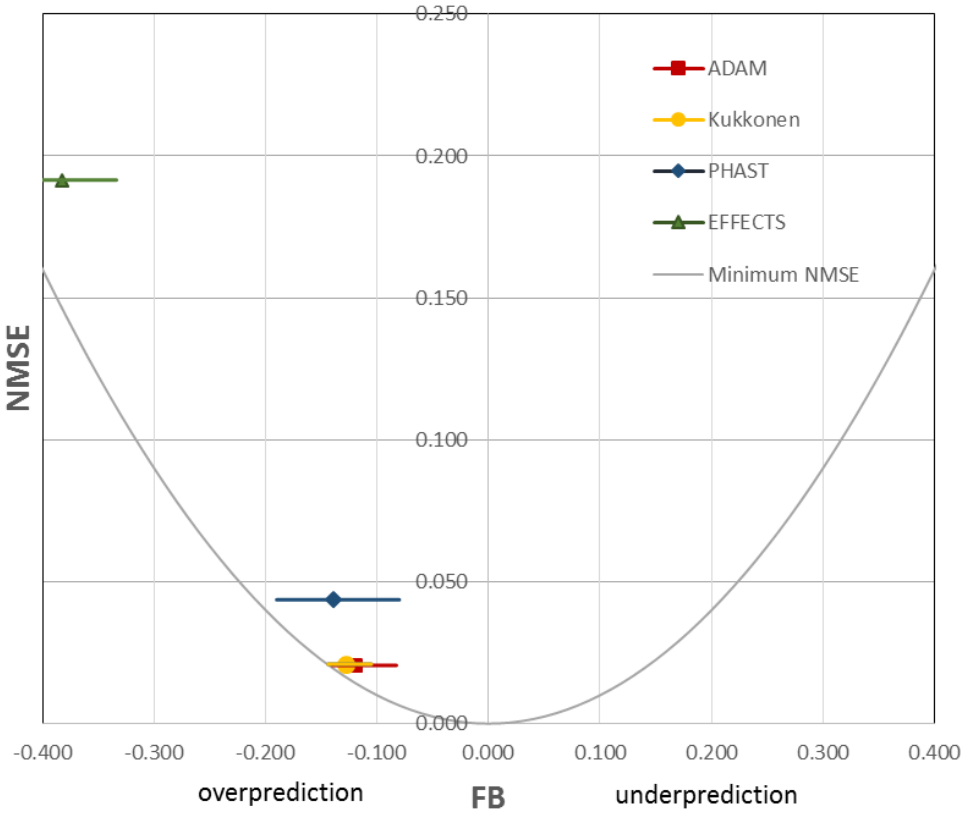

Figure 21: Performance measures (i.e. FB vs NMSE) by using the TRAUMA simulation as the reference values. The 95% confidence intervals on FB are indicated by the horizontal lines. The solid parabola represents the 'Minimum NMSE' curve.

2.4.2 Benchmarking with PHAST

Two sets of reference scenarios were taken from Kukkonen, 2010, which are summarised hereunder:

1. Release from the full-bore rupture of a pipe connected to a vessel at a distance of L = 2m from the pipe inlet. Pipe roughness ε = 0.05 mm, Pipe diameter D = 40 mm. Substances in the vessel: Chlorine, Propane, Ammonia, Sulphur dioxide, Hydrogen fluoride. Storage Temperature in the vessel from -30 to 30 Celsius degrees. Storage Pressure at saturation conditions. (case of fig. 4.2. in Kukkonen, 2010).
2. Release from the full-bore rupture of a pipe connected to a vessel at variable distances from the pipe inlet. Pipe roughness ε = 0.05 mm, variable Pipe diameters (i.e. D = 40 mm and D = 20 mm). Substance in the vessel: Chlorine. Storage Temperature in the vessel 15 Celsius degrees. Storage Pressure at saturation conditions. (case of fig 4.3. in Kukkonen, 2010).

Differently from the case of Kukkonen, where in order to account of the pipe inlet losses a coefficient of contraction of Cd = 0.5 was assumed, the calculation herewith presented was conducted by assuming no losses, as this was not possible to model explicitly with PHAST 5.64.

The comparison of ADAM with PHAST for these two series is depicted in Figure 22 Figure 23, respectively, with a very good agreement for both cases.

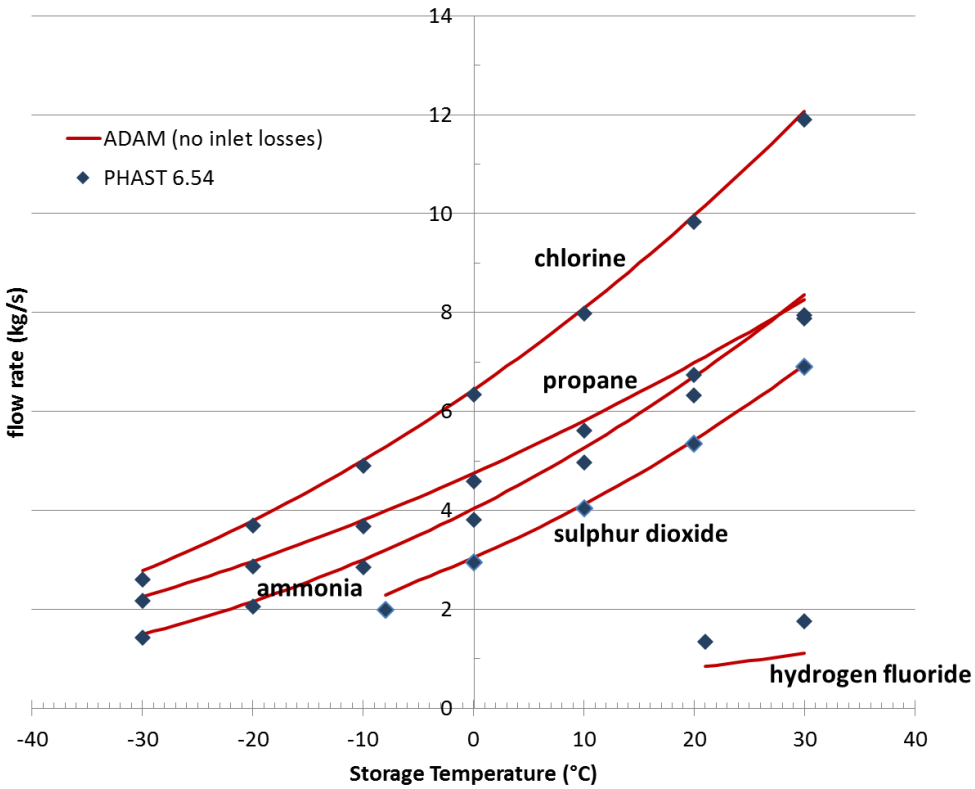

Figure 22: Comparison between ADAM and PHAST on different substances stored at different temperatures and at saturated pressure. Flow rate vs storage temperature (pipe diameter D = 40mm, pipe roughness ε = 0.05 mm, no losses in pipe, pipe length at rupture L = 2m).

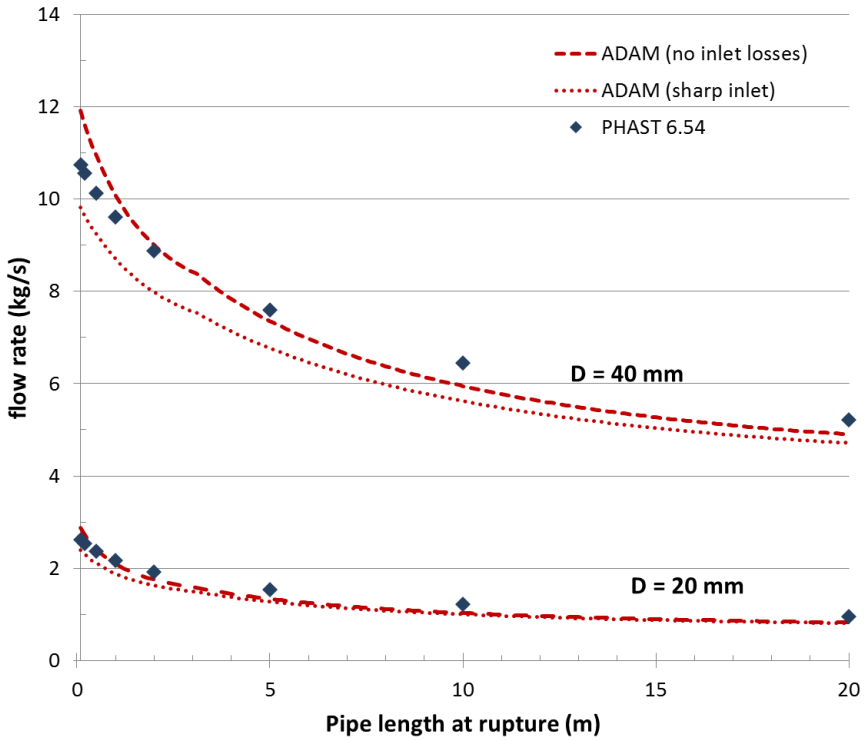

Figure 23: Comparison between ADAM and PHAST on the release from pipe brake from vessel containing chlorine. Flow rate vs pipe length at rupture for two pipe diameters (i.e. 20 mm and 40 mm). Pipe roughness ε = 0.05 mm, no losses inside pipe. For ADAM two cases were considered: no losses at pipe inlet and losses due to a sharp inlet.

2.5 Catastrophic releases

In the case of catastrophic failure of a vessel, the whole content of the dangerous substance is released into the atmosphere. In the case of the release of a pure liquid, the calculus of the source term is rather trivial, since all the stored material will take part in the pool formation. By contrast, in the case of a compressed or liquefied-pressurised gas, the flashing after release might result in the formation of a two-phase material, with droplet formation and rainout. The post-expansion parameters of the released substance (i.e. flash temperature, expansion velocity, and vapour quality) have to be assessed as the serve as an input for the physical effect modules.

The following sections provide a comparison of the post expansion parameters calculated by ADAM and PHAST 6.54.

2.5.1 Release of a compressed gas from vessel (CR1)

The two reference cases are the catastrophic rupture of a vessel containing ethylene and hydrogen, with the following input parameters:

Input Parameter	*Case 1*	*Case 2*
Substance	Ethylene	Hydrogen
Storage temperature	290 K	288.15
Storage absolute pressure	1.5-50 bara	1.5-50 bara
Vessel Volume	50 m^3	1 m^3

The results of the comparison between ADAM and PHAST is given in Figure 24 and Figure 25, which refer to the ethylene and hydrogen cases, respectively. In the first case, the calculus of the expansion velocity was conducted without limiting its maximum value. PHAST uses a rather arbitrary value of 500 m/s to account of turbulence effects, which in the present case did not intervene because the estimated values were below this threshold. In the second case, due to the specific nature of hydrogen, the expansion velocity is much higher for the storage pressures under consideration. Thus, it was decided to limit this value by using the sonic velocity as capping method (this can be selected in both the option menu of ADAM and PHAST.

For both cases, all post-expansion parameters are in a very good agreement for the two tools. In the second case, the vapour quality x_e of the expanded gas was not reported, since, as expected, there was no condensation (i.e. $x_e = 1$).

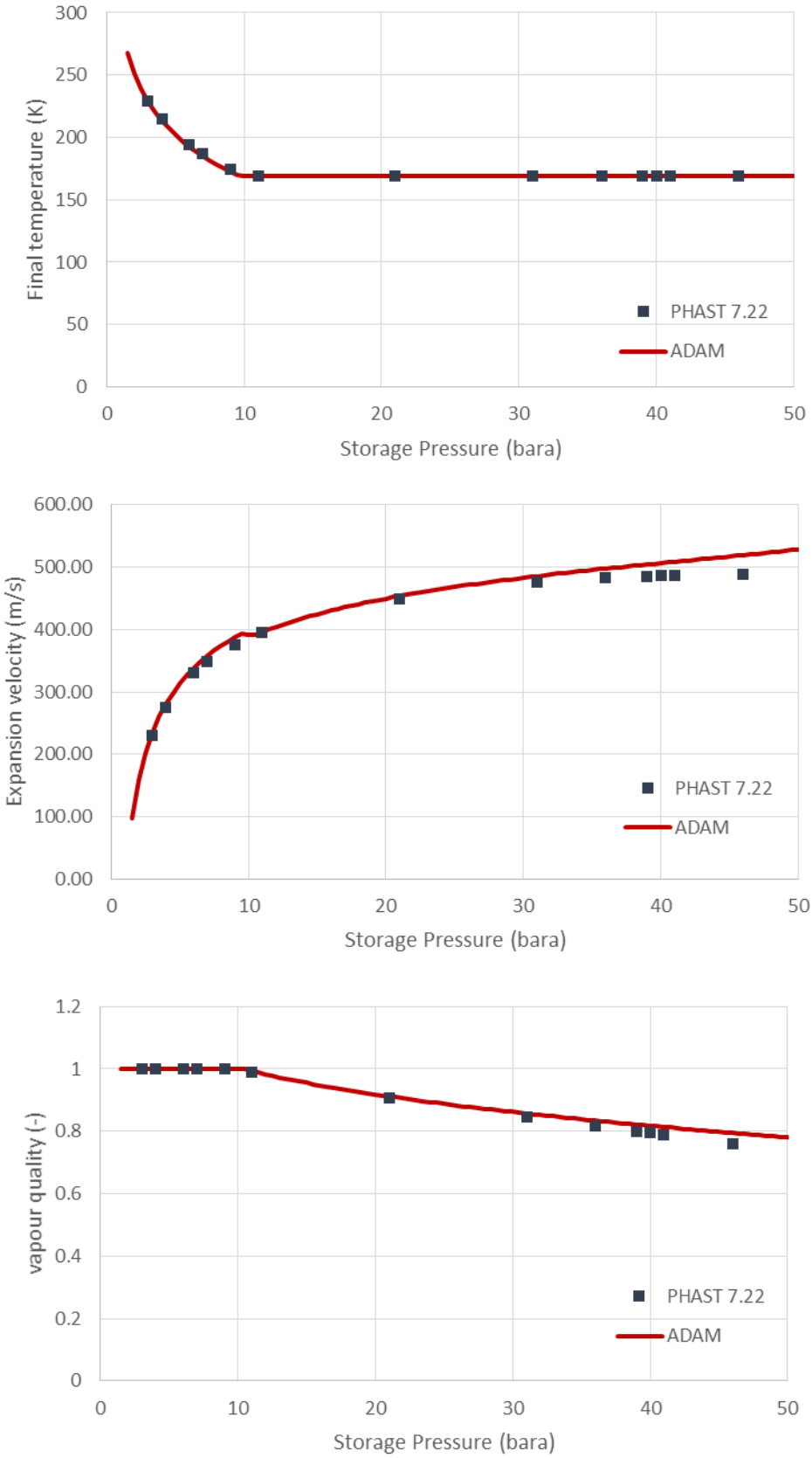

Figure 24: Case 1 (Ethylene). Post expansion parameters vs absolute storage pressure: a) Flash Temperature, b) Expansion velocity, and c) Vapour quality.

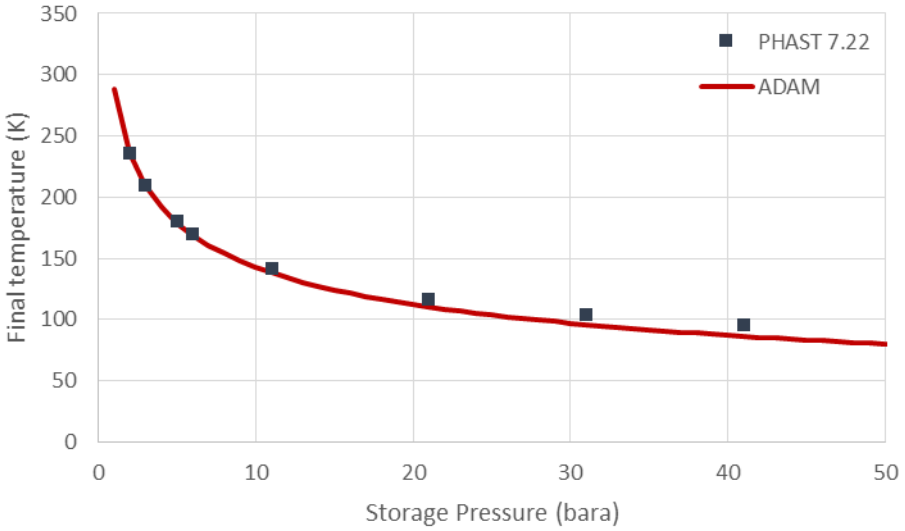

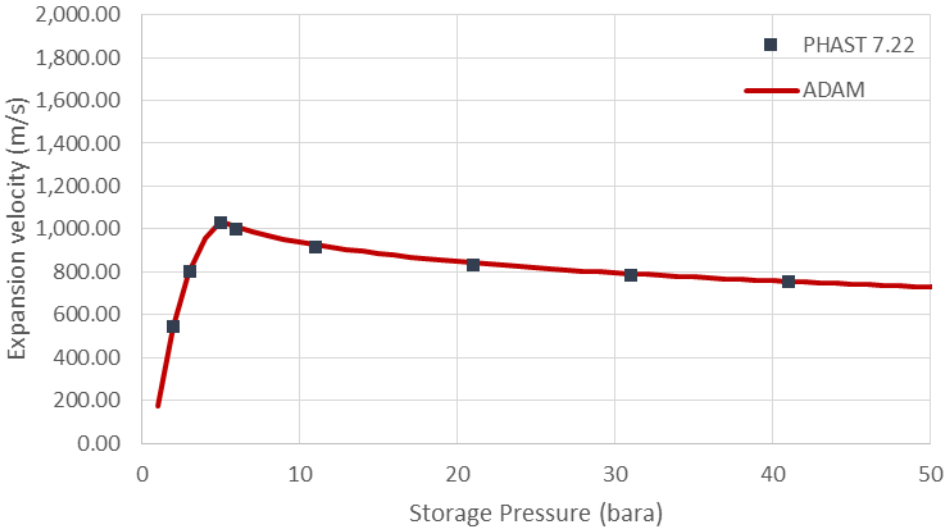

Figure 25: Case 2 (Hydrogen). Post expansion parameters vs absolute storage pressure: a) Flash Temperature, b) Expansion velocity.

2.5.2 Release of a liquefied pressurised gas (superheated) from vessel (CR3)

With reference to the catastrophic release of a vessel containing a superheated gas (i.e. CR3), three cases involving propane, chlorine and ammonia, were considered. The input parameters are reported below, with the pressurised gases at saturated conditions and variable storage temperatures in a quite broad range.

Input Parameter	*Case 1*	*Case 2*	*Case 3*
Substance	Propane	Chlorine	Ammonia
Storage temperature	*variable*		
Storage absolute pressure	*at saturated conditions*		
Vessel Volume	10 m^3	1 m^3	73 m^3

The results for these three cases are reported in Figure 26, Figure 27, and Figure 28, respectively. All post expansion parameters under investigation are reported as a function of the storage temperature in a quite broad range (i.e. 240-350 K). Storage pressure is always considered at saturation.

In general, the agreement is rather good in all cases, with a slighter discrepancy on the estimate of the droplets' size, which tends to deviate especially for intermediate values of the storage temperature.

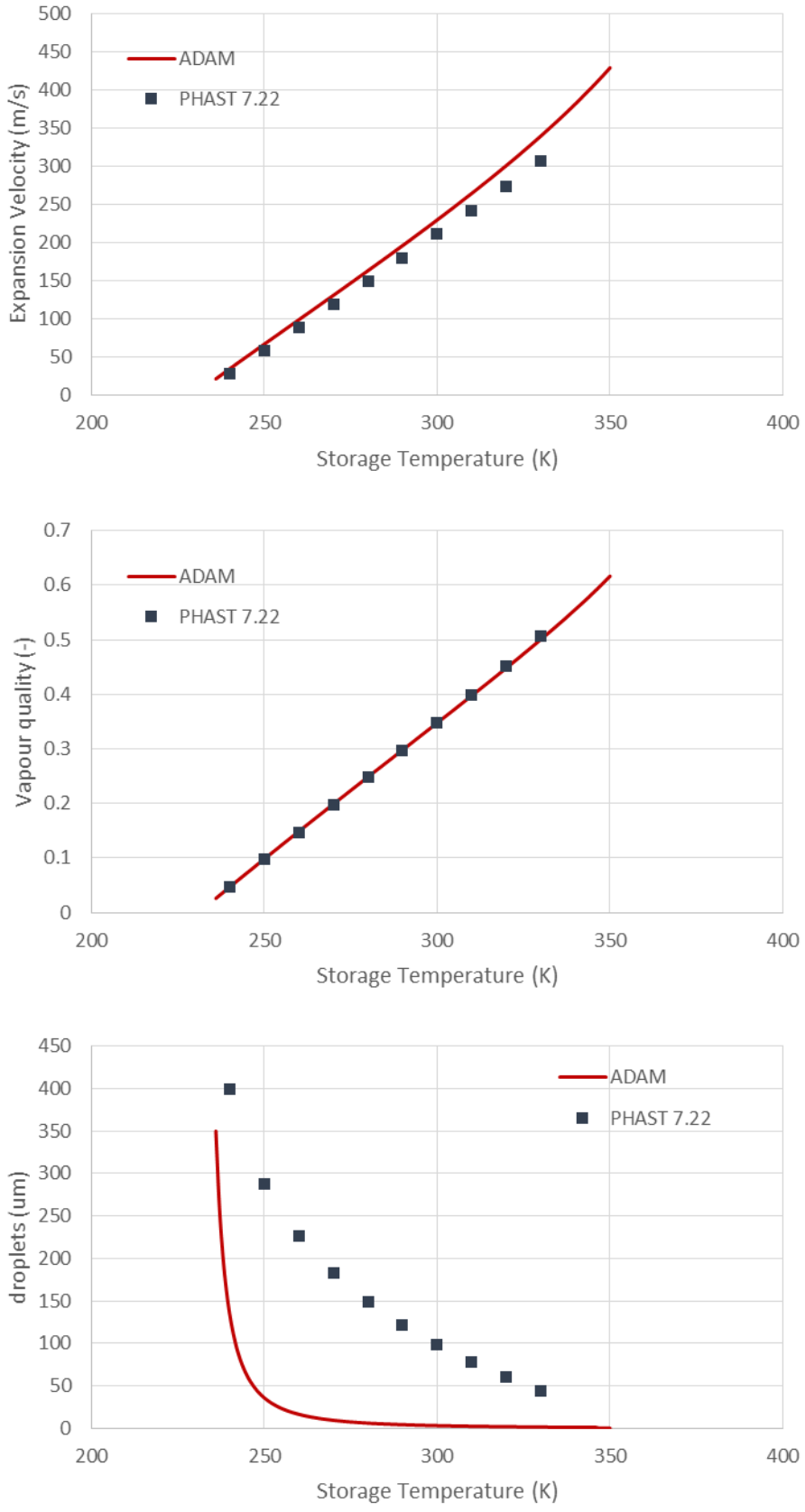

Figure 26: Case 1 (Propane). Post expansion parameters vs absolute storage temperature: a) Expansion velocity, b) Vapour quality, and c) droplets' size.

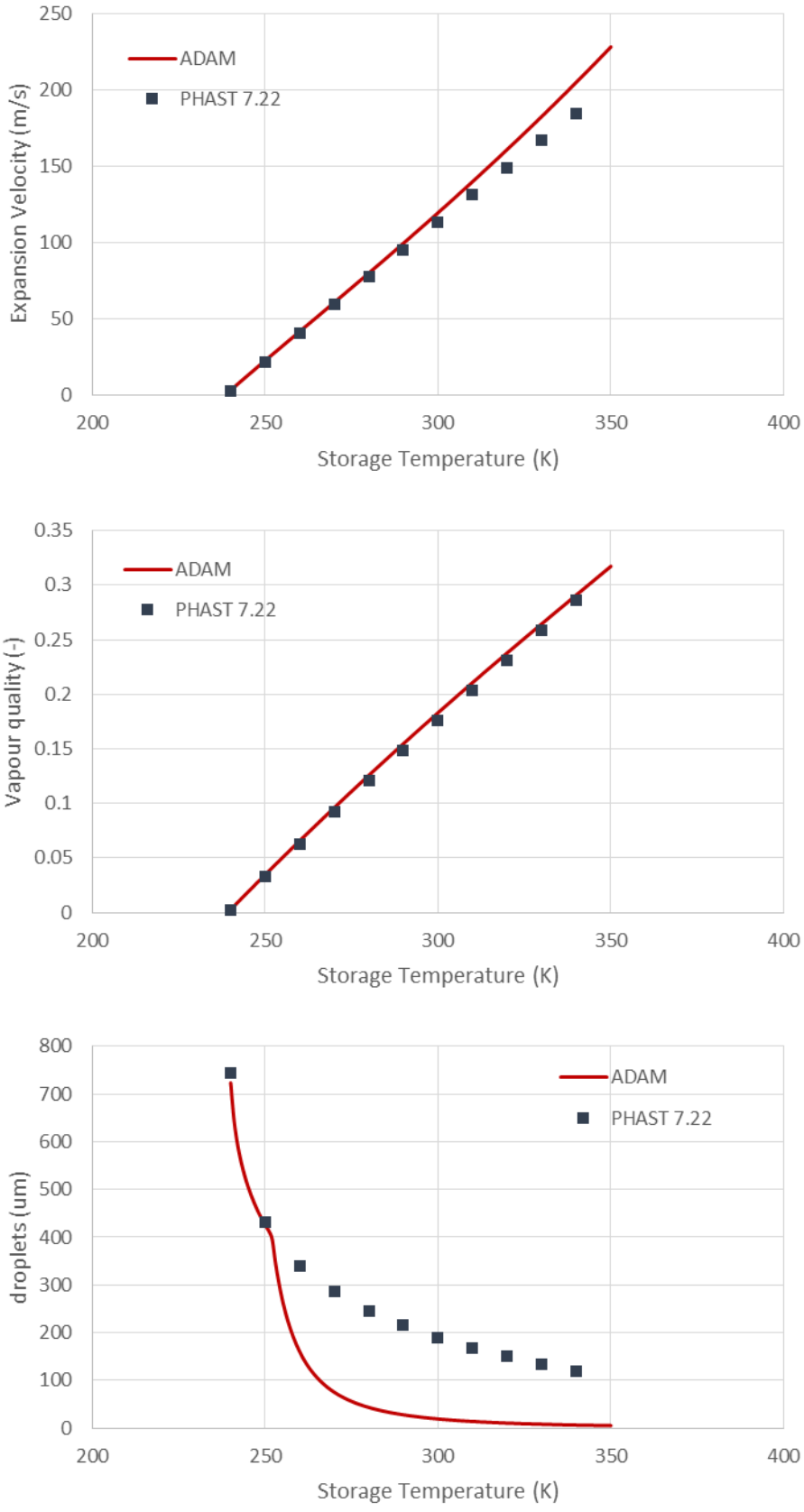

Figure 27: Case 2 (Chlorine). Post expansion parameters vs absolute storage temperature: a) Expansion velocity, b) Vapour quality, and c) droplets' size.

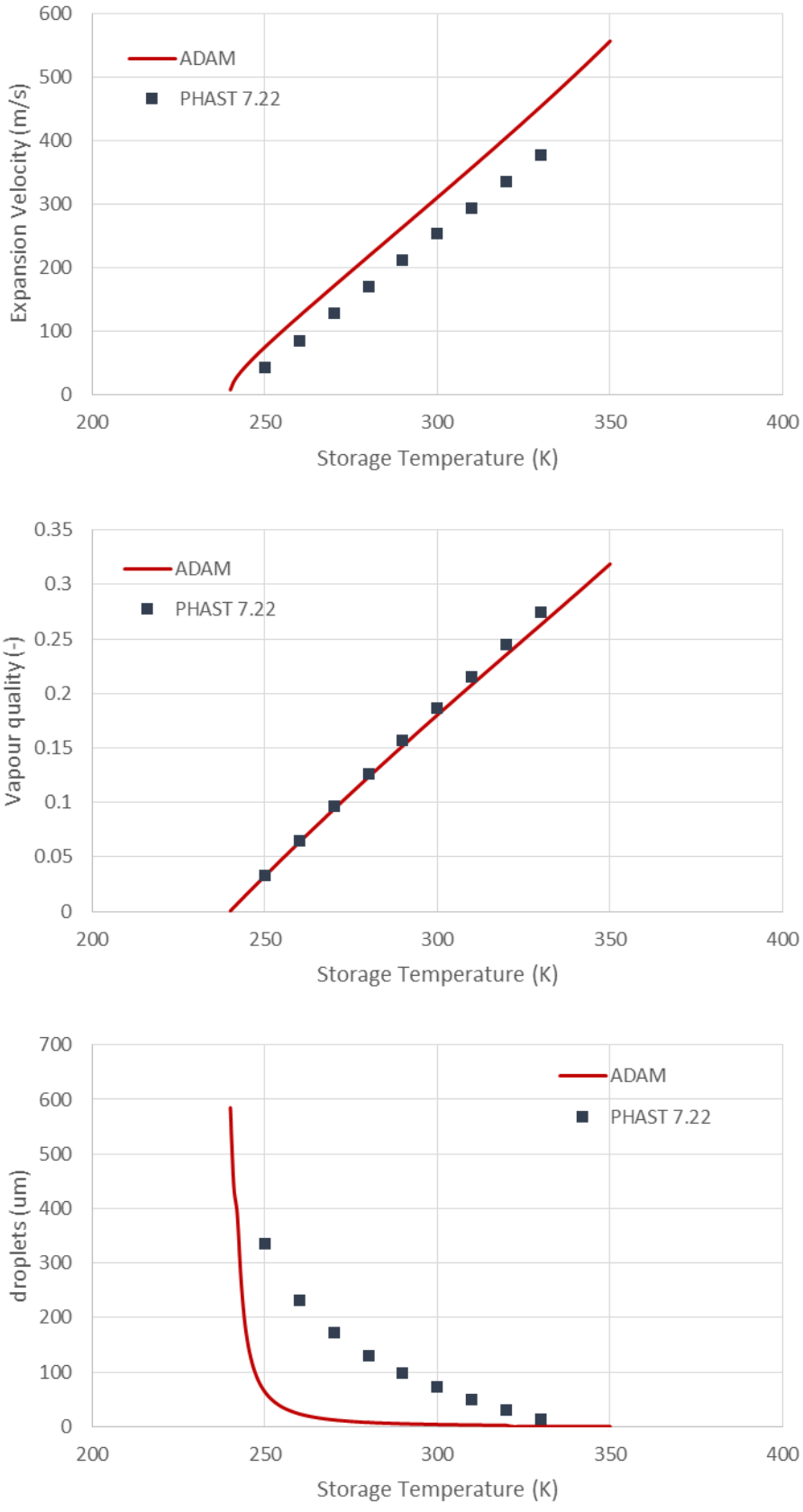

Figure 28: Case 3 (Ammonia). Post expansion parameters vs absolute storage temperature: a) Expansion velocity, b) Vapour quality, and c) droplets' size.

2.6 Pool Spreading and Vaporisation Module

The GASP model, which is the recommended model implemented in ADAM, was already evaluated by its developers (Webber, 1987; Brighthon, 1990; Webber, 1990). As the model and its implementation have a certain level of complexity, a validation was also conducted on the implemented version of ADAM, by using experimental data available from the literature. In general, the evaluation was conducted separately for pool spreading, and vaporisation, by selecting test cases for which one of these two mechanisms is dominant, as described in the following sections.

However, a first verification was conducted by comparing the ADAM results with the pool spreading and vaporisation calculations obtained by the HSE using the original GASP code on Burro 8 trials (Ivings, 2016). Burro 8 trial referred to a continuous release of LNG on water (more details are given in next 3.1.1 section).

This comparison is given in Figure 29 and Figure 30 , which show the pool radius and mass vaporised as a function of time, respectively.

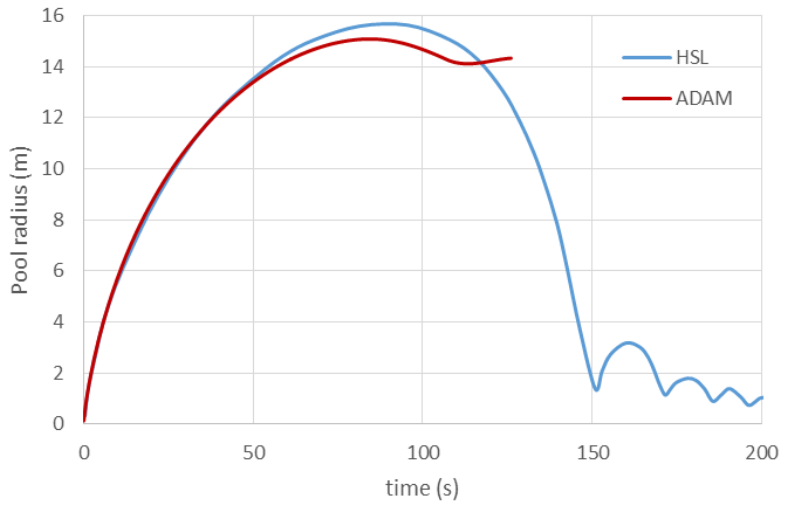

Figure 29: Pool radius vs time for Burro 3 trial, HSL GASP and ADAM GASP calculations.

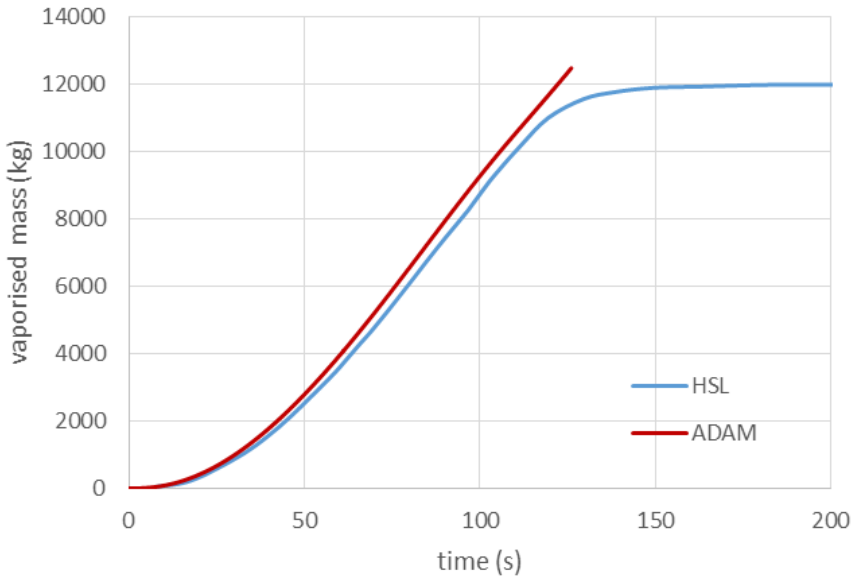

Figure 30: Mass vaporised vs time for Burro 3 trial, HSL GASP and ADAM GASP calculations.

2.6.1 Pool spreading

The pool spreading models implemented in ADAM (i.e. GASP and Raj) were evaluated against experimental data.

For pools spreading on land, the experimental data obtained by Belore and McBean (Belore, 1986) were considered. These referred to the spreading of water due to a continuous discharge over a plywood surface. Due to the very low vaporisation rate, vaporisation is negligible in the considered time frame (i.e. ca. 1 hour), and the process involves pool spreading only. Amongst the different 3D-tests, the ones containing only water were selected (tests containing different solutions with carboxy-methyl-cellulose were excluded because of the absence of related information in the ADAM database. Duration of the release was set as equal to the observation time for each test, since the flow was stopped when the substance reached the test bed, during the experiments. This justifies the assumption of a pure continuous release.

Thermal heat transfer properties for plywood were taken from the www.engineering.com website (i.e. thermal conductivity: 0.12 W/mK, thermal diffusivity: 1.81 10^{-7} m^2/s), whilst the following input parameters where used for the calculations:

Table 5: Belore and McBean tests, input parameters

	Test 28	**Test 29**	**Test 30**
Flow rate (l/min) (Kg/s)	22.04 (0.367)	49.25 (0.8196)	73.1 (1.265)
Storage Temperature (K)	295		
Atm. and ground Temperature (K)	295		
Wind speed at 10m	0.1		
Solar Radiation (W/m^2)	0		

A minimum pool thickness of 5mm was assumed.

The outcome of the simulations of the three tests are reported in Figure 31, Figure 32, and Figure 33, where the different curves were obtained using both models implemented in ADAM i.e., GASP (Webber, 1987; Webber, 1990) and Raj (Raj, 2011). As a comparison, the calculations performed by using PHAST 7.22 were also included. These data practically superimpose the results of ADAM Raj, as expected, since PHAST uses the same formula for pool spreading.

In general, despite of the scatter of experimental data, the results of ADAM GASP are good for both test 28 and test 29, whilst they tend to over-predict the pool radius for test 30. By contrast, ADAM Raj over predicts for all the selected tests. This is in agreements with the deductions of Webber who clearly emphasised that Raj equation rightly "expresses the resistance effect of displaced water, and has absolutely *no* justification for pools spreading on land" (Webber, 2012).

Figure 31: Pool radius vs time for Belore & McBean test 28.

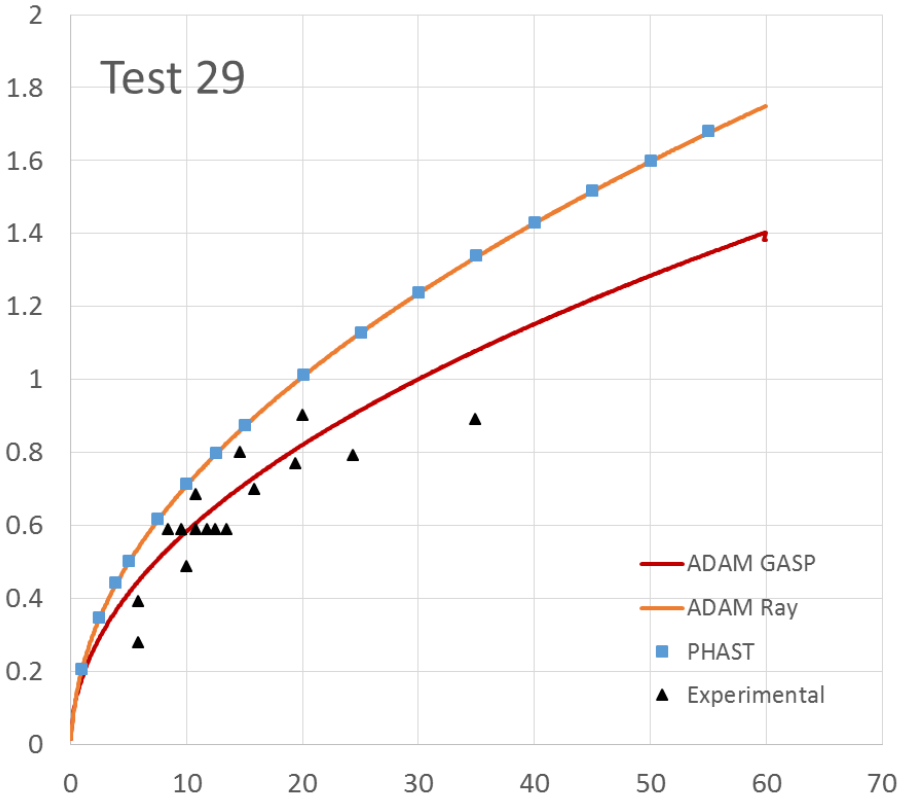

Figure 32: Pool radius vs time for Belore & McBean test 29.

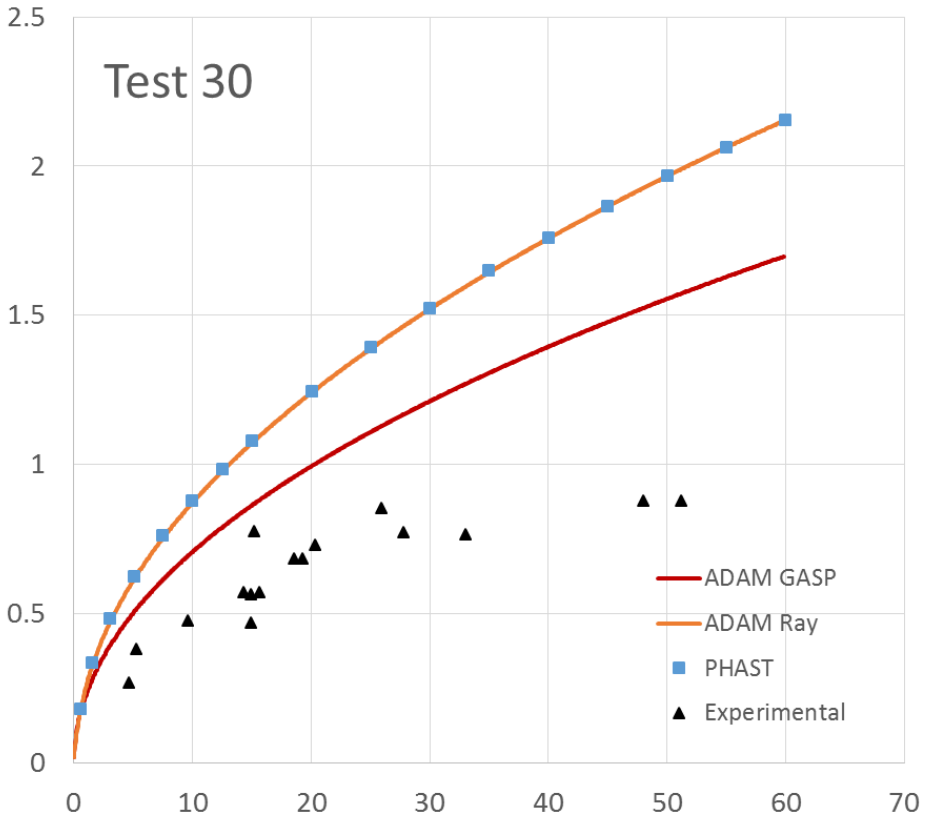

Figure 33: Pool radius vs time for Belore & McBean test 30.

For pools spreading on water, the performance of ADAM was evaluated against the experimental data provided by Dodge et al (Dodge, 1983), which referred to both instantaneous and continuous releases of a series of volatile and non-volatile hydrocarbons.

More specifically, four test series were conducted, with Series I and III involving the instantaneous release different hydrocarbons whilst Series II and IV consisting of continuous spills of different hydrocarbons under different wind conditions.

For the evaluation of ADAM, a number of tests were selected from this report, by picking almost all involved substances, and keeping instantaneous releases with largest amount, and continuous releases with highest and lowest flow rates (i.e. 0.5 and 1.26 liters/s, respectively). The selected cases are reported in Table 6.

The substances spill temperature, the ambient temperature and the water temperature related to each test were not explicitly reported. However, all demonstration cases used for the simulation and described in the Dodge et al. report were set with a single value of for all these three parameters (i.e. 20 Celsius). As such, this was the selected value also for the present simulation.

Solar radiation and air stability was also not reported. Neutral condition was set for all selected tests, with an outdoor solar radiation of 500 W/m^2.

Wind speed was reported only for the releases of volatile substances (i.e. Series III and IV), thus for the other cases (i.e. Series I and II) the lowest wind speed value usable in ADAM was selected (i.e. 0.1 m/s).

Figure 34 and Figure 35 show the comparison between the predicted and experimental radius for tests involving pool spreading following an instantaneous release (i.e. Series I and III). Differently for the case of spreading on land, the Raj model implemented in

ADAM performs slightly better than GASP. This is also noticed in the case of continuous releases (Series II and IV), where the discrepancy between the two models is even more evident. In this case, ADAM GASP tends to systematically under predict the pool radius, whilst ADAM Ray slightly over predict it, as also noticed in Fernandez's PhD thesis, who performed this simulation with the same model (Fernendez, 2013).

Table 6: List of Dodge's at al. tests used for ADAM evaluation.

Test case	**Total Amount (kg)**	**Flow Rate (kg/m^3)**	**Wind speed (m/s)**
Series I (instantaneous)			
I 1-4 n-OCTANE	*28.12*	*n.a.*	*.1*
I 2-4 KEROSENE	*31.80*	*n.a.*	*.1*
I 3-4 n-HEXANOL	*32.76*	*n.a.*	*.1*
I 5.4 m-XYLENE	*34.56*	*n.a.*	*.1*
Series II (continuous)			
II 1-1 n-OCTANE	*n.a.*	*0.3515*	*.1*
II 1-4 n-OCTANE	*n.a.*	*0.8858*	*.1*
II 2-1 KEROSENE	*n.a.*	*0.3975*	*.1*
II 2-4 KEROSENE	*n.a.*	*1.002*	*.1*
Series III (instantaneous)			
III 1-4 n-PENTANE	*25.04*	*n.a.*	*1.83*
III 2-4 HEPTANE	*27.36*	*n.a.*	*1.69*
III 3-4 n-OCTANE	*28.12*	*n.a.*	*1.30*
III 5-4 ETHYL ACETATE	*36.04*	*n.a.*	*1.83*
Series IV (continuous)			
IV 1-4 n-PENTANE	*n.a.*	*0.7888*	*2.62*
IV 2-1 HEPTANE	*n.a.*	*0.3420*	*1.57*
IV 3-4 n-OCTANE	*n.a.*	*0.8858*	*1.24*
IV 5-1 ETHYL ACETATE	*n.a.*	*0.4505*	*0.67*

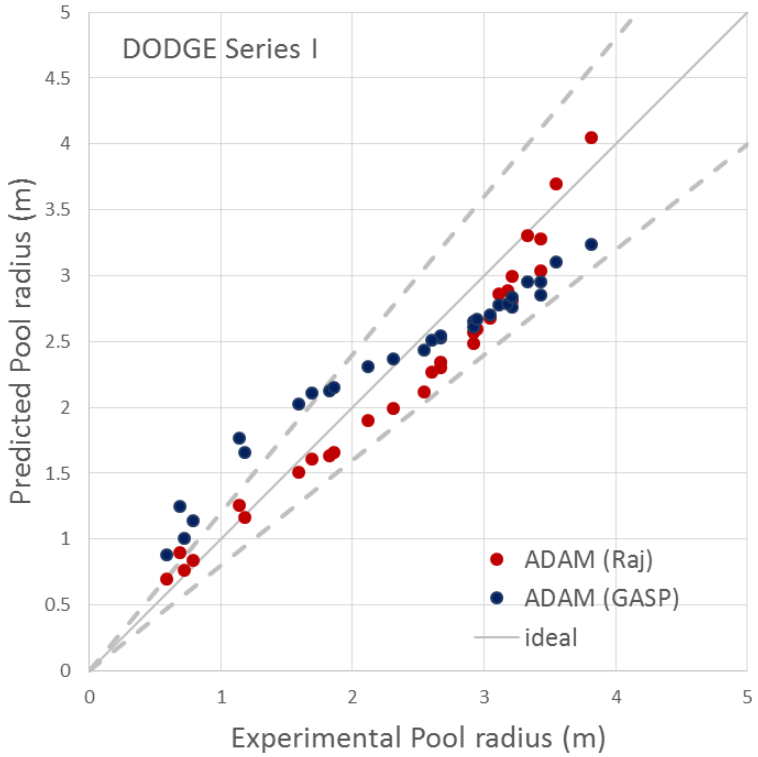

Figure 34: Predicted vs Experimental pool radius for Series for the instantaneous releases (Series I tests, Dodges, 1983). The solid line represents the ideal case whilst the dashed lines represents a ±20% scatter from ideal.

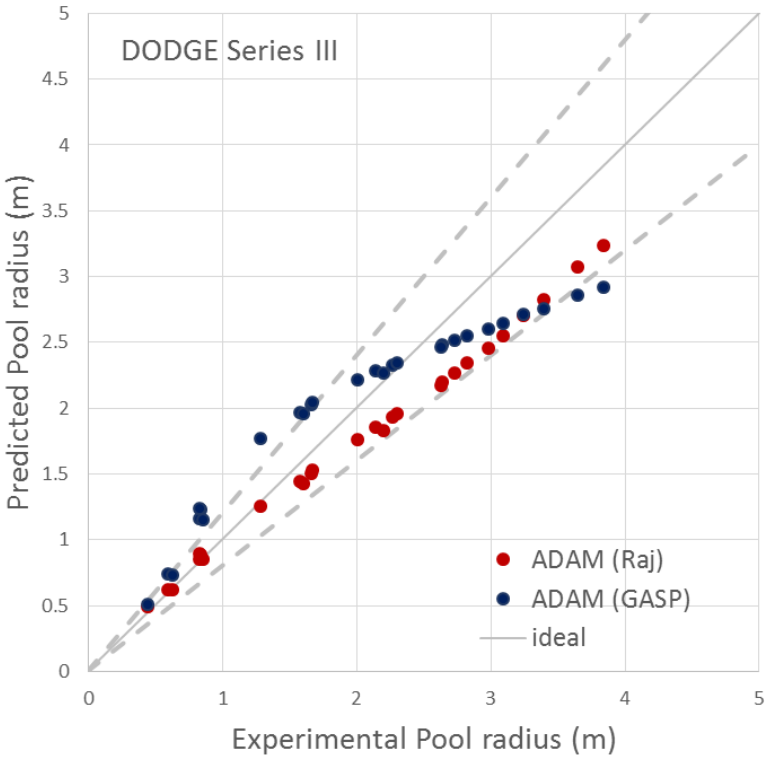

Figure 35: Predicted vs Experimental pool radius for Series for the instantaneous releases (Series III tests, Dodges, 1983). The solid line represents the ideal case whilst the dashed lines represents a ±20% scatter from ideal.

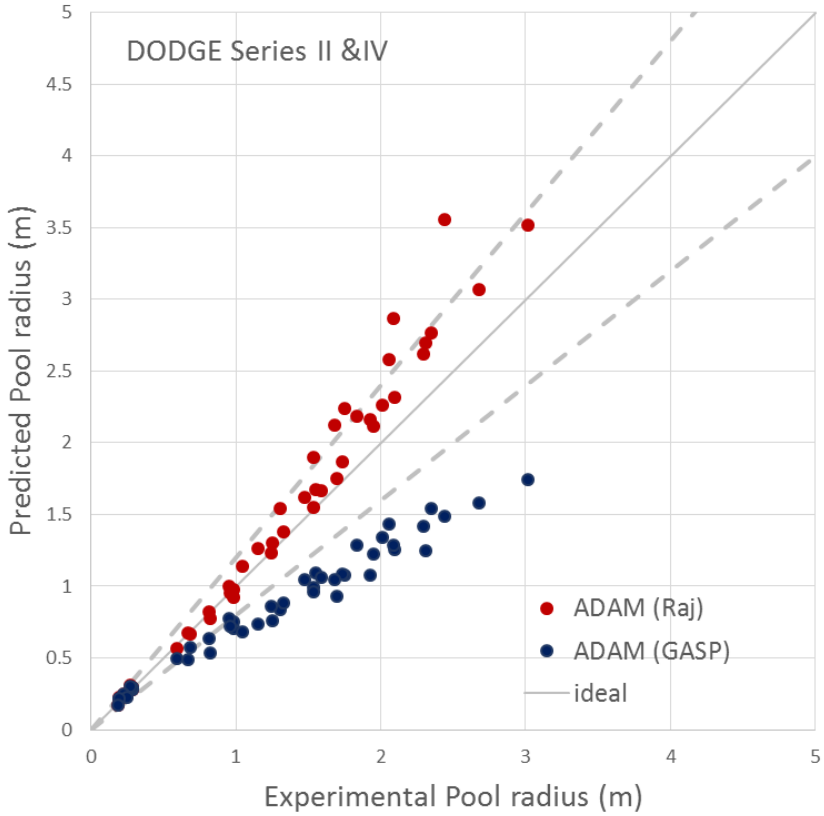

Figure 36: Predicted vs Experimental pool radius for the continuous releases (Series II and IV tests, Dodges, 1983). The solid line represents the ideal case whilst the dashed lines represents a ±20% scatter from ideal.

In order to quantitatively assess the model implemented in ADAM that performs best for poos spreading in water, statistical performance indicators where calculated and reported in Table 7. The data confirm that ADAM Ray performed better for the selected tests, since the performance indicators are significantly different within their 95% confidence interval calculated using the Bootstrap technique.

Table 7: Performance measures on Dodge tests

	FB	**MG**	**NMSE**	**VG**	**P**	**FAC2**
ADAM (GASP)	0.084	1.055	0.056	1.077	0.911	1
95% confidence interval	*0.046*	*0.061*	*0.018*	*0.020*	*0.036*	*0*
ADAM (Raj)	0.050	1.026	0.024	1.016	0.962	1
95% confidence interval	*0.031*	*0.029*	*0.004*	*0.003*	*0.016*	*0*
Ideal model	0	1	0	1	1	1

As a general conclusion of these preliminary tests on pool spreading, within the limits of the ADAM implementation, the GASP model is recommended for pool spreading on land whilst the Raj model is recommended in case of spreading on water.

2.6.2 Pool Vaporisation

The pool vaporisation models implemented in ADAM (i.e. GASP and Mackay & Matsugu) were evaluated against experimental data. The selected cases referred to releases in bund, in which the spreading mechanism has no relevance (i.e. with a complete pool formation occurring in fractions of second. This allowed isolating the processes involving heat exchange and vaporisation from pool spreading.

For pools on land, the experimental tests carried out by Kawamura and Mackay were used for this evaluation (Kawamura, 1987). These consisted of experiments on seven instantaneous releases of volatile substances from a circular pan of inner diameter equal to 0.46m. The presence of the containment allowed the complete formation in fractions of second, which makes the evaporation mechanism independent of the pool spreading.

The series of tests and the input data used for the simulation are given in Table 8.

Table 8: Kawamura and Mackay, input parameters

	Test 18	**Test 19**	**Test 20**	**Test 21**	**Test 22**	**Test 23**
Substance	Toluene	Hexane	Cyclohexane	n-Pentane	n-Pentane	Freon 11
Released mass (kg)	3.44	3.08	2.61	4.36	2.48	10.35
Air Temperature (K)	298.15	302.15	300.15	296.15	298.15	304.15
Solar radiation (W/m^2)	872	894	728	647	861	853
Wind speed at 10m (m/s)*	2.65	3.14	1.59	4.94	5.42	1.17
Simulation duration (h)	3.5	1.67	1.5	1.07	0.58	1.5

*wind speed data collected from Nawaz, 2014 and Fernandez, 2013

Spill temperature and ground temperature were not explicitly reported by the authors of the tests. Thus, they were supposed to be in equilibrium with air temperature, with the exception of Test 23, since air temperature was above the substance normal boiling point (i.e. 269.76 K). In this case, therefore, spill temperature was set as just below this value. Wet sand terrain was assumed, with thermal conductivity and diffusivity as taken from the ADAM database (i.e. 0.6 W/m/K, and 3.310^{-6} cm^2/s, respectively).

Experimental data reported evaporation rates (per unit surface) averaged over the whole experiment duration. Thus, the evaporation rate predicted values were obtained through the following expression:

$$q_{av}^{ev} = \frac{1}{t_{\max}} \sum q_i^{ev} \, \Delta t_i$$

where q_{av}^{ev} is the average predicted evaporation rate, $t_{\max}$ is the reported time duration of the experiment (i.e. the simulation duration in the above table), q_i^{ev} is the simulated evaporation rate at the *i*-th time step Δt_i.

The outcome of the simulation is depicted in Figure 37 and shown in Table 9, which provides a comparison between predicted and experimental data. The results obtained by using ADAM GASP and ADAM MacKay & Matsugu models are also compared to the values obtained by Fernandez (Fernandez, 2013) using the PVAP-MC model, which is one of the implemented models in PHAST.

Overall, the performance of ADAM GASP is very good, which as obtained using the Brighton value for the pool roughness length (i.e., 0.00023 m), which is the recommended value in ADAM.

Table 9: Predicted and simulated average vaporisation rate per unit area of the Kawamura & MacKay Tests. (Percentage deviations from experimental value are within parenthesis)

Average Evaporation rate (Kg/m²/h)	**Test 18**	**Test 19**	**Test 20**	**Test 21**	**Test 22**	**Test 23**
Experimental values (Kawamura, 1987)	*3.9*	*9.38*	*7.28*	*23*	*27.1*	*34.88*
ADAM (GASP)	4.00 (2.7%)	9.06 (-3.4%)	6.95 (-4.5%)	22.37 (-2.8%)	29.65 (9.4%)	30.85 (-12%)
ADAM (MacKay & Matsugu)	5.91 (52%)	12.71 (36%)	11.05 (52%)	28.40 (24%)	35.91 (32%)	37.36 (7.1%)
PVAP-MC (Fernandez, 2013)	4.42 (13%)		10.31 (42%)	27.08 (18%)	33.79 (25%)	

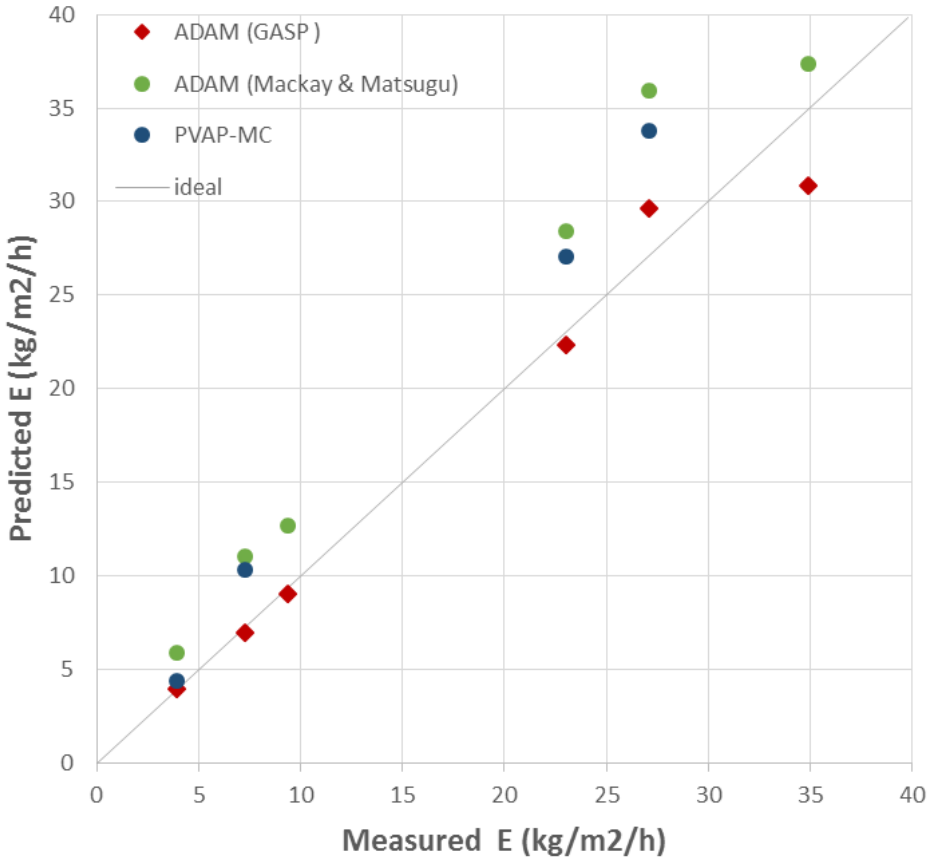

Figure 37: Predicted vs Experimental average vaporisation rate for Kawamura & MacKay trials (Kawamura, 1987). The simulation carried out with ADAM GASP and ADAM MacKay & Matsugu, are compared with the data obtained using the PVAP-MC model reported in Fernandez, 2013.

For pools on water, ADAM was evaluated against the data of the U.S. Bureau of Mines (Burgess, 1972), which referred to several tests involving instantaneous releases of LNG, liquid Nitrogen and liquid methane. The tests were conducted on a 0.0742 m^3 reservoir of water placed on a balance to measure the weight loss due to vaporisation. For each involved substance, the releases were repeated under the same conditions to ensure reproducibility of the results and to get average values for the vaporisation rate.

More specifically, the number of tests and the measured averaged evaporation rates (calculated during the first 20 seconds after the release), together with the input parameters used for the simulation are given in Table 10.

This table reports also the average vaporisation rates as calculated with ADAM GASP under the two different assumptions that film boiling between the pool and the water substrate takes place, or not. From the results, it is quite evident that ADAM GASP reproduces quite well the experimental results for the LNG and Methane trials without the film boiling assumption (i.e. with a deviation of ca. 5%), whilst this assumption play an important role in the case of liquid Nitrogen. This is also evident in the following figures, that depict the vaporised mass vs time for the different test series (Figure 38 for LNG, Figure 39 for Nitrogen, and Figure 40 for Methane).

Table 10: U.S. Bureau of Mines tests on LNG, liquid Nitrogen and Methane (Burgess, 1972). Number of tests for each series, average values of the measured vaporisation rate, input parameters used for the simulation, and ADAM results.

	LNG	**Liquid Nitrogen**	**Liquid Methane**
Number of Tests	7 (from N.18 to 24)	4 (from N.35 to 38)	11 (from N.44 to 49 and from N. 56 to 60)
Spill temperature (K)	111	77.3	111
Temperature of water (K)	294.15	294.15	293.15
Exp. Vaporisation rate (kg/s)	0.0115 *(average 0-20s)*	0.0122 *(average 0-20s)*	0.0125 *(average 30-60s)*
Vaporisation rate (kg/s) *ADAM (no film boiling)*	0.0121 (5.2%)	0.0405 (>200%)	0.0132 (5.6%)
Vaporisation rate (kg/s) *ADAM (film boiling)*	0.00387 (>50%)	0.0109 (10.6%)	0.00422 (>50%)
Due to the small-scale nature of the tests, stable conditions (F Pasquill stability call) and low wind speed (i.e. 0.1 m/s) were considered for the simulation.			

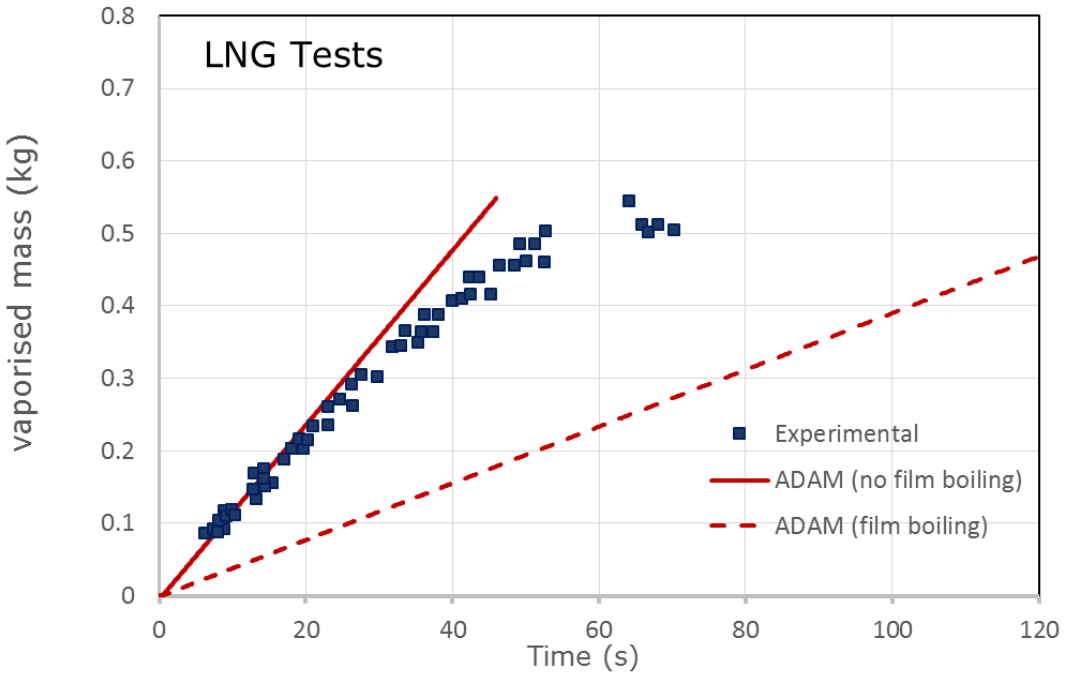

Figure 38: Vaporised mass vs time for the LNG instantaneous releases carried out by the U.S. Bureau of Mines (Burgess et al, 1972). Experimental data are reported together with ADAM simulation in absence and presence of film boiling.

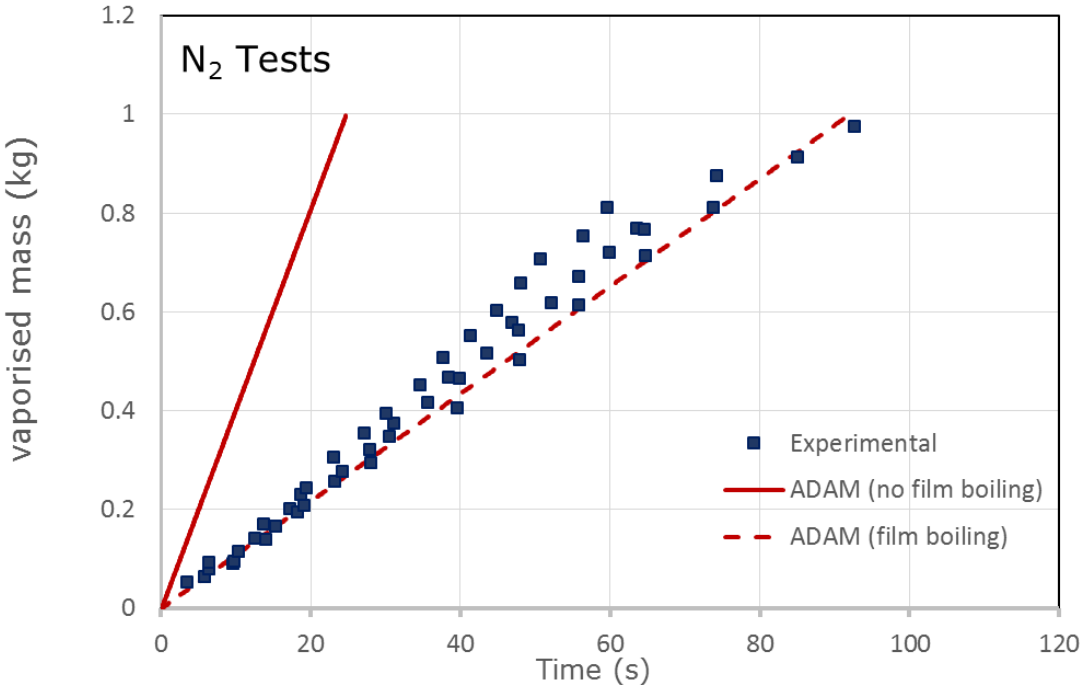

Figure 39: Vaporised mass vs time for the liquid Nitrogen instantaneous releases carried out by the U.S. Bureau of Mines (Burgess et al, 1972). Experimental data are reported together with ADAM simulation in absence and presence of film boiling.

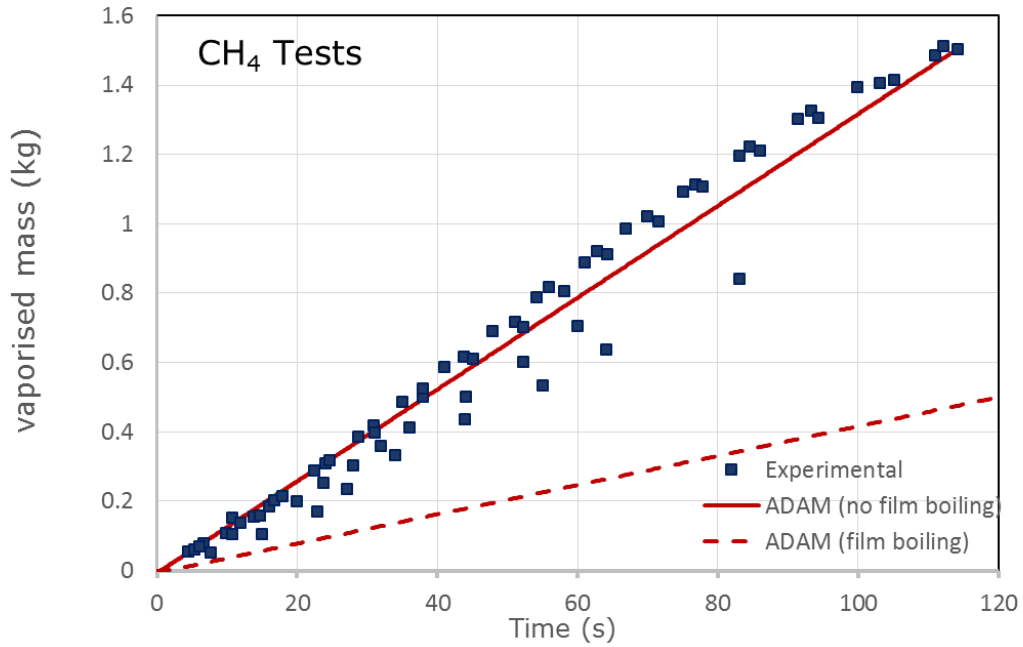

Figure 40: Vaporised mass vs time for the Methane instantaneous releases carried out by the U.S. Bureau of Mines (Burgess et al, 1972). Experimental data are reported together with ADAM simulation in absence and presence of film boiling.

3 Physical Effects (Module 2)

3.1 Atmospheric Dispersions

ADAM-SLAB is the Physical Effect Module for airborne dispersion calculations. This software originates from the former dispersion model developed by the Lawrence Livermore National Laboratory (SLAB), which is a widely used, validated and quality assured to treat heavier-than-air clouds but that can be applied also to neutral buoyant or lighter-than-air clouds. In particular, SLAB addresses various types of releases, including a ground-level evaporating pool, an elevated horizontal jet, a stack or elevated vertical jet, and an instantaneous volume source. With the exception of the evaporating pool, in which the source term is assumed to be all vapour, the other sources may consists of either pure vapour or a mixture of vapour and liquid droplets. The atmospheric dispersion is calculated by solving spatially averaged conservation equations of mass, momentum, energy, species. The conservation equations are spatially averaged in order to treat the cloud as a steady state plume, a transient puff, or a combination of the two depending on the duration of the release. In this respect, it should be considered that the solution to spatially averaged equations leads to spatially averaged cloud properties.

In ADAM, the SLAB algorithm that was originally written in FORTRAN has been completely rewritten in a more efficient code by using the C++ language. Before introducing novel methodological aspects, the code transformation procedure was fully verified in a large number of scenarios. A special software was written to verify the new code by comparing its outcome with the results of the original SLAB. This software was designed to execute parallel runs of the original and the new SLAB by varying all the input parameters in a wide range. Clearly, the same environmental data such as the ambient pressure and the thermophysical properties of air and water, which are coded in SLAB, were also used in the ADAM version of SLAB. A special feature of the software was that it allowed checking whether all the lines of the ADAM code were used in the series of run. This in order to verify whether the choice of the reference accident scenarios and of the parameters' range used for this benchmarking would cover all the software lines. The comparison led to very consistent results between the original SLAB version and the SLAB transformation into the ADAM code.

After this verification exercise, some methodological improvements were introduced in ADAM. These include:

- the possibility to use other environmental data extracted from the ADAM database instead of those coded in the original SLAB (e.g., properties of air and water);
- the direct linkage with the source term module;
- the increase of the number of points in the downwind direction for the construction of proper effect maps;
- an alternative calculus of the average concentration for instantaneous releases;
- the calculus for time-varying releases;
- the inclusion of the separate contribution from pool evaporation in case of rainout.

All these modifications are described in detail in the ADAM Technical Guidance document (Fabbri, 2017).

3.1.1 Overview of reference field campaigns

The set of field trials used for this evaluation are summarised in the table below and described hereunder.

Table 11: Field campaigns for atmospheric dispersion

Field campaign	substance	Release type	Reference
Burro	LNG	Evaporating Pools	Koopman, 1982a and 1982b
Coyote	LNG	Evaporating Pools	Goldwire, 1983
Desert Tortoise	Ammonia	Horizontal jets (2phases)	Goldwire, 1985
Goldfish	Hydrogen Fluoride	Horizontal jets (2phases)	Blewitt, 1987
Fladis	Ammonia	Horizontal/Vertical jets (2phases)	Nielsen, 1996b
Thorney Island	Freon12+N2	Instantaneous release	McQuaid, 1985

Burro and Coyote: These series of trials were performed over a dry lake bed at the US Naval Weapon Center at China lake, California. The trials consisted of a series of releases of LNG into a water basis, which formed pools 58 m wide. The 8 Burro trials focussed on the dispersion of evaporating vapours. The 4 Coyote tests were conducted later on and expanded from Burro by studying the occurrence of phase transitions, and the fires resulting from the cloud ignition.

Desert Tortoise and Goldfish: These two series of trials were conducted over at the Frenchman Flat desert area of the Nevada Test Site. The Desert Tortoise consisted of a series of 4 two-phase releases of pressurised ammonia from a pipe pointing horizontally downwind at a height of 1m from the ground. Ammonia concentrations were measured with sensors located on towers distributed along arcs at distances of 10m and 800m downwind from the source and at different heights (in the range 1-8.5m). Other two measuring portable stations were placed at higher distances. The Goldfish tests were conducted on the same site and consisted of a series of 3 releases of pressurised Hydrogen Fluoride. HF sensors were located on cross wind lines at distances of 300m, 1000m and 3000m from the source and at different heights (in the range 1-8.5m).

Fladis: These field experiments were conducted by a team from Risoe, Hydro-Care, FOA and CBDE on consisted of a series of pressurised ammonia releases on a flat terrain at a height of 1.5m. The main difference with Desert Tortoise trials was due to the much lower flow rates that allowed investigating on far field passive effects. The measuring setup in consisted of three main arcs of sensors at 20, 70, 150 and 238m downwind from the source at 0, 1.5 and 10m height.

Thorney Island: These heavy gas dispersion trials conducted by the UK Health and Safety Executive and involved a series of large (i.e. 2000m3) instantaneous releases of a mixture of Freon12 and N2 from a collapsible tent-like structure. The dispersions took place on an airfield, which could be considered as relatively flat mostly and in absence of obstacles, as existing building were not placed in the dispersion direction.

3.1.2 Model evaluation procedure

Since ADAM has introduced several methodological changes, in some circumstances the model outcome may vary from the results obtained by using the original SLAB. For this reason, it is necessary to conduct a novel evaluation campaign.

As mentioned in the introduction, the validation process of consequence assessment models is not always very straightforward, and the case of airborne dispersion models is extremely complex. Some of the measurement data used to evaluate the model performance are never accurate enough and some observed data cannot be reproduced even by a 'perfectly accurate' method. For instance, the random nature of the dispersion process, i.e. due to local fluctuations of the wind or atmosphere properties, leads to a scatter of local concentration measured during the field tests and used as the reference values for modelling evaluation. For this reason, these reference data are often grouped according to certain criteria by obtaining ensemble-averaged mean data, which are then compared to those calculated by the models.

The statistical measures used to compare experimental data with predictions are those described in the introduction (see Table 1), which are based on the concentration observed values (i.e. the measured average or peak concentrations *Co*) and the model output (i.e. the calculated average or peak concentrations *Cp*). In order to apply the calculus of performance measures on a consistent number of observation/prediction pairs, for each experimental trial dataset blocks were built by grouping the data associated with each monitoring arc.

A point to note is that, compared to other engineering fields, acceptance standards for validation of dispersion models are less stringent. Commonly, a model is considered to provide acceptable performance if predictions are within a factor of two of the measurement data for half of the time (CCPS, 1996). This partially reflects the level of uncertainty in many of the sets of measurement data. It was shown by Davies (Davies,1987) that multiple repeats of an instantaneous release of a dense gas under nominally identical conditions in a wind tunnel can produce concentrations at downstream locations, which vary by roughly a factor of two. In addition, the study conducted by Hanna et al. (Hanna, 1993) in their evaluation of 14 hazardous gas models, highlighted that the range of acceptability of performance measures is described by the conditions outlined below:

- Fraction of prediction within a factor of two of observation is about 50% or greater (i.e. FAC2>0.5).
- Mean bias within 30% of the mean (i.e., -0.3 < FB < 0.3 or 0.7 < MG < 1.3).
- Random errors is about a factor of two or three of the mean (i.e. NMSE < 1.5 or VG < 4).

Consequently, the same acceptability range is used for the purpose of this evaluation exercise.

In addition to the above quantitative measures, scatter plots of predicted vs observed concentration values were always presented in order to provide a general idea of the overall trend.

3.1.3 Results and discussion

Burro, Coyote and Fladis

For three set of trials (i.e. Burro, Coyotes and Fladis), all experimental information and results were collected from the Rediphem database (Nielsen, 1996a). This database contains both the auxiliary data which are necessary to run the dispersion models (meteo and environmental information), and the data on local concentrations which were measured through sensors positioned at different locations during the trials. The data on concentration are given as a function of time, which were processed to obtain average values within the release time duration. These data formed the observations' data set (i.e., Co) to be compared with the model output (i.e., *Cp*).

As the exact location of the sensor was known, ADAM calculations were conducted at the specific spatial coordinates of these locations, which allows making the comparison more appropriate. An example of sensor positioning for the Burro 8 trial is depicted in Figure 41, which shows the downwind and crosswind coordinates of the sensors that are displaced in equidistance arcs. Most of the sensors were placed at three different heights, i.e. 1, 3, and 8m.

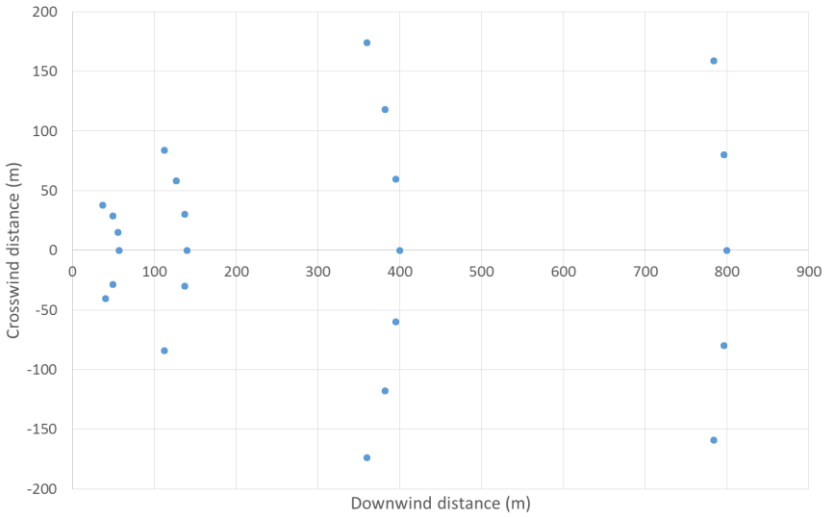

Figure 41: Burro 8 trial, positioning of sensors for concentration measurements

Since all integral models as the one implemented in ADAM do not directly take into account of the fluctuations of wind direction around the central axis (the meandering effect addressed averaged effects only), the punctual comparison of the observation/prediction pairs does not make very much sense. Thus, these data were grouped to form pairs (observed and simulated data) belonging to the same arc, and the values to compare were those averaged amongst data of the same arc. In other words, the procedure consisted of comparing the average concentrations observed on the sensors in the same arc (i.e. those with comparable x-values) with the values calculated by averaging the simulations obtained on the single points of each arc. In such a way, the unavoidable under/over predictions at the single point due to wind direction displacement were slightly compensated. The number of arcs for the different trials was: 4 for Burro, 5 for Coyote, and 3 for Fladis.

The result of these comparisons for three different trials of Burro are given in Figure 42, which shows a very good agreement between predicted and experimental data. Similarly, Figure 43 and Figure 44 shows the results of the comparison conducted on 3 Coyote trials and 14 Fladis trials.

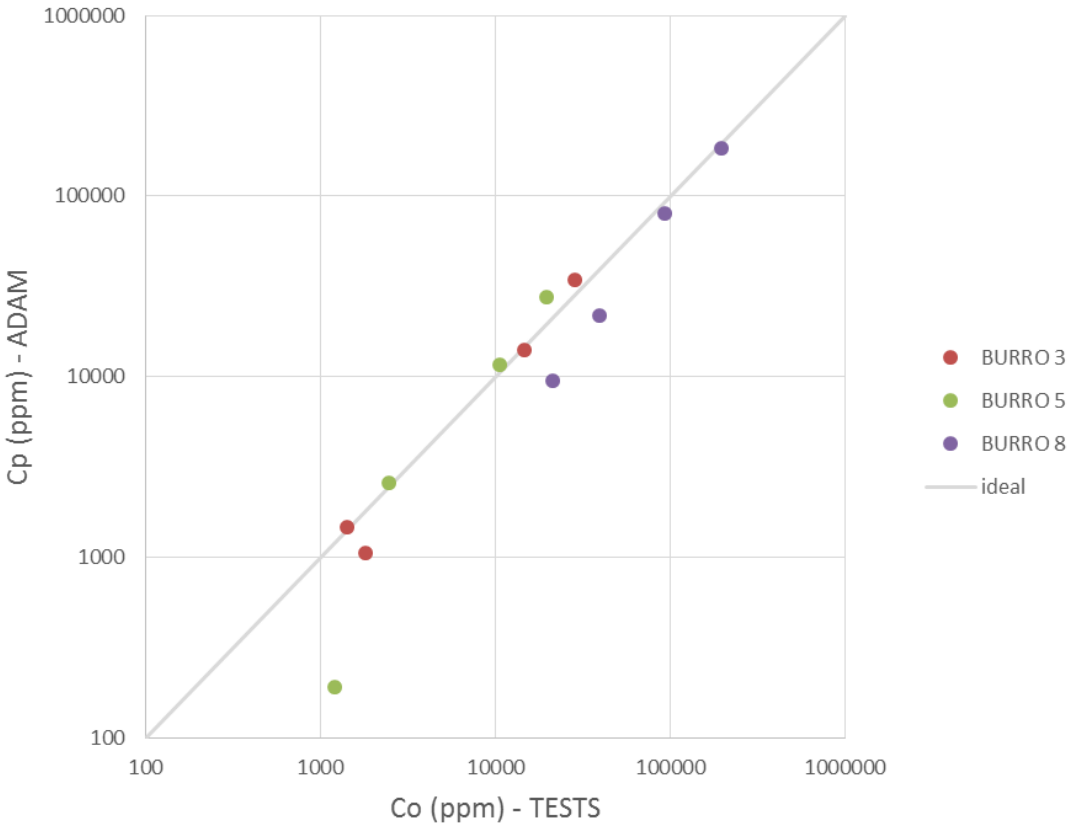

Figure 42: Burro -scatter plot of observation/prediction pairs.

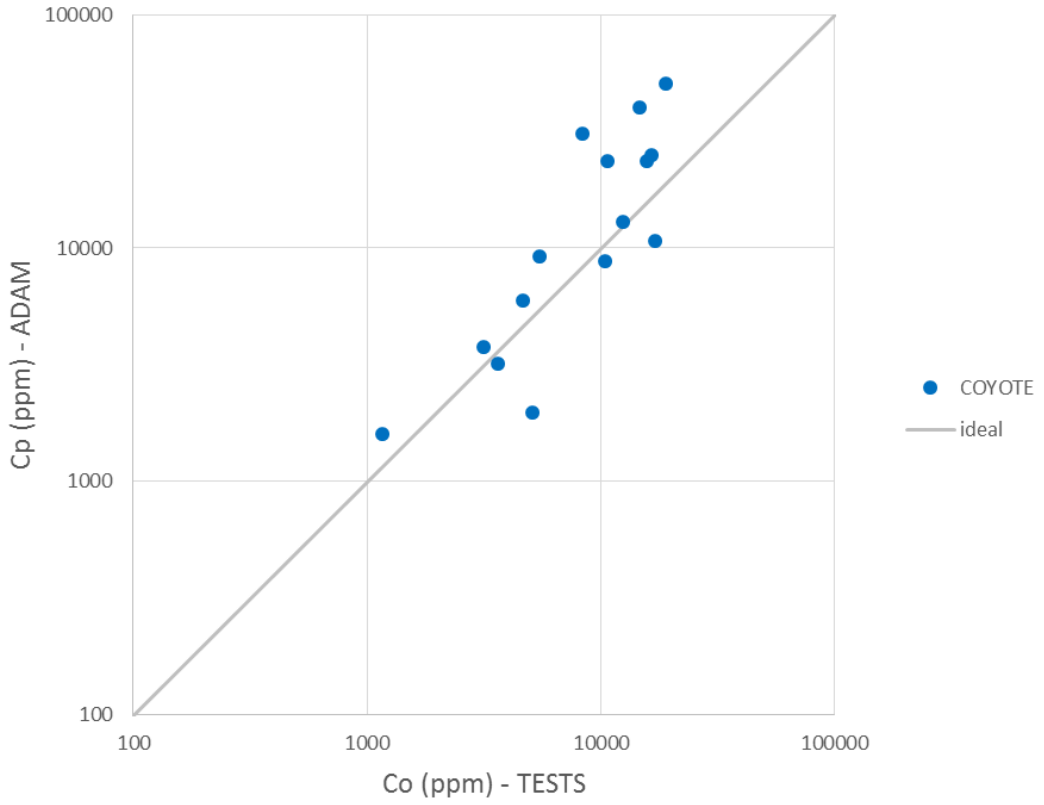

Figure 43: Coyote - scatter plot of observation/prediction pairs.

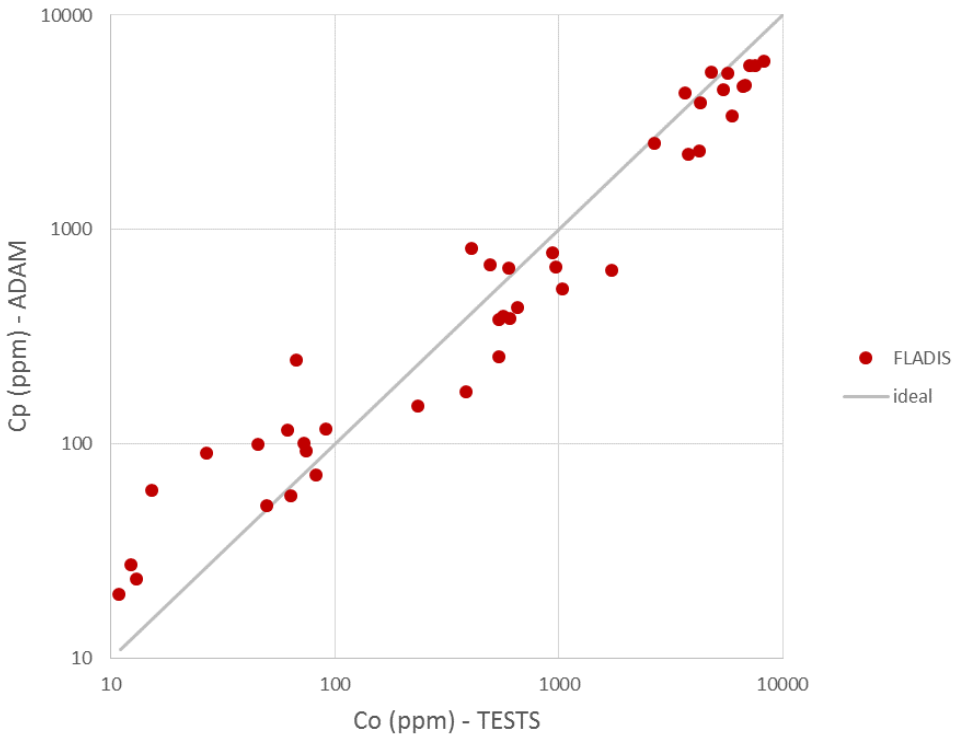

Figure 44: Fladis - scatter plot of observation/prediction pairs.

Desert Tortoise and Goldfish

For the Desert Tortoise and Goldfish trials, the data on single sensor concentrations vs time were not available at the JRC, therefore, the average concentration data on the centreline reported in the literature (Hanna, 1991), were used as the reference data. The scatter plot of observed and predicted concentrations on the centreline is given in Figure 45, which shows that whilst the match is excellent for the Desert Tortoise trials, ADAM tend to under predict in the Goldfish case.

Thorney Island

The ADAM test on Thorney Island data is particularly important since it refers to the case of instantaneous release. For such a release type, ADAM has, indeed, introduced some significant modifications to the original SLAB model by producing different results. The observed maximum ground concentration centreline concentrations of the different trials were compared to the model predicted values. This comparison is shown in Figure 46 that shows an excellent agreement for the majority of field tests.

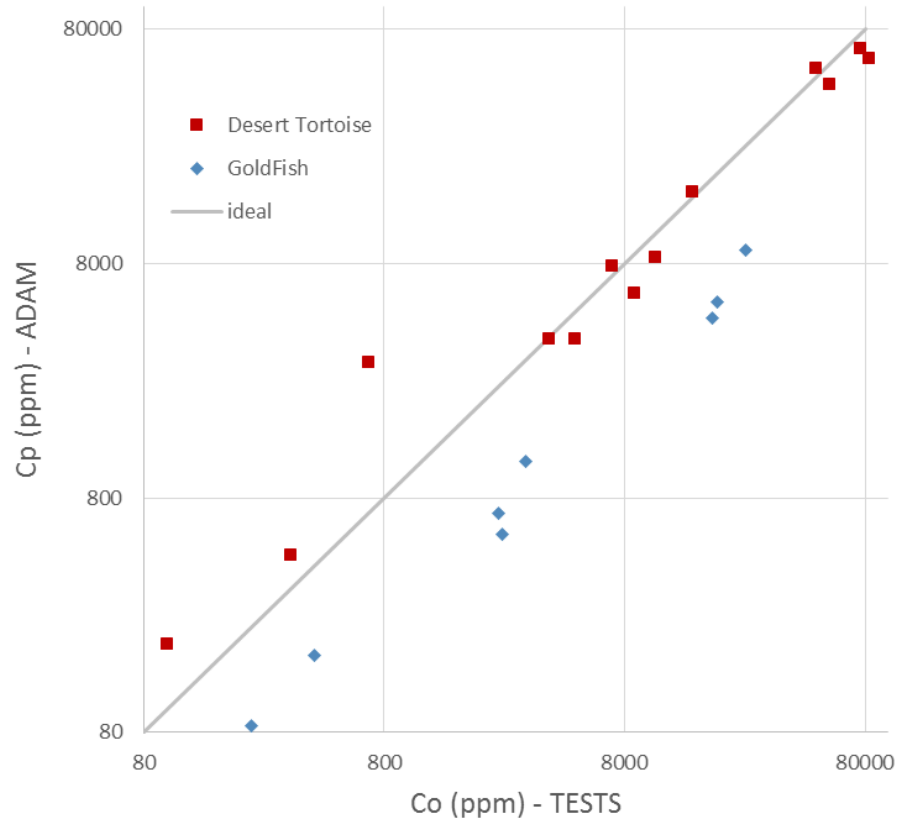

Figure 45: Desert Tortoise & Goldfish trials - scatter plot of observation/prediction pairs

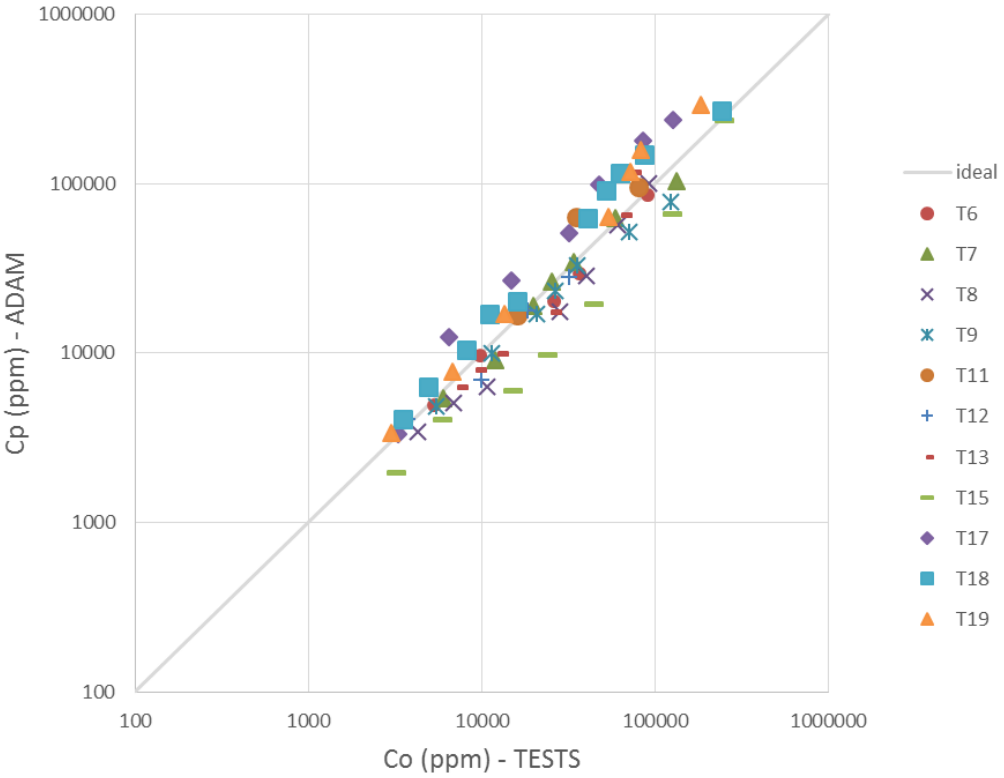

Figure 46: Thorney Island instantaneous release (Freon + N_2) - scatter plot of observation/prediction pairs

Statistical model evaluation

In order to quantify all the above results, the statistical performance measures defined in the introduction were calculated for the different trials' set. The outcome of this calculus is given on Table 12, which shows the general good performance of ADAM. In general, all performance measures are within the acceptability range, with the exception of the Goldfish trials, for which ADAM underpredicted the concentration values. For Coyote trials, the fractional bias and the geometrical mean bias were just above the acceptability threshold.

Finally, Figure 47 shows the overall geometrical mean bias, MG and the geometric variance, VG, values for the different trials. Here, an experimental trial "perfectly" reproduced by the model would be placed at the (1,1) point. The case with no random scatter but with a mean bias different from zero would be placed somewhere along the parabolic line that represents the minimum possible value of the geometric variance for the corresponding value of the geometrical mean bias. Thus, all points should lie within this parabola. As a reference, the two vertical lines represent the 'factor-of-two' between mean predictions and observations.

Each point reported in the figure is given with its MG 95% confidence interval as calculated by using the Bootstrap technique. Overall, the performance of ADAM is very good.

Table 12: ADAM Performance measures on the different field trials*

	FB	**MG**	**NMSE**	**VG**	**P**	**FAC2**
BURRO	0.11	1.32	0.06	1.50	0.99	0.83
COYOTE	*-0.52*	*0.74*	1.03	1.52	0.74	0.67
FLADIS	0.23	1.00	0.24	1.38	0.97	0.81
DESERT TORTOISE	0.14	0.96	0.11	1.26	0.98	0.92
GOLDFISH	*1.07*	*3.13*	*3.76*	*3.81*	0.98	*0.00*
THORNEY ISLAND	-0.25	0.93	1.22	1.59	0.70	0.92
Ideal model	0	1	0	0	1	1

** values in italics are outside the acceptability range*

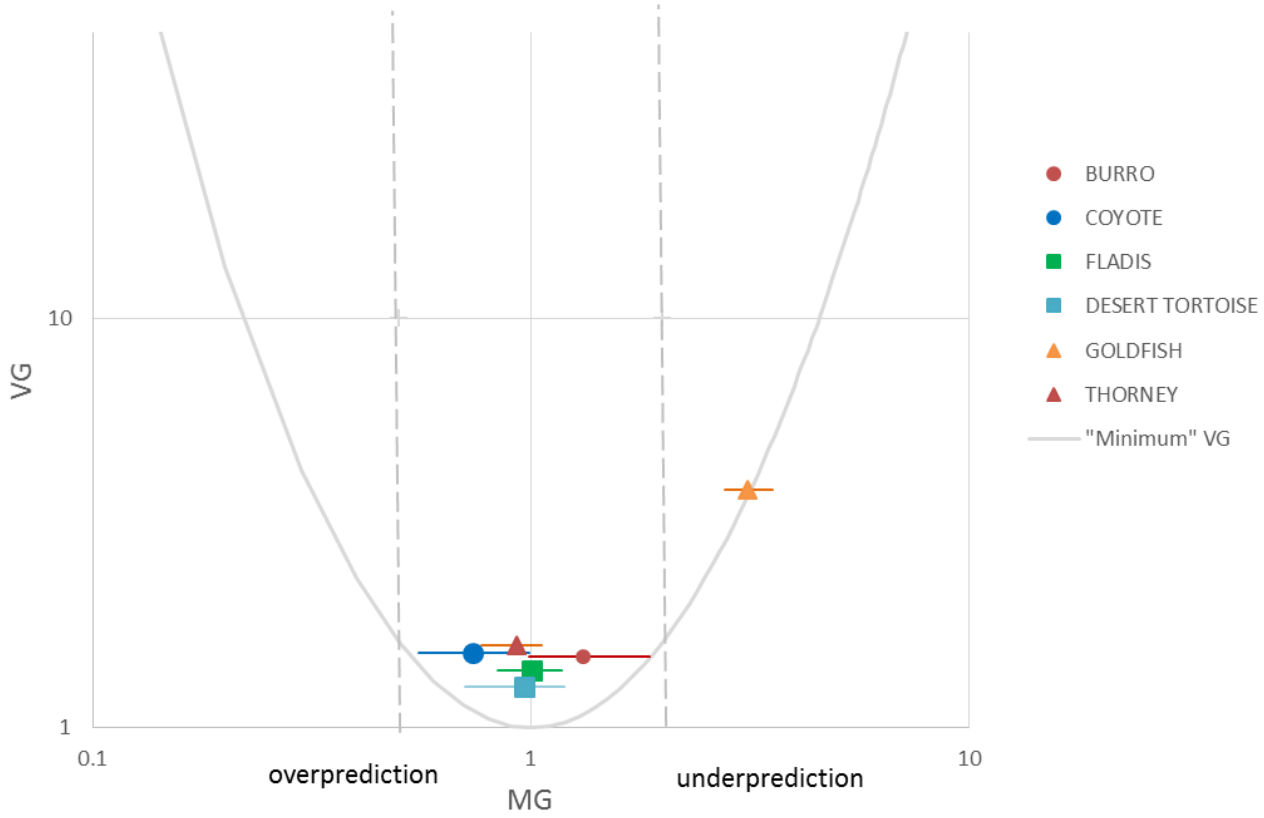

Figure 47: Model performance indicators, geometrical mean bias MG and geometric variance VG for concentration prediction and observations. The horizontal lines on MG represent 95% confidence intervals; the solid parabola is the "minimum" VG curve. The vertical dotted lines represent the 'factor-of-two' between mean predictions and observations

3.2 Fires

This section deals with the evaluation of flammable effect models implemented in ADAM, which are all based on semi-empirical correlations. For fire related effects, the evaluation was conducted by comparing the ADAM predictions with the experimental data available from the literature. The fire flame geometry, the radiative properties of the flame and the calculation of the radiant flux at receptor location were not analysed separately, but were studied in terms of the overall final effect. For both pool and jet fire calculations, because of some modifications introduced in the models in terms of the flame geometry, the novel procedure for the calculus of the view factor, and alternative correlations to address the effects of atmospheric absorption, full evaluation was conducted. For fireballs, since the implemented model is very well established and simple to verify by hand calculations, its evaluation was not reported here.

3.2.1 Pool fires

The models implemented in ADAM have been evaluated against experimental trials for LNG (Johnson, 1992) and LPG (Welker & Cavin, 1982) pool fires. Specifically three different empirical models are implemented in ADAM: (*i*) the Modified TNO model, (*ii*) the Shokry and Beyler model, and (*iii*) the Mudan model (Fabbri, 2017). Separate simulations were conducted on these three.

Johnson trials

The fields trials used for the evaluation refer to field trial 1, 6 and 7 conducted by Shell Research Ltd and British Gas, which were reported in tabular form by Johnson (1992). The main input parameters are summarised hereunder:

Table 13: Input parameters for the LNG pool fire trials (Johnson, 1992)

Trial number	**Pool diameter (m)**	**Wind speed (m/s)**	**Ambient Pressure (bar)**	**Ambient Temp. (C)**	**Humidity (%)**	**Points**
1	1.8	2.4	-	-	-	5
6	6.1	6.6	.943	7	83	13
7	10.6	4	.943	9.3	87	13

The pool was formed by refrigerated LNG that for the purpose of the calculations was set at a temperature of 110K.

For the thermal radiation comparison, a proper transformation of the coordinate system for the location of radiometers had to be implemented. The simulation was conducted by assuming the radiometer pointing at the axis of the pool, which was placed at 1m (trial 1), 0.7-1.07 m (trial 6), and 1.25 m (trial 7) heights.

Table 14 provides the result of the evaluation in terms of the associated statistical measures for the three different models implemented in ADAM. This resulted from the comparison of experimental data as obtained from Johnson, 1992 with the ADAM simulation. In this case, the *C*o coefficients of Table 1 refer to the observed thermal radiation, whilst *Cp* is the thermal radiation predicted by ADAM for each measuring point (31 for the present case). As it results from the table, both the Modified TNO and Mudan methods perform very well, whilst the results obtained with the Shokri and Beyler method are quite questionable.

Scatter plots for the TNO modified and Mudan models implemented in ADAM are shown in Figure 48 where the observed vs predicted thermal radiations are given. For a

comparison, the figure includes also the values calculated in the reference paper (Johnson, 1992). Also from the plot it result the better performance of the TNO method if compared to Mudan.

Table 14: Performance measures on Jonhson trials (Pool fire) for the different models implemented in ADAM

	FB	MG	NMSE	VG	P	FAC2
Modified TNO	-0.024	0.994	0.032	1.023	0.936	1.000
SHOKRI and BEYLER	0.412	1.558	0.444	1.547	0.386	0.677
MUDAN	-0.043	0.967	0.068	1.063	0.831	1.000
Ideal model	0	1	0	1	1	1

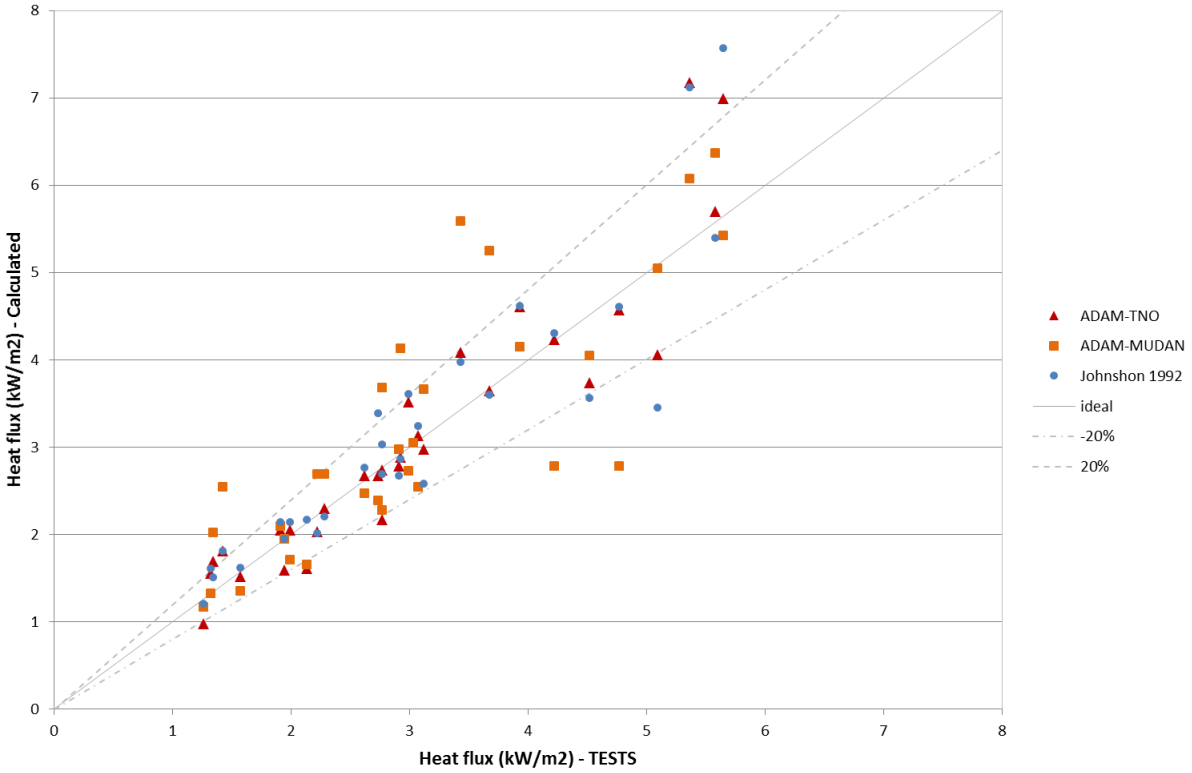

Figure 48: LNG pool fires. Comparison with experimental trials from Johnson, 1992 (Trial 1, 6,7). Scatter plot of observation/prediction pairs

Welker and Cavin trials

Radiation data obtained from experimental trials on LPG pool fires were extracted from Part II of the DOE report on Vaporisation, Dispersion, and radiant Fluxes from LPG spills, (Welker & Cavin, 1982).

Since the LPG was unloaded into concrete pits 5, 10, 20, and 40 pits square. Pool fires with diameter equivalent of 1.86, 3.58, 7.02, and 13.9 were obtained. Measuring radiometers were positioned at an elevation of 5 ft. above the top of the pit and were generally placed in the crosswind direction, 1 and 2 pit widths from the edge of the pit (rear and front radiometers).

All thermal radiation data available in the report are associated to a specific field test characterised by certain wind conditions (i.e. speed and direction), and correspond to the rear and front radiometer responses. The number of available tests were ca. 60, with two

measurements each from the front and rear radiometers. In ADAM, the radiometer was modelled as a vertical target and a suitable coordinate transformation was implemented to take into account of the different wind directions associated with each test.

The result of the evaluation of ADAM against the Welker and Cavin trials for the three implemented models is provided in terms of the performance indicators reported in Table 15. Again, the modified TNO and Mudan are the implemented models that perform the best.

Scatter plots for the TNO modified and Mudan models implemented in ADAM are shown in Figure 48 and Figure 49, respectively, where the observed vs predicted thermal radiations are given.

Table 15: Performance measures on Welker and Cavin trials (Pool fire) for the different models implemented in ADAM

	FB	**MG**	**NMSE**	**VG**	**P**	**FAC2**
Modified TNO	0.025	1.073	0.140	1.118	0.719	0.956
SHOKRI and BEYLER	0.606	1.863	0.626	1.681	0.559	0.596
MUDAN	-0.083	0.974	0.173	1.107	0.725	0.965
Ideal model	0	1	0	1	1	1

Finally, Figure 48 shows the overall geometrical mean bias, MG and the geometric variance, VG, values for the different pool fires for both the Johnson and Welker&Cavin trials. As usual, the figure reports also the parabolic line representing the minimum possible value of the geometric variance, with the two vertical lines indicating the 'factor-of-two' between mean predictions and observations.

As it can be seen from the figure, the modified TNO and the Mudan methods implemented in ADAM performs very well whilst the Shorky and Bayler method is characterised by lower performance. Overall, the modified TNO is selected as the default method in ADAM for pool fires.

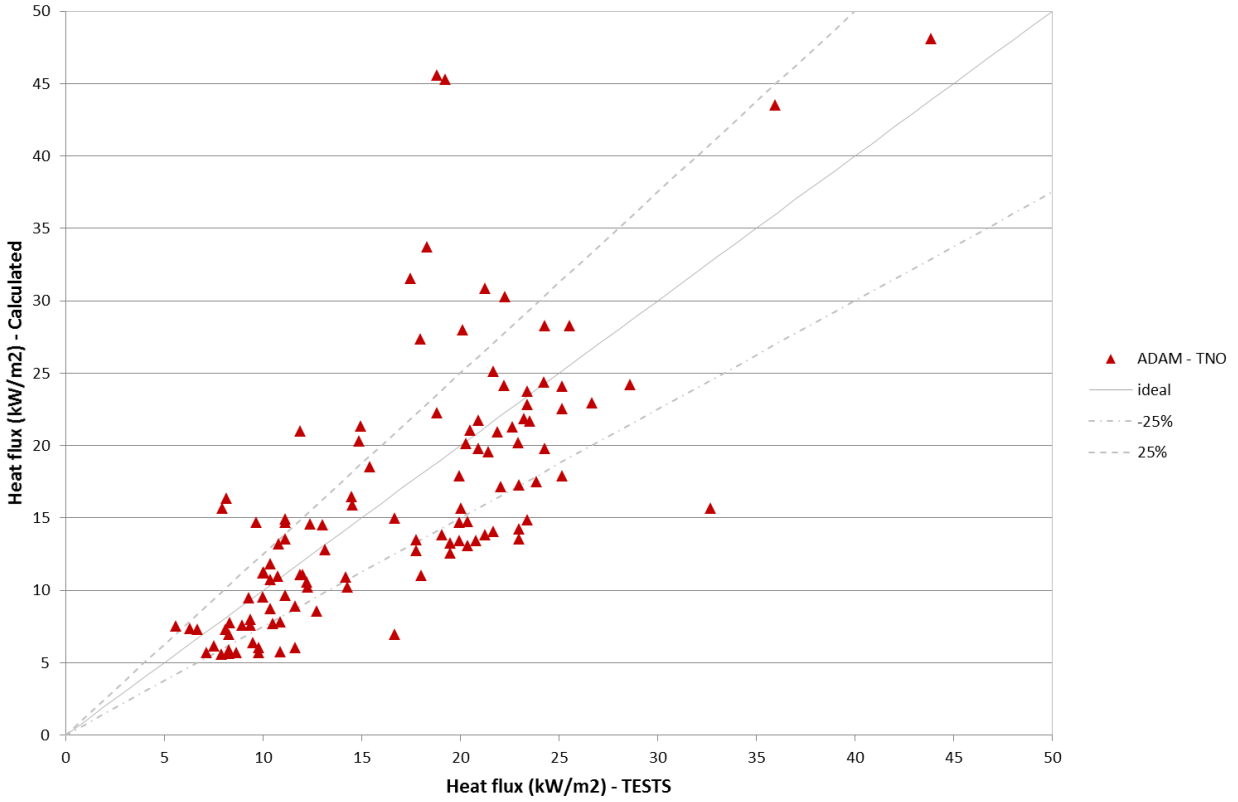

Figure 49: LPG pool fires. Comparison of ADAM TNO with experimental trials from Welker and Cavin, 1982. Scatter plot of observation/prediction pairs

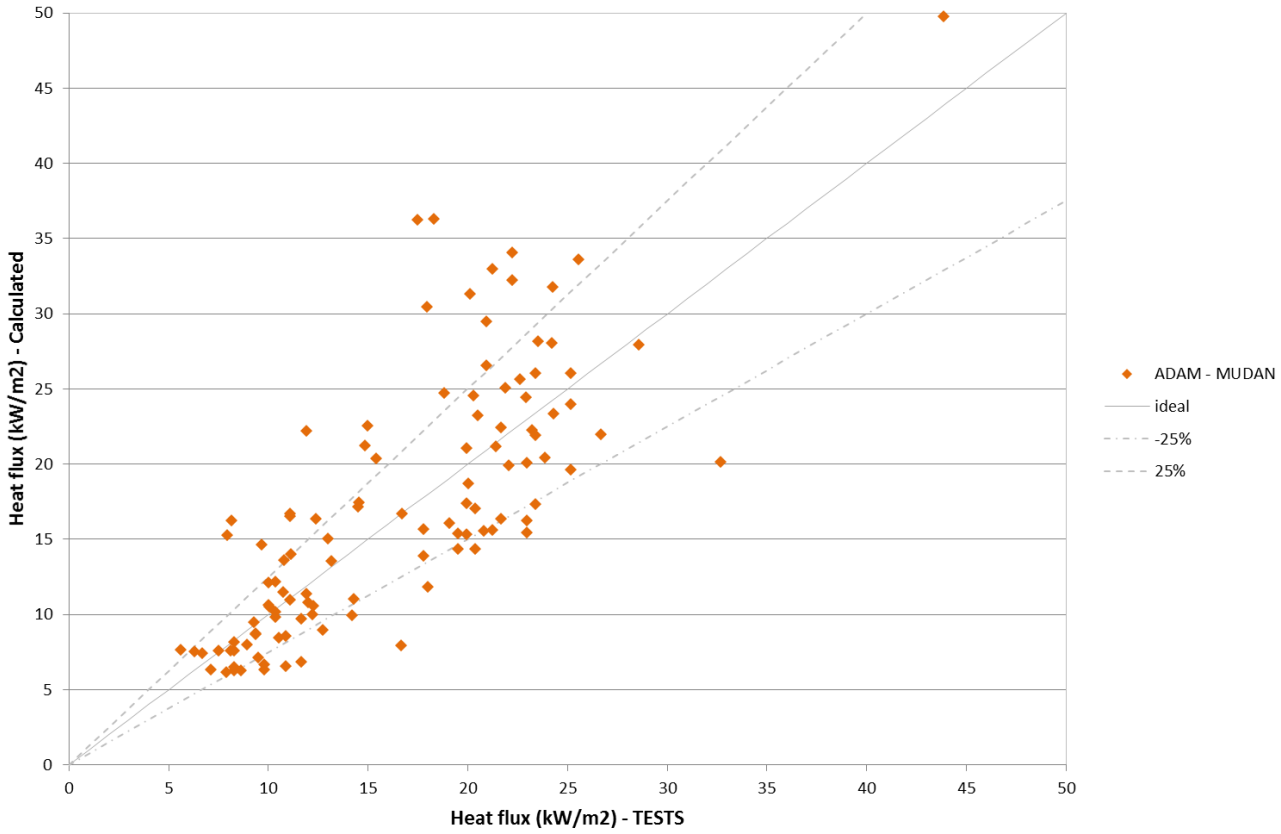

Figure 50: LPG pool fires. Comparison of ADAM - MUDAN with experimental trials from Welker and Cavin, 1982. Scatter plot of observation/prediction pairs

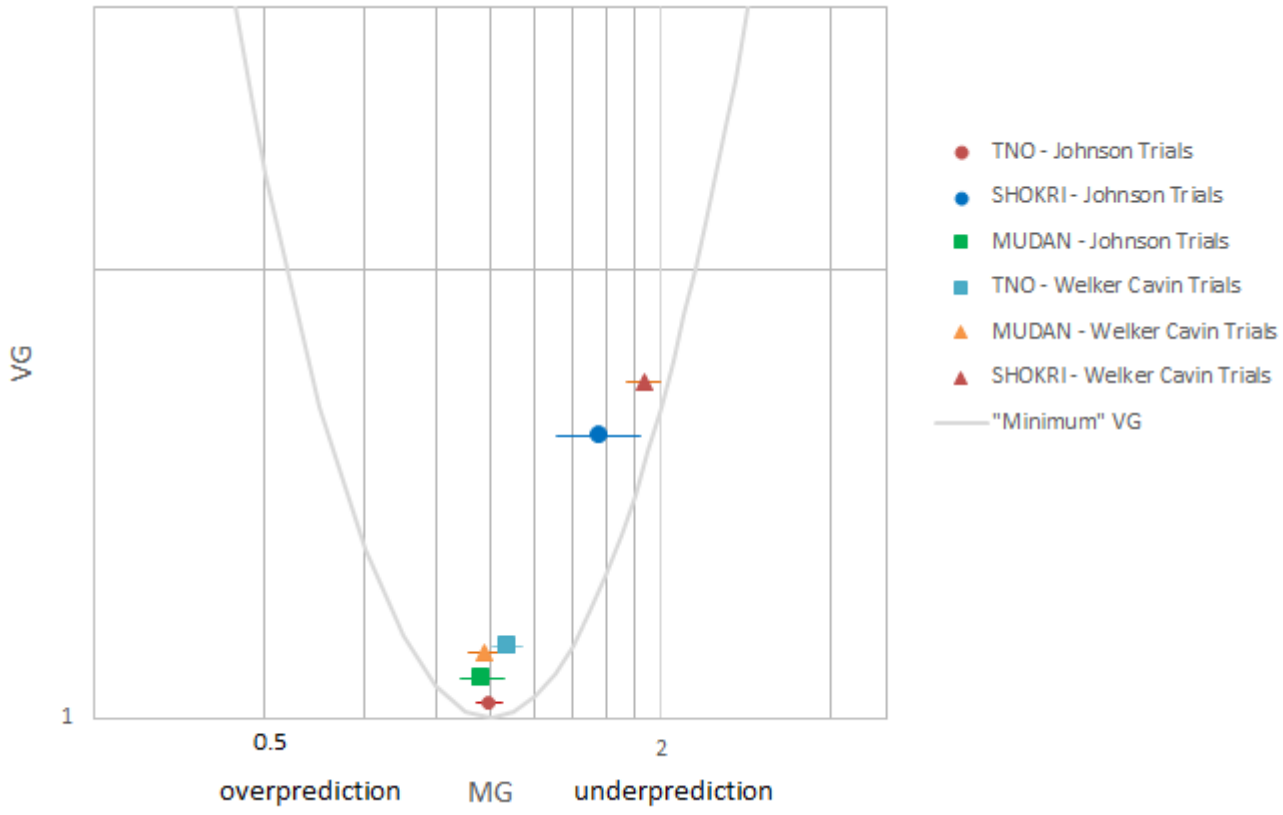

Figure 51: Model performance indicators, for the pool fire trials. The different models included in ADAM were tested separately. The horizontal lines on MG represent 95% confidence intervals; the solid parabola is the "minimum" VG curve.

3.2.2 Jet fires

The ADAM model implementation for vertical and horizontal jet fires was evaluated against experimental trials involving LNG (Chamberlain, 1987 and Johnson, 1994)

Vertical Jets

For vertical jets, one reasonable source of test data is reported by Chamberlain (1987), which contains data from large-scale trials involving natural gas releases carried out at onshore oil installation in Cumbria (Trial 4), with three tests (A, B, C) with different variables (jet diameter, wind speed, flow rate, and environmental conditions) as outlined in the table below. Stagnation temperature and pressure were not reported. Thus, they were fixed in ADAM together with a discharge coefficient of 0.86, in such a way to produce the reported flow rate

Table 16: Input parameters for Trial 4 (Chamberlain, 1987)

	Test A	**Test B**	**Test C**
Flow rate (kg/s)	5.6	11.2	22.2
Orifice diameter (mm)	152	203	305
Ambient temperature (°C)	16.3	14.2	14.3
Humidity (%)	50	60	51
Wind speed (m/s)	8.1	6.3	10.3
Wind direction (from north ,deg)	268	268	270

For each test, several data points at different receptor locations were reported. A suitable coordinate transformation had to be carried out in order to adapt ADAM reference system with the Chamberlain's original coordinate system. For the calculation, the radiometer was modelled as being placed horizontally, with the normal to its sensitive surface pointing at the z-axis (i.e. vertical direction placed at release origin). Figure 52 shows the comparison of thermal radiation data predicted by ADAM vs the observed values in the different locations. As a reference, the original data calculated by Chamberlain (1987) were also included.

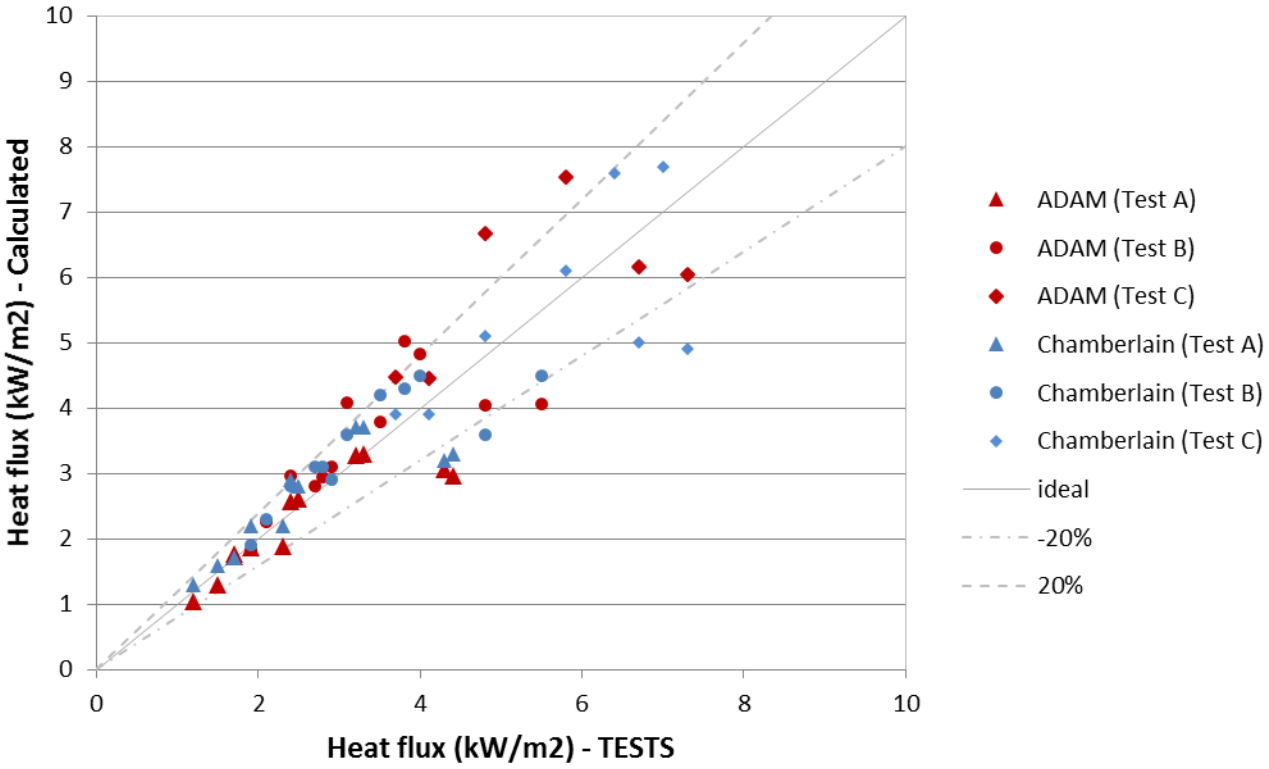

Figure 52: LNG vertical fires. Comparison of ADAM with Cumbria experimental trial 4 from Chamberlain, 1987. Scatter plot of observation/prediction pairs for the different Tests (i.e. A, B, and C).

Horizontal Jets

For horizontal jets, the field trials carried out at the British Gas test site (Bennet, 1991) and reported in the paper by Johnson et al. (1994) were used. These involved four different tests involving natural gas horizontal jets (B, C, D, and E), originated from different orifice diameters and under different operative and environmental conditions. Also in this case, measurements at different locations and at two different heights (i.e. 1.7 and 2m) were available. For the calculation, the radiometer was considered as oriented horizontally, with the normal to its sensitive surface pointing at the z-axis (i.e. vertical direction placed at release origin).

Table 17: Input parameters for horizontal jet field trials (Johnson, 1994)

	Test B	Test C	Test D	Test E
Stagnation overpressure (barg)	0.3	2.1	11.1	66
Stagnation Temperature (K)	277	267	279	281
Flow rate (kg/s)	2.8	8.4	7.9	3.8
Orifice diameter (mm)	152	152	75	20
Ambient temperature (K)	279	281	282	286
Humidity (%)	89	80	81	91
Wind speed (m/s)	1.7	0.3	3.9	6.9
Wind direction (from north ,deg)	247	326	271	269

The comparison of thermal radiation data predicted by ADAM with the observed values in all different locations is shown in Figure 53. The original calculations reported in Johnson et al. (1994) are also reported in the graph.

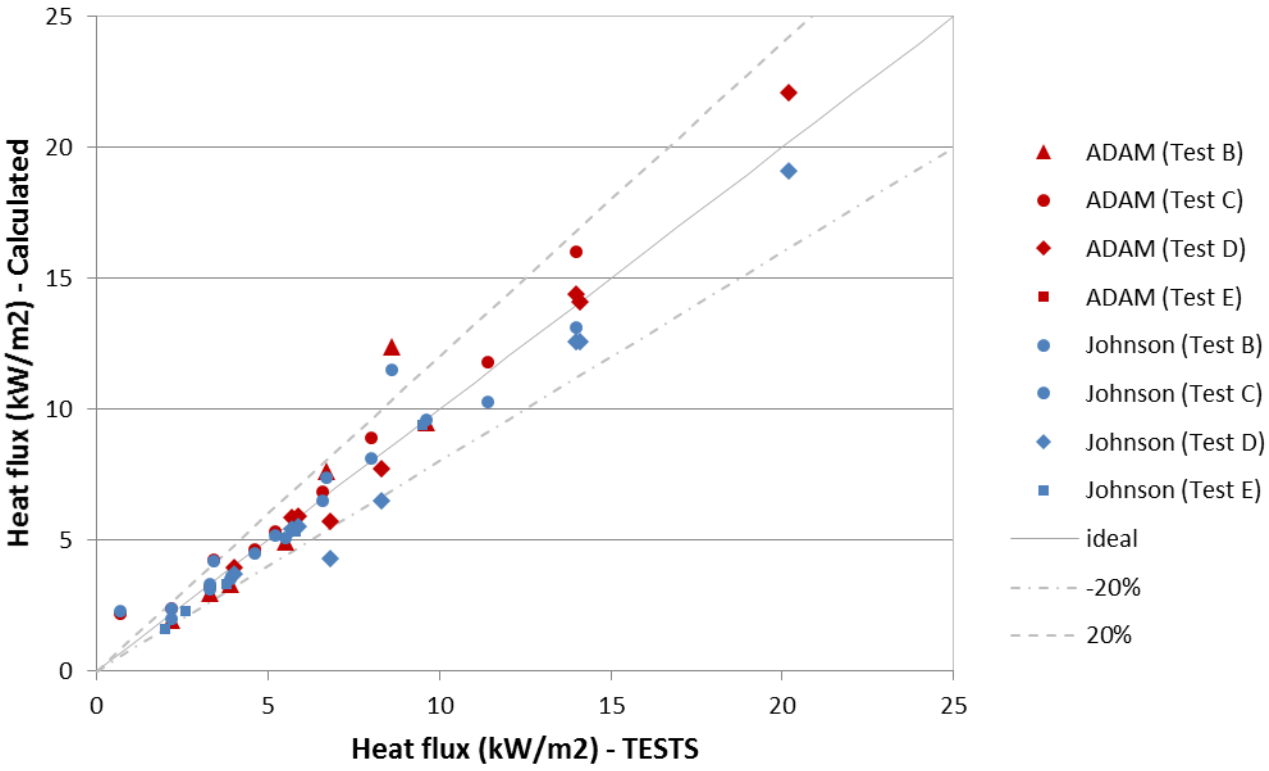

Figure 53: LNG horizontal fires. Comparison of ADAM experimental data from Johnson 1994. Scatter plot of observation/prediction pairs for the different Tests (i.e. B, C, D, and E).

Statistical measures

The result of the evaluation of ADAM against the Chamberlain and Johnson Trials (i.e., vertical and horizontal LNG jets) is reported in Table 18, in which the whole set of statistical performance measures is provided, and in Figure 54 that shows the geometric variance as a function of the geometrical mean bias. Also in the present case, ADAM shows good performance.

Table 18: Performance measures of ADAM for the fire jets.

	FB	MG	NMSE	VG	P	FAC2
Chamberlain (vert. jet)	-0.153	0.891	0.115	1.063	0.855	1.000
Johnson (horiz. Jet)	-0.052	0.946	0.021	1.057	0.983	0.967

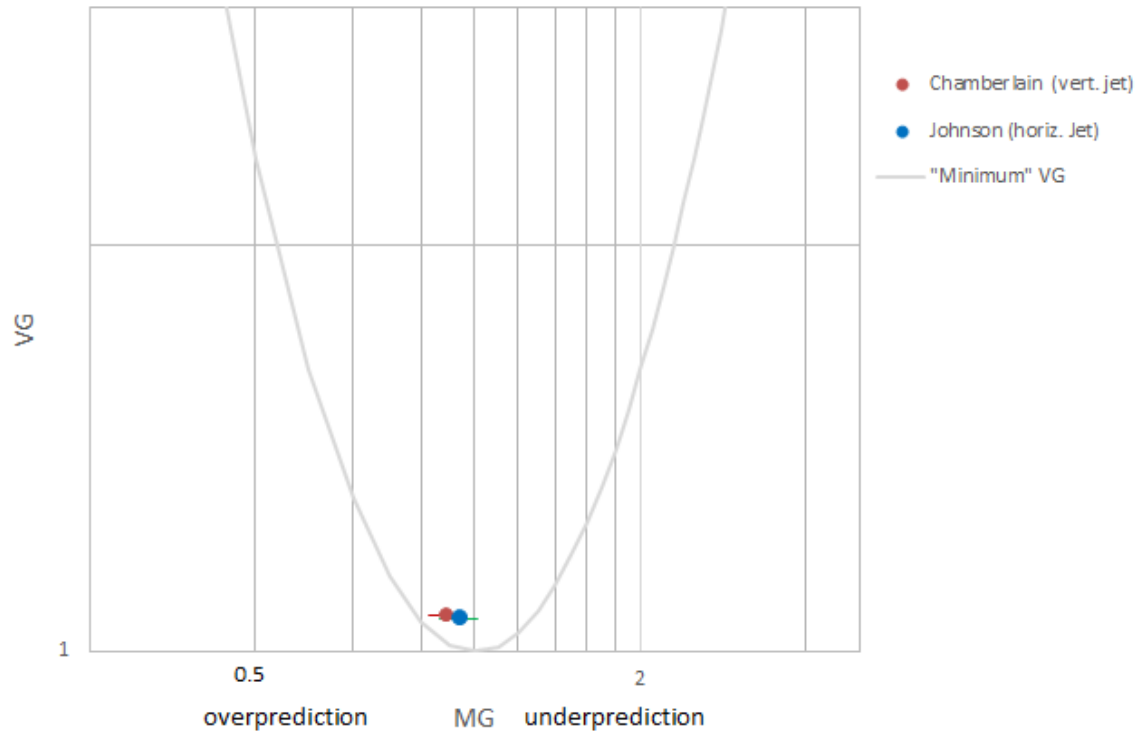

Figure 54: Model performance indicators, for the jet fire trials. The horizontal lines on MG represent 95% confidence intervals; the solid parabola is the "minimum" VG curve.

3.3 Vapour cloud explosions

All VCE models implemented in ADAM (i.e. Equivalent TNT, MultiEnergy (ME) and Backer-Strehlow-Tang(BST) are based on a set of scaled curves for peak-overpressure and blast duration (or equivalently positive impulse), which refer to different blast severities.

For the ME method, the ten scaled-curves of the peak overpressure and of the positive phase duration, which correspond to the 10 blast strength levels, were extracted from the original graph produced by the model developers (van den Berg, 2005; Mercx, 2005). Each scaled curve was digitised by producing 1000 points and uploaded on the ADAM code.

The same was done for the 9 scaled-curves of the peak overpressure and positive impulse of the BTS method, which were extracted from the original work of the model developer (Tang, 1999; Tang, 2005). Since the available 9 scaled curves are associated to flame speeds that do not cover all Mach values of Pierorazio's table (Pierorazio, 2005), intermediate curves were created by using the spline interpolation method.

All scaled curves uploaded in ADAM were carefully verified on the original graphs by superimposition.

3.3.1 Test Programme BFETS3a (Full scale VCE)

The BTETS3a experiments conducted by British Energy (BFETS BG Technology, 2000; Fitzgerald, 2001) were designed as a follow up of the previous BFETS2 programme (VCE in 1D confinement) to explore more complex confinement geometries. All of BTETS3a tests were conducted with Methane.

The following table lists the input data used for the ADAM evaluation. The blast Energy E, used for the determination of the explosive mass, which is an ADAM input, was taken from the paper of Fitzgerald (Fitzgerald, 2001). that reports simulations performed by using Backer Strehlow Tang (BTS) and the Multi-energy (ME) methods on these tests. All other relevant parameters i.e., confinement, congestion for BST and the blast strength for ME were also taken from this paper. ADAM simulations were performed by considering and explosive mass as given in Table 19 and assuming a stoichiometric mixture with air. The explosive mass was calculated from the blast energy by considering a heat of combustion per unit mass of the flammable equal to 50031 kJ kg^{-1}, as extracted from the ADAM database. The flame speed Mach number M_f was taken from Pierorazio's table according to the new version of the BST method (Pierorazio, 2005)

Table 19: Input parameters for BTETS3a simulations.

			For BTS				*For ME*
Tests n.	**Mass(kg)**	**Energy (J)***	**Confinement**	**Congestion**	**Reactivity**	**M_f**	**Strength**
1-4	83.56	4.18E+09	2D	High	low	0.66	6.908
16,17,19,22	83.56	4.18E+09	2.5D	High	low	0.5	6.908
24-26,29,32	167.11	8.36E+09	2.5D	High	low	0.5	7.452
37,28	167.11	8.36E+09	2.5D	High	low	0.5	7.557
39-44	83.56	4.18E+09	2.5D	High	low	0.5	6.976

* for BTS blast energy is doubled due to a ground reflection factor of 2

The outcome of the simulations on the separate groups of BFETS3a tests performed with ADAM are shown in Figure 55- Figure 59. These data confirms also the results of Fitzgerald i.e., the BST method underestimate the experimental data with the ME method performing better, which is evident by comparing Figure 60 with Figure 61.

Improved predictions were obtained by applying the ground correction method described by Xu et al. (Xu, 2009). The average error of the BST model with the ground correction method has reduced to 60% that is significantly lower if compared to the average error obtained with the original BST method that applies a ground reflection factor of 2 (i.e. ca. -60%.) (see also Figure 60).

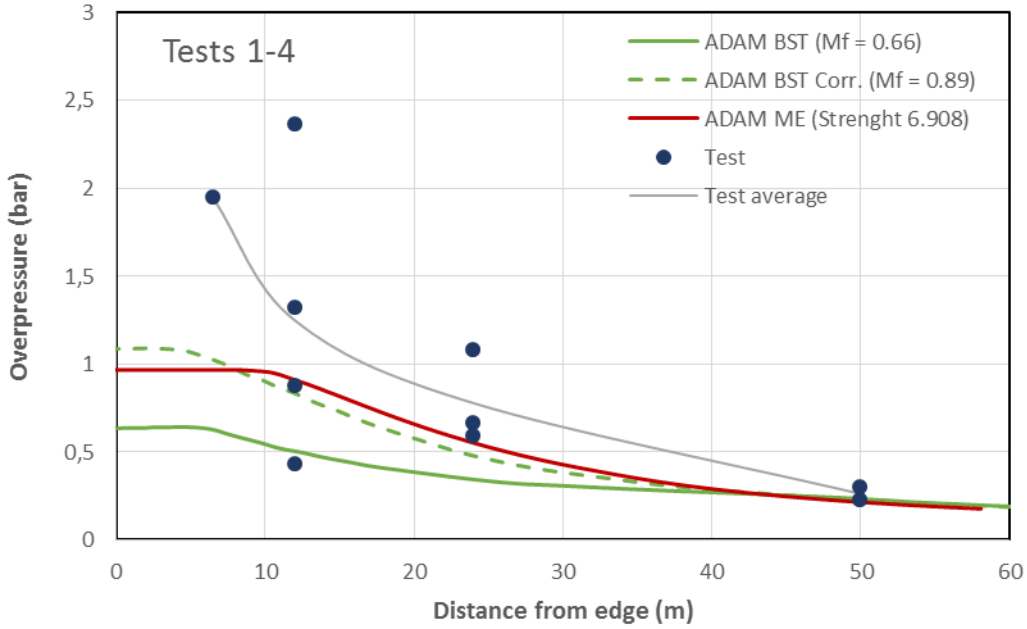

Figure 55: ADAM Simulation of BFETS3a Tests 1-4 vs. experimental results.

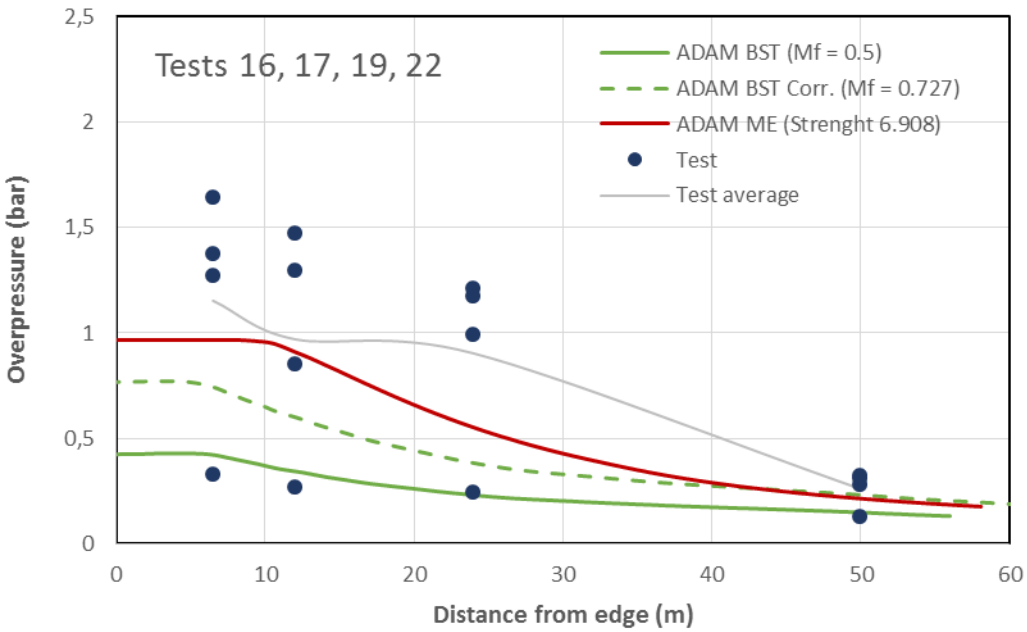

Figure 56: ADAM Simulation of BFETS3a Tests 16, 17, 19, 22 vs. experimental results.

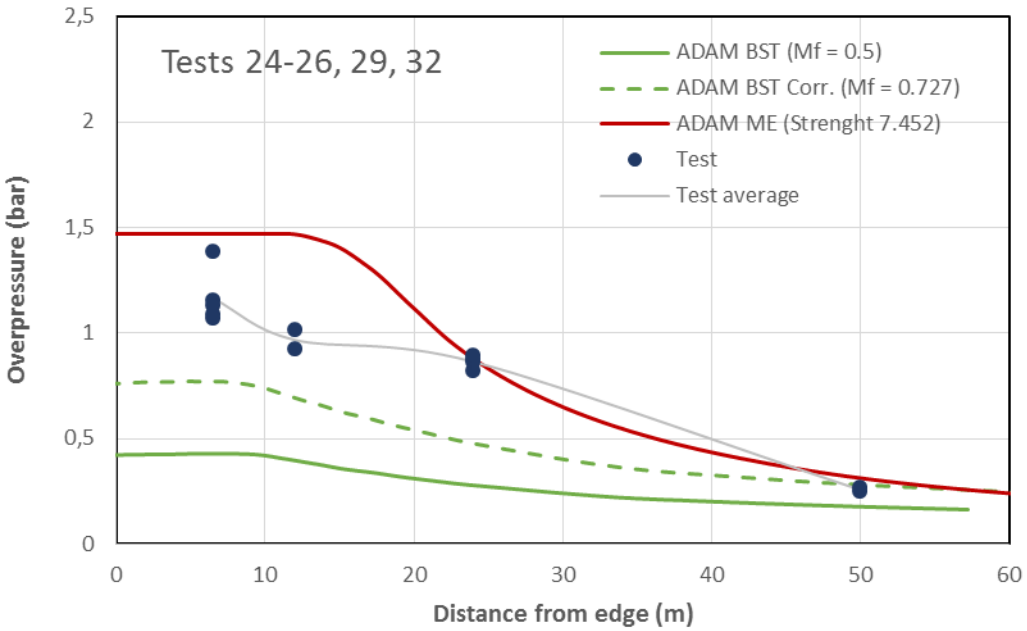

Figure 57: ADAM Simulation of BFETS3a Tests 24-26, 29, 32 vs. experimental results.

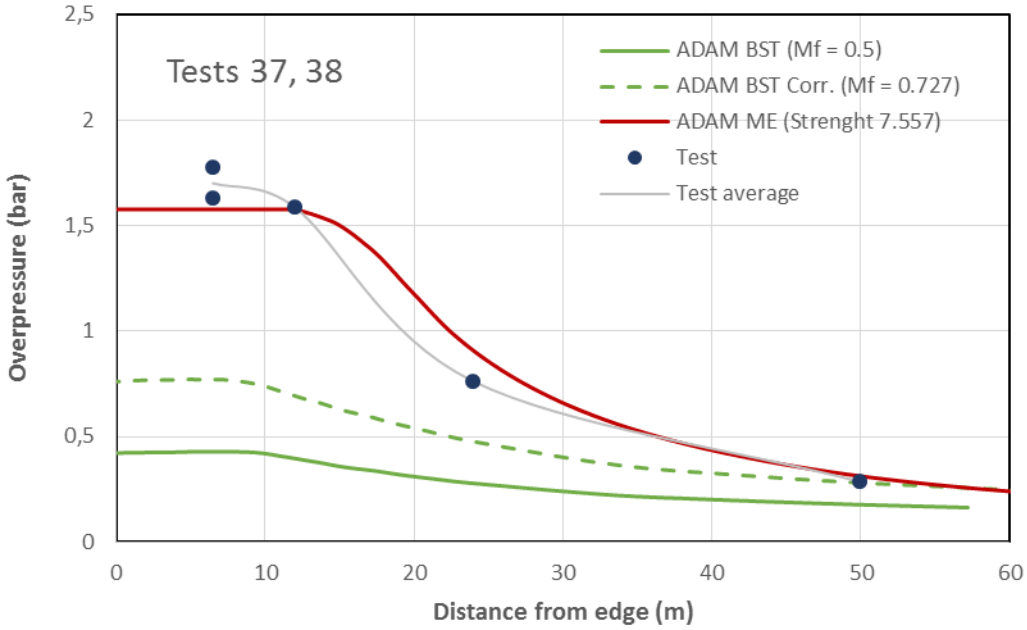

Figure 58: ADAM Simulation of BFETS3a Tests 37, 38 vs. experimental results.

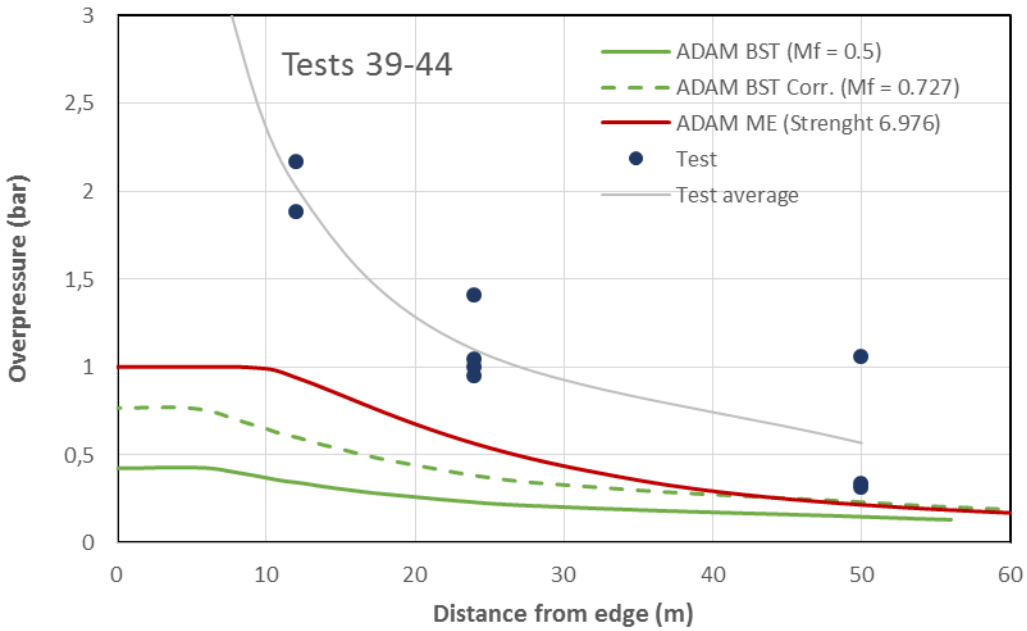

Figure 59: ADAM Simulation of BFETS3a Tests 39-44 vs. experimental results.

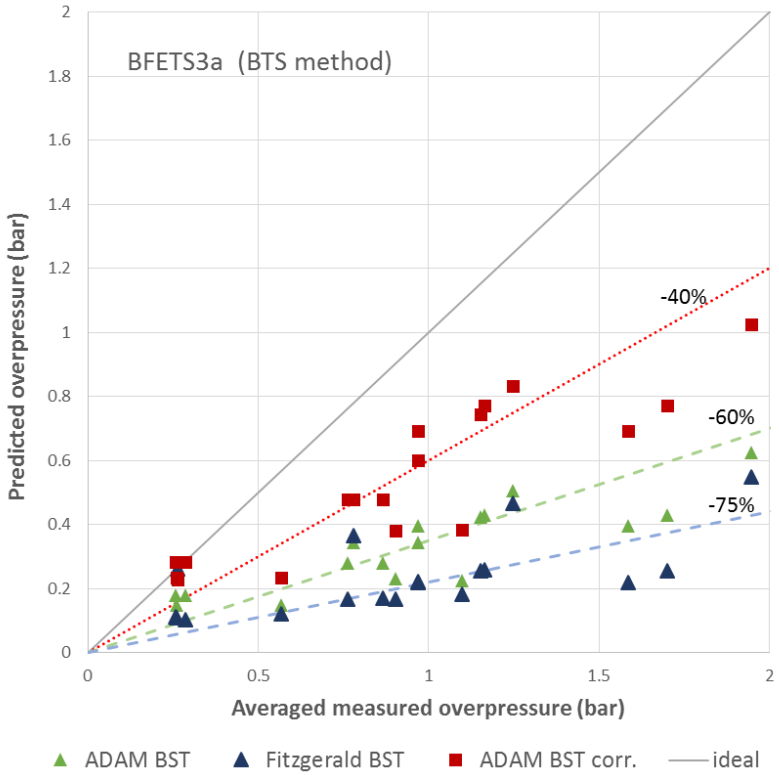

Figure 60: Predicted overpressure vs. average measured overpressure on BFETS3a Tests. Comparison of ADAM results obtained with original BST method (orange triangle) and corrected for the ground effect (red squares) with the Fitzgerald, 2001 results (blue triangle).

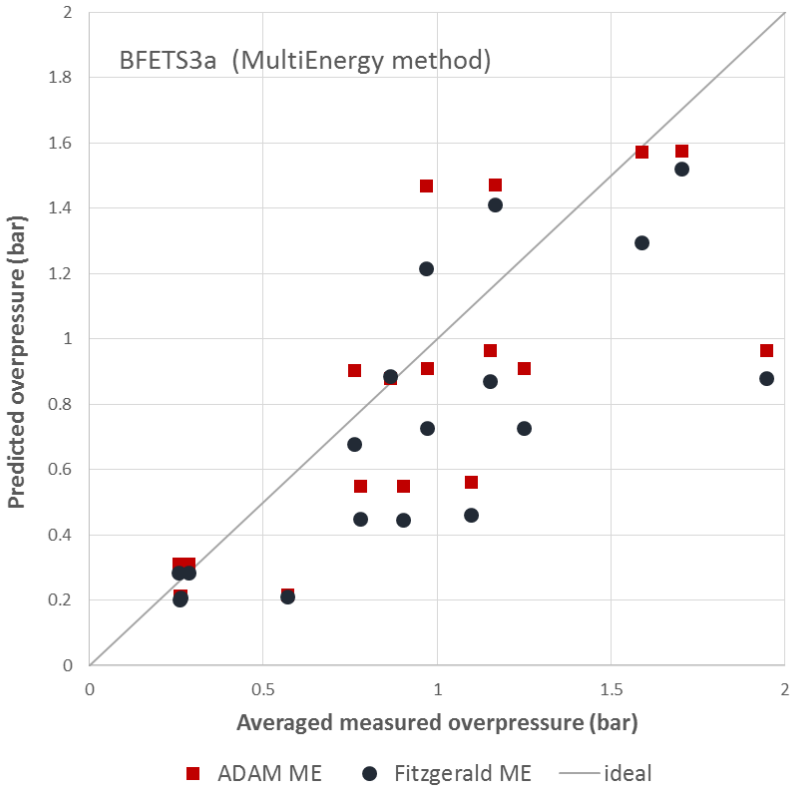

Figure 61: Predicted overpressure vs. average measured overpressure on BFETS3a Tests. Comparison of ADAM with the Fitzgerald, 2001 results obtained using the Multi Energy method.

3.3.2 Test Programme: EMERGE

The EMERGE tests were performed by TNO, BG, and CMR to study vapour cloud explosions involving methane and propane under different congestions conditions (EMERGE, 1998).

The information given in the table below provides the input parameters for VCE modelling used by Fitzgerald (Fitzgerald, 2001). These were used also for the simulation with ADAM. The blast Energy E was used for the determination of the explosive mass, input to ADAM, which was calculated by considering a heat of combustion per unit mass for methane and propane of 50031 kJ kg^{-1}, and 46360 kJ kg^{-1}, respectively (from the ADAM database).

Table 20: Input parameters for EMERGE tests' simulations.

				For BST				*For ME*
Tests		**Mass(kg)**	**Energy (J)***	**Confinement**	**Congestion**	**Reactivity**	**Mf**	**Strength**
Methane	28-31,32-34	0.248	1.24E+07	3D	High	low	0.34	7.051
	A1,4	1.987	9.94E+07		High		0.34	7.378
	F1,3,6,7	1.987	9.94E+07		Medium		0.23	4.815
	L1,2	16.03	8.02E+08		High		0.34	8.139
Propane	40-42,50,52	0.292	1.36E+07	3D	High	Medium	0.5	7.577
	A2-3	2.315	1.07E+08		High		0.5	7.904
	F2,4, 5	2.315	1.07E+08		Medium		0.44	5.285
	L3,4	18.52	8.59E+08		High		0.5	8.586

* for BTS blast energy is doubled due to a ground reflection factor of 2

The outcome of the simulations on the separate groups of EMERGE tests performed with ADAM are shown in Figure 62Figure 69. These data confirms also the results of Fitzgerald i.e., the BST method underestimate the experimental data with the ME method performing better, which is evident by comparing Figure 60 with Figure 61.

A point to note is, however, that small and medium scale tests were considered not realistic for industrial scenarios, and where not taken into consideration in the conclusions of Fitzgerald's paper, in which it was argued that none of the selected models are reliable enough to represent these cases. This is also the conclusion with ADAM.

Amongst the large-scale tests, which were considered in Fitzgerald's analysis, only tests L1,2 (methane) had reliable overpressure data. For the tests with propane (L3, 4) it was not possible to extract the part the pressure wave due to deflagration and no reliable overpressure data were available. In the first case, the ME method provides the best estimate whilst BST under predicts the overpressure quite significantly (see Figure 65). In the second case, since no experimental data were available, the ADAM simulations were compared to those calculated by Fitzgerald. The results are very similar in the case of ME, whilst Fitzgerald results with BST are less conservative than ADAM (see Figure 69). This is probably because Fitzgerald made use of the former BS method, which does not make use of the revised Pierorazio table.

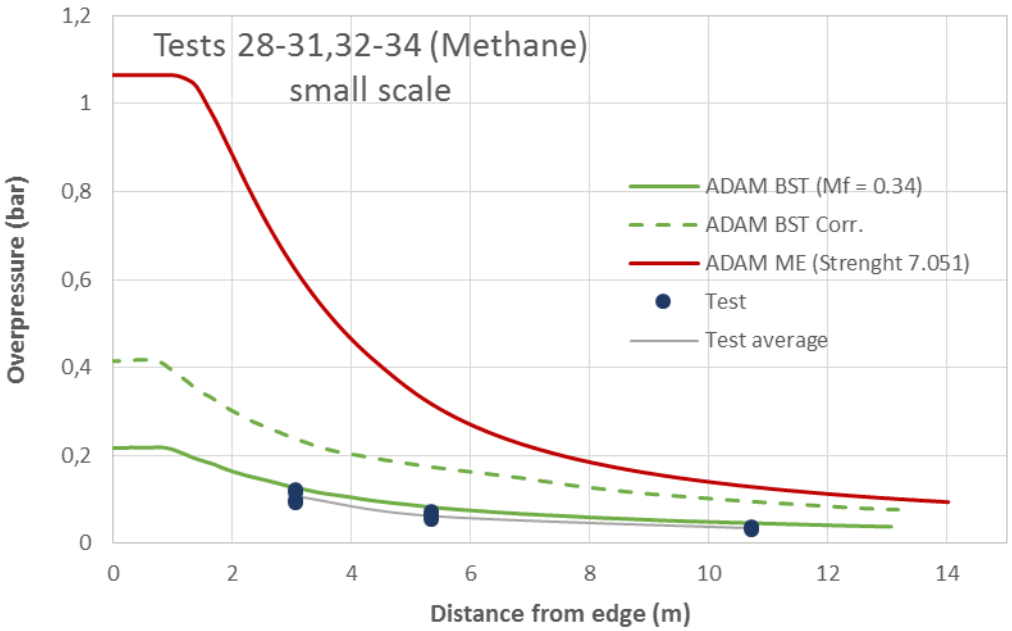

Figure 62: ADAM Simulation of EMERGE Tests 28-31,32-34 (methane VCE small scale, high congestion. Confinement 3D). Test data, ME/BST calculations vs. distance.

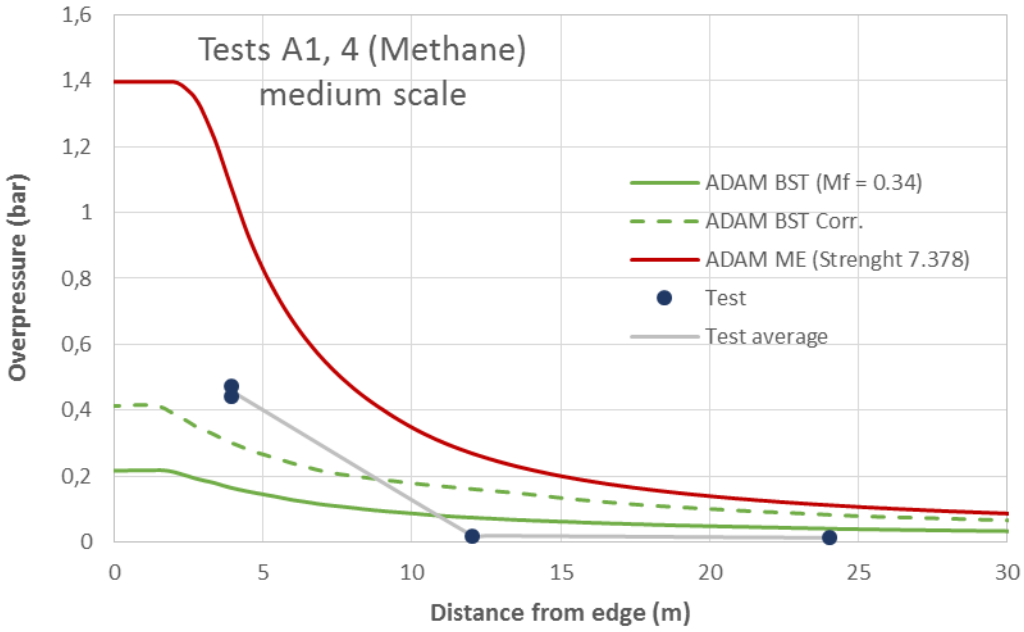

Figure 63: ADAM Simulation of EMERGE Tests A1, 4 (methane VCE medium scale, high congestion. Confinement 3D). Test data, ME/BST calculations vs. distance.

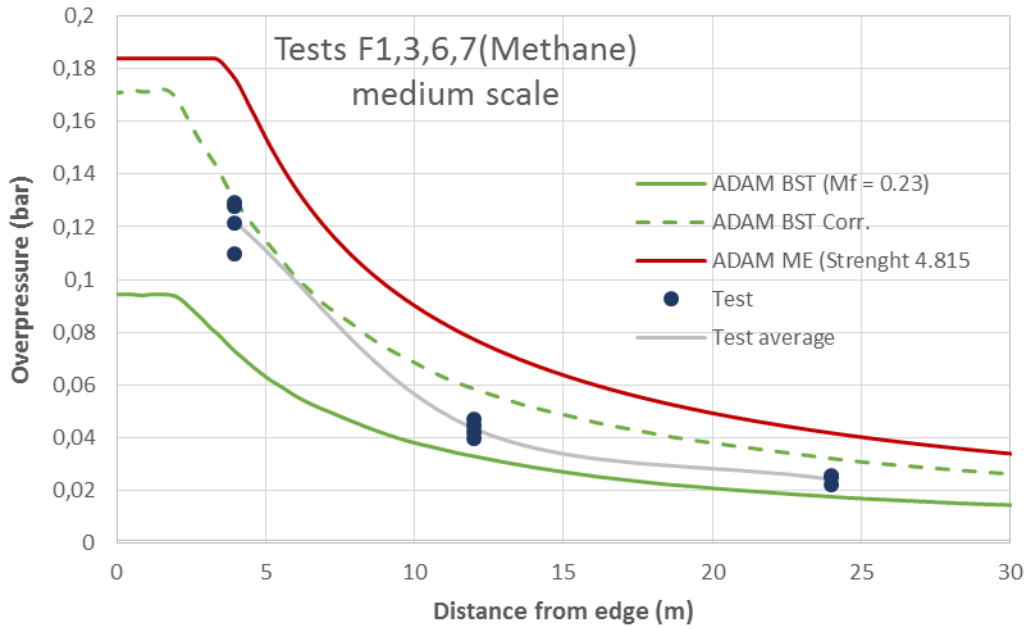

Figure 64: ADAM Simulation of EMERGE Tests F1, 3, 6, 7 (methane VCE medium scale, medium congestion. Confinement 3D). Test data, ME/BST calculations vs. distance.

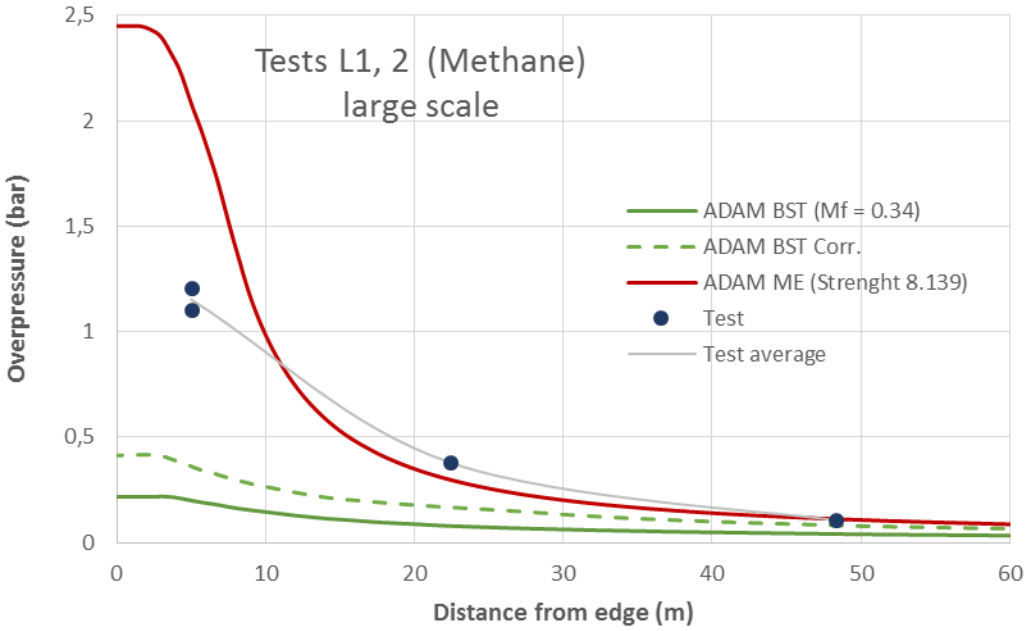

Figure 65: ADAM Simulation of EMERGE Tests L1, 2 (methane VCE large scale, high congestion. Confinement 3D). Test data, ME/BST calculations vs. distance.

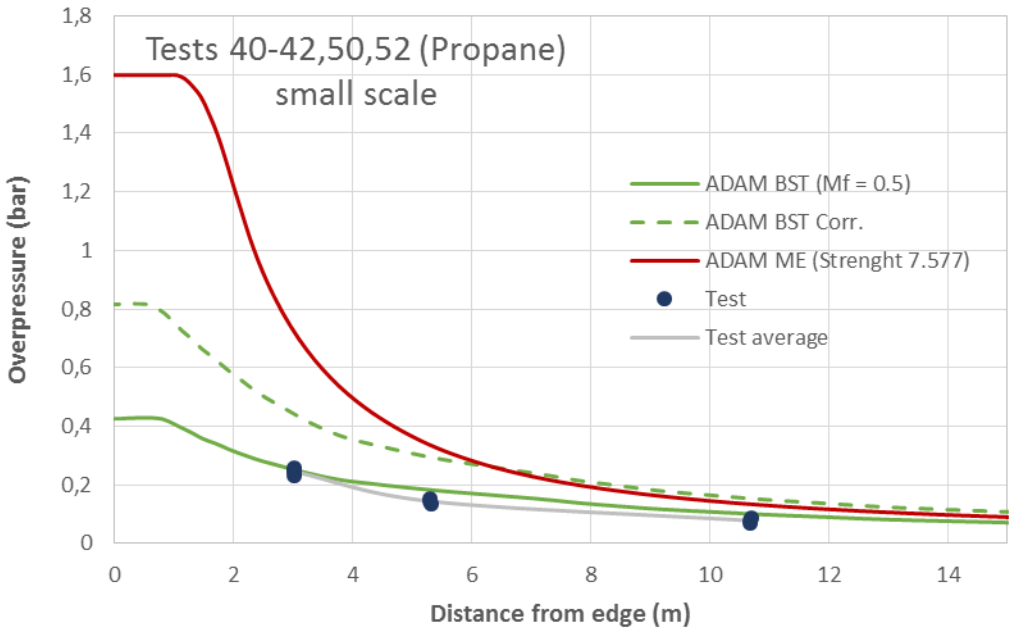

Figure 66: ADAM Simulation of EMERGE Tests 40-42, 50, 52 (propane VCE small scale, high congestion. Confinement 3D). Test data, ME/BST calculations vs. distance.

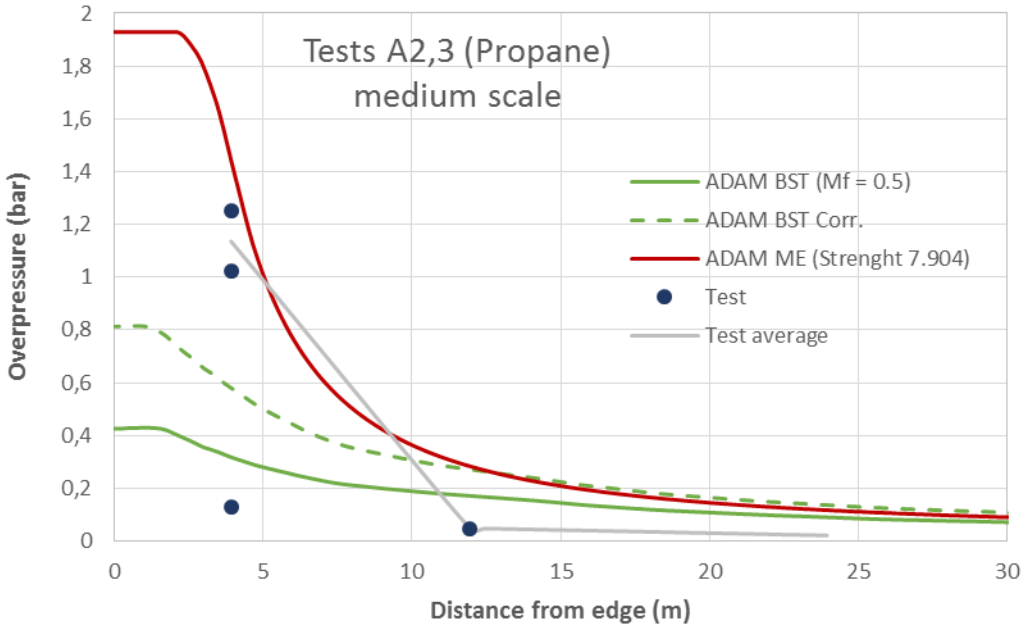

Figure 67: ADAM Simulation of EMERGE Tests A2-3 (propane VCE medium scale, high congestion. Confinement 3D). Test data, ME/BST calculations vs. distance.

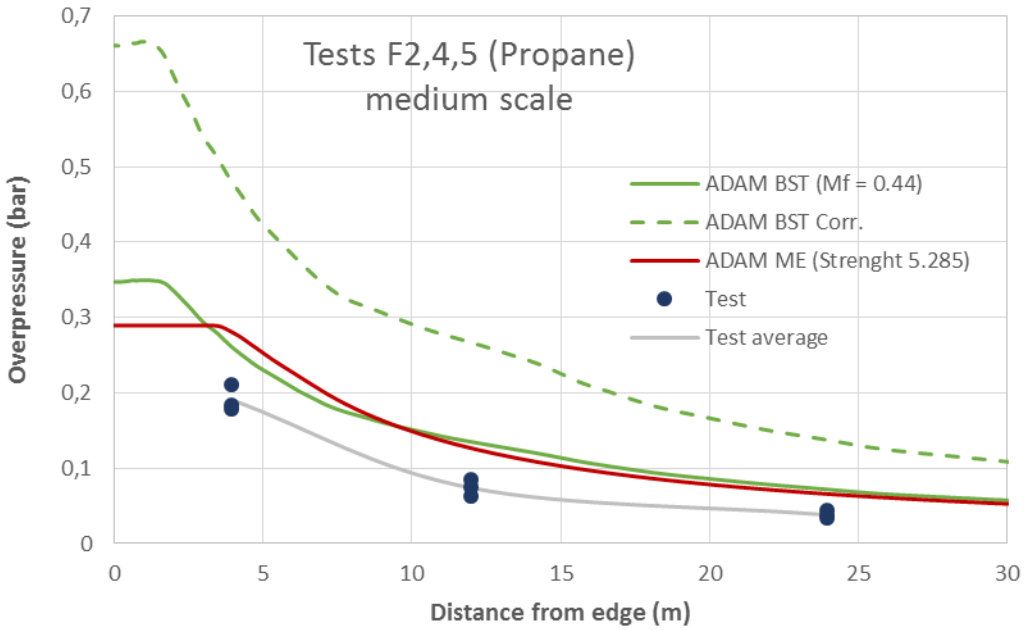

Figure 68: ADAM Simulation of EMERGE Tests F2,4, 5 (propane VCE medium scale, medium congestion. Confinement 3D). Test data, ME/BST calculations vs. distance.

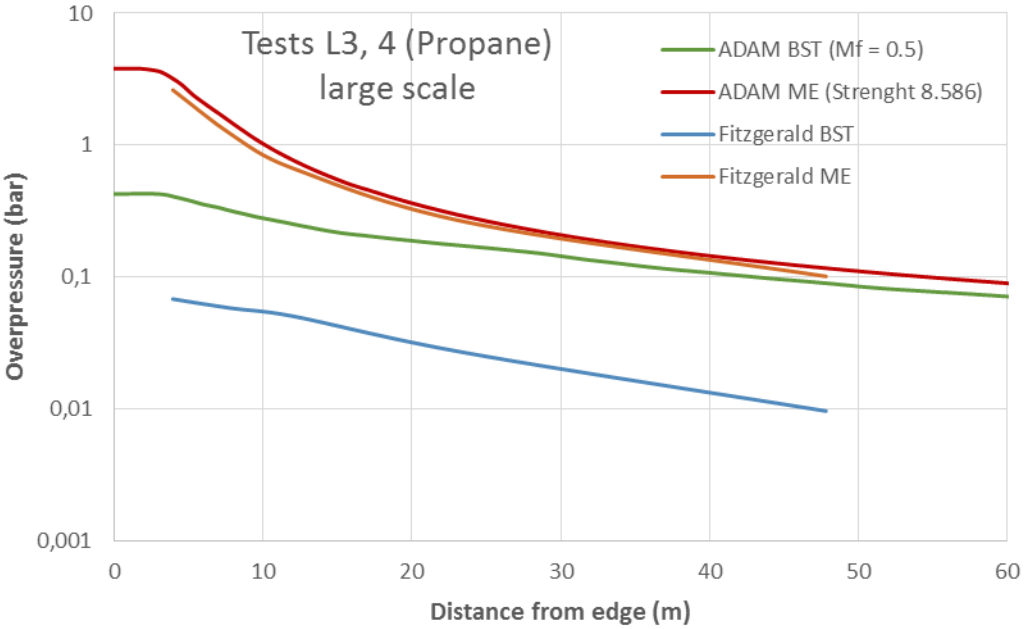

Figure 69: ADAM Simulation of EMERGE Tests L3,4 (propane VCE large scale, high congestion. Confinement 3D). In this case, no test data were reported because of the experienced transition to detonation.
The ME/BST calculations vs. distance obtained with ADAM is compared to the same calculations reported by Fitzgerald, 2001.

3.3.3 Shell Deer Park case

The last comparison was conducted on the observed overpressure data resulting from a large VCE of an accident case occurred at the Shell Company plant in Deer Park, Texas (EPA, 1998). Far field overpressures were estimated based on different observed levels of windows breakage. Although the present comparison is relevant in the far field, differently from the previous tests it represents a typical industrial case with a VCE with potential off-site effects.

The following table lists the input data used for the ADAM evaluation as taken from Fitzgerald (Fitzgerald, 2001). The blast Energy E was multiplied by the heat of combustion per unit mass of the flammable to determine the explosive mass, which is an input of ADAM. The heat of combustion per unit mass of was estimated by using the rule of mixtures and the corresponding values for hydrogen and ethylene as taken from the ADAM database (111155.8 kJ kg^{-1}). Flame speed Mach number Mf and blast strength were selected to maximise the overpressure effect (i.e. 5.2 and 10, respectively)

Table 21: Input parameters for Deer Park case simulations.

			For BST				*For ME*
Material	**Mass(kg)**	**Energy (J)***	**Confinement**	**Congestion**	**Reactivity**	**Mf**	**Strength**
19%H_2 81% Ethylene	610	6.78E+10	2.5D	High	High	5.2	10
* for BTS blast energy is doubled due to a ground reflection factor of 2							

The results of the simulation carried out with ME and BTS in ADAM is given in

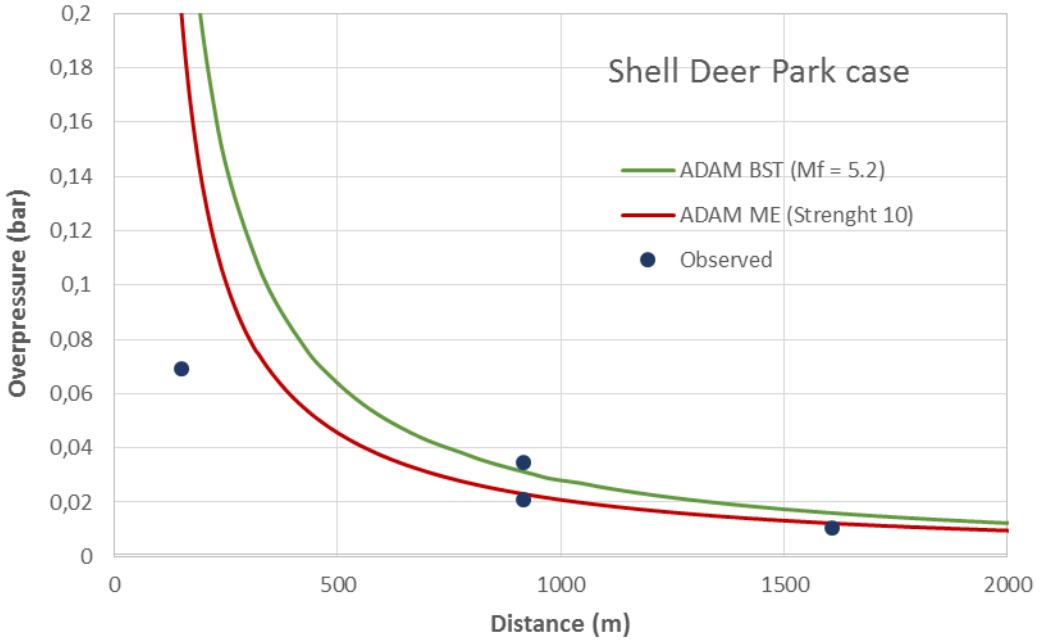

Figure 70, which shows that both methods produced similar results especially in the far field. In this case, the ground correction method on BST is not applied, since the flame speed is already the highest (i.e. M_f = 5.2).

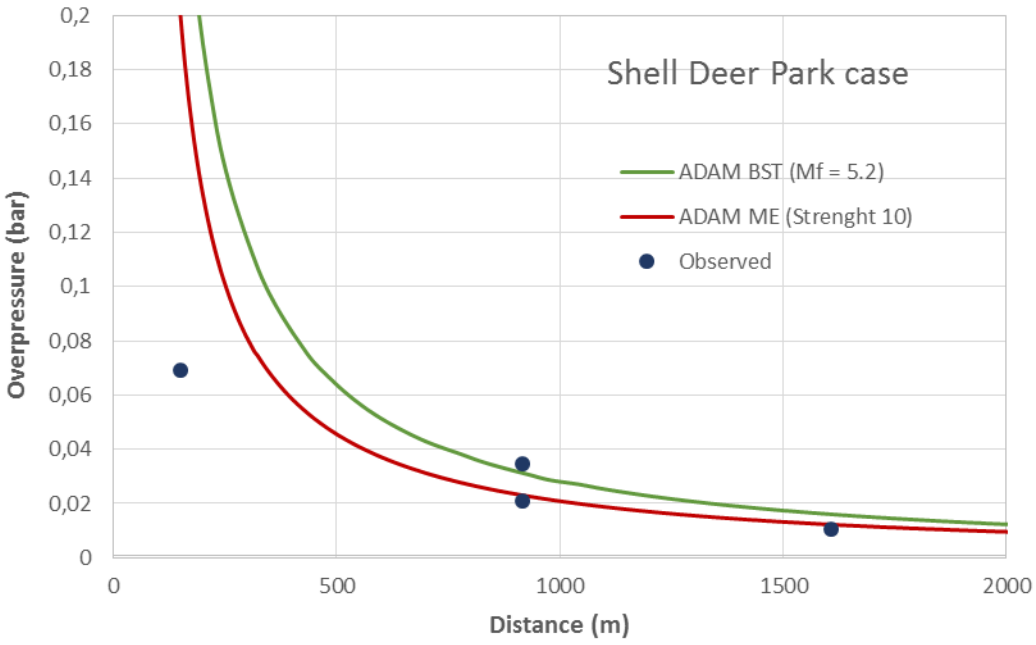

Figure 70: Shell Deer Park case, overpressure in the far field. Comparison of ADAM BST (Mf = 5.2) and ME (strength 10) vs observed data.

References

Bennett, JF, Cowley, LT, Davenport, JN, and Rowson, JJ (1991), "Large scale natural gas and LPG jet fires - final report to the CEC", TNER 91.022

Blewitt, RE Yohn, JF Koopman, RP Brown, TC (1987), "Conduct of anhydrous hydrofluoric acid spill experiments", Proc. Int. Conf. on Vapour Cloud Modelling, AIChE, New York, pp. 1-38

Brighton, P. (1990), "Further verification of a theory for mass and heat transfer from evaporating pools", J. Hazard. Mater. 23, 215-234

Burgess, D.S, Biordi, J. and Murphy, J.N. (1972), "Hazards of spillage of LNG into water", Final report. PMSRC Report No 4177, US Department of Interior, Bureau of Mines.

BFETS BG Technology HSE (2000) "Explosions in full scale Offshore module geometries-Main Report" Offshore Technology Report – OTO 1999 043, Project No 3522, prepared for Health and Safety Executive by BG Technology

CCPS (1996), "Guidelines for use of vapour cloud dispersion models, Center for Chemical Process Safety (CCPS)", American Institute of Chemical Engineers, New York, USA

Chamberlain, GA (1987), "Developments in design methods for predicting thermal radiation from flares", Chem. Eng. Res. Des., 65: 299–309

Chang JC and Hanna JC, (2004), "Air quality model performance evaluation", Meteorol. Atmos. Phys. 87, pp. 167-196

Cleary, V Bowen, P Witlox, H (2007) "Flashing liquid jets and two-phase droplet dispersion – part 1, experiments for derivation of droplet atomisation correlations", Journal of Hazardous Materials, 142, pp. 786–796

Davies, JKW (1987), "A comparison between the variability exhibited in small scale experiments and in the Thorney Island Phase I trials", J. Hazard. Mater. 16, pp.339-356

De Vaull, G. E. King, J. A. (1992), "Similarity scaling of droplet evaporation and liquid rain-out following the release of a superheated flashing liquid to the environment", 85th Annual Meeting, Air and Waste Management Assoc., Kansas City, MO, June 21-26.

Dodge, F. T., Park, J. T., Buckingham, J. C. & Magott, R. J. (1983), "Revision and experimental verification of the hazard assessment computer system models for spreading, movement, dissolution, and dissipation of insoluble chemicals spilled into water": test data volume. -Final Report- Department of US Transportation, United States Coast Guard

Efron B (1987) "Better bootstrap confidence intervals", J. Amer. Stat. Ass., 82, pp.171-185

Elkotb, MM (1982), "Fuel atomisation for spray modelling", Progress in Energy and Combustion Science, 8(1), pp. 61-91

EMERGE (1998), "Extended Modelling and Extended Research into Gas Explosions", Final Summary Report of the CEC Contract Ev5V-CT93-0274.1998

EPA (1998), "EPA/OSHA Joint Chemical Accident Investigation Report", prepared by US Environmental Environment Agency and US Occupational Safety and Health Administration for Shell, Deer Park, Texas, EPA 550-R-98-005

Fabbri, L Binda, M Bruinen de Bruin, Y; "Accident Damage Analysis Module (ADAM) – Technical Guidance", EUR 28732 EN, 2017, ISBN 978-92-79-71879-3, doi 10.2760/719457

Fitzgerald G, (2001), "A comparison of simple vapor cloud explosion prediction methodologies", Second Annual Symposium, Mary Kay O'Connor Process Safety Center, Texas October 30-31, 2001

Goldwire HC Jr, McRae TG, Johnson GW, Hipple DL, Koopman RP, McClure JW, Morris LK, Cederwall RT (1983) "Desert Tortoise data series report", UCID-20562, Lawrence Livermore National Laboratories, Livermore

Goldwire HC Jr, Rodean HC, Cederwall RT, Kansa EJ, Koopman RP, McClure JW, McRae TG, Morris LK, Kamppinen L, Kiefer RD, Urtiew PA, Lind CD, (1983). "Coyote series data report, LLNL/NWC 1981 LNG spill tests dispersion, vapor burn and rapid phase transition", Vols. 1 and 2, UCID - 19953. Lawrence Livermore National Laboratories, Livermore

Hanna Consultants, (2006), "Source Term Estimation Methods for Releases of Hazardous Chemicals to the Atmosphere Due to Accidental and Terrorist Incidents at Industrial Facilities and during Transportation", Report No. P081-F, Final Report to H.E. Cramer Company under contract 343-HEC0001-05-0001 in support for DARPA Pentagon Shield Program, 181 pp.

Hanna SR, Chang J.C. and Strimaitis DG, (1993) "Hazardous gas model evaluation with field observations", Atmos. Environ., 27A, pp. 2265-2285

Hanna SR, Dharmavaram, Zhang. JC, Sykes I, Witlox H WM, (2008) "Comparison of six widely-used dense gas dispersion models for three recent chlorine railcar accidents", Process Safety Progress, 27 pp 248-259

Hanna SR, Strimaitis DG, and Chang JC (1991) "Evaluation of fourteen hazardous gas models with ammonia and hydrogen fluoride field data", J. Hazard. Mater. 26, pp. 127-158

Ivings M.J., Gant S.E., Jagger S.F, Lea C.J., Stewart J.R., and Webber, D.M. (2016), "Evaluating vapour dispersion models for safety analysis of LNG facilities". HSE report, 2nd Edition MSU/2016/27

Johnson DW, Woodward, JL (1999) "A Model with Data to Predict Aerosol Rainout in Accidental Releases", Center of Chemical Process Safety (CCPS), New York

Johnson, A.D., 1992, "A model for predicting thermal radiation hazards from large-scale LNG pool fires", IChemE Symp. Series, 130: 507–524

Johnson, A.D., Brightwell, H.M., and Carsley, A.J., (1994), "A model for predicting the thermal radiation hazard from large scale horizontally released natural gas jet fires", Trans. IChemE., 72B: 157–166

Kay, P J, Bowen, PJ Witlox, H W M, (2010) "Sub-cooled and flashing liquid jets and droplet dispersion II. Scaled experiments and derivation of droplet size correlations", Journal of Loss Prevention in the Process Industries Volume 23, Issue 6, pp. 849–856

Kay, P.J. Witlox, H. W.M. Bowen, P. J., (2010), "Sub-cooled and flashing liquid jets and droplet dispersion II. Scaled experiments and derivation of droplet size correlations", Journal of Loss Prevention in the Process Industries, 23, pp. 849-856

Koopman RP , Baker J , Cederwall RT , Goldwire HC Jr. , Hogan WJ , Kamppinen,LM , Kiefer RD , McClure JW , McCrae TG , Morgan DL , Morris LK , Spann MW Jr. , Lind CD (1982a). Burro Series Date Report, LLNL/NWC 1980 LNG Spill Tests, UCID - 19075 , Lawrence Livermore Laboratory, Livermore, CA, Dec. https://e-reports-ext.llnl.gov/pdf/194414.pdf and https://e-reportsext.llnl.gov/pdf/194606.pdf .

Koopman RP , Cederwall RT , Ermak DL , Goldwire HC Jr. , Hogan WJ , McClure, JW McCrae, TG Morgan, DL Rodean, HC Shinn, JH (1982b). "Analysis of Burro series 40 m^3 LNG Spill experiments". J. Hazard. Mater. 6, pp. 43 – 83.

Kukkonen J, (1990) "Modelling source terms for the atmospheric dispersion of hazardous substances", Physico-Mathematicae 115/1990, Dissertation N0 34, The Finnish Society of Sciences and Letters

Lautkaski R. (2008), "Experimental correlations for the estimation of the rainout of flashing liquid releases - Revisited," Journal of Loss Prevention in the Process Industries vol. 21, pp. 506-511.

Lois, E., and Swithenbank, J., 1979, "Fire hazards in oil tank arrays in a wind", 17th Symposium (Int.) on Combustion, Leeds, Combustion Institute, Pittsburgh, PA, 1087–1098

McQuaid J, Roebuck B. (1985). "Large-scale field trials on dense vapour dispersion". EUR 10029 EN. Brussels: Health and Safety Executive

McQuaid, J. (1985) Proceeding of the symposium on heavy gas dispersion trials at Thorney Island. J. Hazard. Mater. 11.

Mercx W.P.M., van den Berg A.C. (2005), "Vapour Cloud Explosions", TNO-Yellow-Book-CPR-14E, Chapter 5, Editors: C.J.H. van den Bosch, R.A.P.M. Weterings, third revision

Nedelka, D., Moorhouse, J., and Tucker, R. F., (1990), "The Montoir 35m diameter LNG pool fire experiments", Proc. 9th Intl. Cong and Exposition on LNG, LNG9, Nice, 17–20 October 1989, Published by Institute of Gas technology, Chicago,

Nielsen M., Ott S. (1996b), "Fladis field experiments Final Report", (Denmark. Forskningscenter Risoe. RisoeR; No. 898(EN))

Nielsen M., Ott S., (1996a) "A collection of data from dense gas experiments", (Denmark. Forskningscenter Risoe. RisoeR; No. 845(EN))

Pierorazio A. J., Thomas J. K., Baker J. K., and Ketchum D. E., (2005). "An update to the Baker Strehlow-Tang vapor cloud explosion prediction methodology flame speed table" Process Safety Progress 24 (1) pp. 59-65

Selby, C.A., and Burgan, B.A., (1998), "Blast and fire engineering for topside structures - phase 2: final summary report", SCI Publication No. 253, Steel Construction Institute, UK

Tang M.J., Baker Q.A. (1999) "A new set of blast curves from vapour cloud explosions", Process Safety Progress 18, pp. 235-240

Tang M.J., Baker Q.A. (2000) "Comparison of blast curves for vapour cloud explosions", J. Loss Prev. Proc. Indus., 13 pp. 433-438

van den Berg A.C., Mos A.L. (2005) "Research to improve guidance on separation distance for multi-energy method (RIGOS)", HSE Research Report 369, ISBN 0 7176 6146 6

van den Bosch C.J.H., Duijm N.J. (2005), "Outflow and Spray release", TNO-Yellow-Book-CPR-14E, Chapter 2, Editors: C.J.H. van den Bosch, R.A.P.M. Weterings, third revision 2005

Webber M.D., Jones, S.J. (1987). A model of spreading vaporising pools. In J. Woodward (ed.) International conference on vapor cloud modeling. Boston Massachusset, USA, AIChE

Webber M.D. (1990), "A model for pool spreading and vaporisation and its implementation in the computer code G*A*S*P*", HSE Report SRD/HSE/R507.

Webber M.D. (2012), "On models of spreading pools" Journal of Loss Prevention in the Process Industry 25, 923-926.

Welker, J. R., and W. D. Cavin, (1982) Vaporization, Dispersion, and Radiant Fluxes from LPG Spills. Final Report No. DOE-EP-0042, Department of Energy Contract No. DOE-AC05-78EV-06020-1, May, 1982 (NTIS No. DOE-EV-06020-1).

Wheatley, CJ (1994) A theoretical study of NH3 concentrations in moist air arising from accidental releases of liquefied NH3 using the computer code TRAUMA, Volume 393 UKAEA Safety and Reliability Directorate, 1987, ISBN: 0853562148, 9780853562146 Oreskes N, Shrader-Frechette K, Beliz K, "Verification, validation and confirmation of numerical methods of numerical methods in earth science", Science 263, pp.641-646

Witlox, H.W.M. Harper, M. (2013) Two phase jet release, droplet dispersion and rainout I. Overvire and model validation. Journal of Loss Prevention in the Process Industries 26453-461

Woodward J.L. (2014), "Source Modelling – Aerosol formation and rainout, Reference Module in Chemistry", Molecular Sciences and Chemical Engineering, pp. 1-27

GETTING IN TOUCH WITH THE EU

In person

All over the European Union there are hundreds of Europe Direct information centres. You can find the address of the centre nearest you at: https://europa.eu/european-union/contact_en

On the phone or by email

Europe Direct is a service that answers your questions about the European Union. You can contact this service:

- by freephone: 00 800 6 7 8 9 10 11 (certain operators may charge for these calls),

- at the following standard number: +32 22999696, or

- by electronic mail via: https://europa.eu/european-union/contact_en

FINDING INFORMATION ABOUT THE EU

Online

Information about the European Union in all the official languages of the EU is available on the Europa website at: https://europa.eu/european-union/index_en

EU publications
You can download or order free and priced EU publications from EU Bookshop at: https://publications.europa.eu/en/publications. Multiple copies of free publications may be obtained by contacting Europe Direct or your local information centre (see https://europa.eu/european-union/contact_en).

KJ-NA-29363-EN-N

The European Commission's science and knowledge service
Joint Research Centre

JRC Mission
As the science and knowledge service of the European Commission, the Joint Research Centre's mission is to support EU policies with independent evidence throughout the whole policy cycle.

EU Science Hub
ec.europa.eu/jrc

@EU_ScienceHub
EU Science Hub - Joint Research Centre
Joint Research Centre
EU Science Hub

Publications Office

doi:10.2760/582513
ISBN 978-92-79-94668-4